The Ramifications of Maximally Coupled Electromagnetic Interactions

A DISSERTATION
SUBMITTED TO THE DEPARTMENT OF PHYSICS
OF CANTERBURY UNIVERSITY
IN PARTIAL FULFILLMENT OF THE REQUIREMENTS
FOR THE DEGREE OF
DOCTOR OF PHILOSOPHY

G. Robert Burling–Claridge

June 1990

Abstract

In this thesis I study several applications of a maximally coupled QED model to particle interactions. The seminal work on the subject is Rosenbluth (1950), who studied the maximally coupled proton in electron-proton scattering. His analysis involves three assumptions which were starting points for the research reported here.

1. There was no derivation given (or referenced) for the maximally coupled vertex.
2. The dipole moment of the electron is ignored on the grounds that it is "quite small and decreases rapidly at higher energies".
3. He assumes that the proton is a distributed particle and attempts to fit his theoretical results using structure constants intended to reflect the details of the proton structure.

I present a derivation of the maximally coupled vertex first used by Rosenbluth. The resultant vertex disagrees with that used by Rosenbluth (and all subsequent workers in the field) in the sign of the magnetic dipole parameter. I explore the ramifications of this discrepancy for the other two assumptions.

Using the sign derived here for both the electron and the proton I show that the full maximally coupled cross-section to first order for electron-proton scattering to be in far better agreement with experiment than the commonly employed Rosenbluth model. Further, at around 200 MeV the prediction developed here agrees with experiment to within the experimental uncertainties. At higher energies (and hence exchange momenta) this agreement falls away, however it is always in better agreement than the bare Rosenbluth expression.

I show that for exchanged momentum of about the proton rest mass, the dipole-dipole terms are comparable to or larger than the monopole-monopole terms. Hence the dipole terms become more important as the exchanged energy increases. This is true for either vertex. Taking Rosenbluth's second assumption, but using the vertex derived here, I find little difference from the minimally coupled result.

I discuss the difficulty of trying to re-develop the form factor approach of fitting the theoretical curves to experiment.

I apply the maximally coupled QED model to neutron decay and obtain a neutron lifetime within 15% of the latest experimental value from a first order analysis involving no free

parameters.

Maximally coupled QED neutron-proton scattering is shown to account for about 10^{-4} of the measured scattering. This is as expected since this interaction is dominated by the strong nuclear force. I find poor agreement between the maximally coupled QED model and experiment for electron-neutron scattering. However, the application of a basically minimally coupled model for extracting electron-neutron scattering from the experimentally measured electron-deuteron scattering data is discussed and questioned.

All of the two-photon scattering matrix elements for any two non-identical fermions are calculated, up to the integrations over the extra 4-momentum. These integrals are partially completed here, and all of the 4-space integrations are performed and presented. The development of a systematic approach to these integrals will allow their solution in later research.

Contents

List of Tables

List of Figures

Chapter 1

Introduction

1.1 Historical

In 1949 Feynman introduced the concept of representing an interaction between particles by a series of diagrams or graphs, where each symbol in the diagram had a particular quantum mechanical operator associated with it. These Feynman diagrams have proven to be extremely useful. They allow a simple interpretation to be made of a complex interaction by viewing the process as a series of 'common sense' diagrams. The diagram techniques have since been extended from the original Quantum Electro–Dynamics (QED) into general quantum field theory, covering all types of particle interactions.

One very important aspect of the diagram method is the physical and mathematical details of the operator describing the way in which the particles couple to the underlying field structure. This operator is commonly called the vertex operator, because of the way in which the diagrams are drawn.

Feynman assumed the interaction could be described by the covariant Dirac operator for the minimally coupled electromagnetic interaction of spin-$\frac{1}{2}$ particles,

$$O_D = \not{p} - q_i \not{A} - m \tag{1.1}$$

which has the particles interacting solely through their electric monopole charges (q_i). He deduced from this that the QED vertex operator was $(-i\ q_i \gamma^\alpha)$, the coefficient of the interaction field term (A_α).

Previously, Pauli and Weisskopf (1934) had pointed out that there was one other term that could appear in an (electromagnetic) covariant Dirac operator for spin-$\frac{1}{2}$ particles. They suggested adding the contracted form of the electromagnetic field tensor, $F^{\alpha\beta}$, in such a way that the operator would remain covariant and Poincarè invariant.

Recent work on this suggestion (Sachs, 1982, Barut and McEwan, 1984) has shown that the term $\not{F} = \sigma_{\alpha\beta} F^{\alpha\beta}$ is the only other Poincarè invariant term in the covariant Dirac interaction operator. Sachs also looks at other possible additional terms if Poincarè invariance is not retained, but I do not follow this path here.

Pauli and Weisskopf's suggested interaction operator (the Pauli–Dirac operator) was

$$O_{PD} = \not{p} - q_i \not{A} - m - \xi \not{F} \tag{1.2}$$

The coupling constant, ξ, associated with the Pauli modification is easily identified with the anomalous magnetic moment, μ_a. The extra $\xi \not{F}$ term in the operator allows the particles to interact through their electromagnetic dipoles (since $F_{\alpha\beta} \sim \partial_\alpha A_\beta$) as well as their monopoles (electric charges).

I shall call this Pauli–Dirac coupling 'maximal coupling', since the coupling is via the electromagnetic dipole as well as the monopole, in contrast to the 'minimal coupling' (electromagnetic monopole only) of Dirac's original interaction operator.

Minimal coupling predicts a magnetic moment for a spin-$\frac{1}{2}$ particle

$$\mu_D = \frac{q_i}{2m_i} \tag{1.3}$$

although, as several authors have shown (see for example Corben 1968, Bohm, 1979, §9.3), this 'Dirac' magnetic moment can be derived classically i.e. it is a Lorentz relativistic, rather than a quantum, phenomenon.

Experimental measurement of the magnetic moments of electrons, protons and neutrons show the measured value in each case to be of larger magnitude than the minimal coupling prediction. This 'extra' moment is commonly referred to as the 'anomalous magnetic moment', μ_a.

As discussed, the Dirac magnetic moment derives directly from a spinning, point monopole. The distance dependence of the potential corresponding to the minimal coupling (Dirac) magnetic moment is as for the monopole it derives from, as can be seen in the standard solution to a Dirac hydrogen atom. The anomalous magnetic moment on the other hand, arises from the spatial differentiation of the electromagnetic potential, A_α. This is a dipole term, and hence the distance dependence of the anomalous moment or dipole charge is quite different to that for the monopole charge.

This is a critical distinction. As the energy of the colliding particles increases the closest approach distances will decrease, and hence the relative importance of the monopole and the dipole interactions will alter. In Chapter 5 I prove this to be the case for electron proton scattering and estimate the value of exchanged momentum about which the dipole-dipole contribution to the interaction begins to dominate the monopole-monopole contribution.

It is customary to quote the experimentally measured magnetic moment in terms of g-factors, a multiplier of the minimal coupling magnetic moment, rather than the actual value

$$\mu_{exp} = g \left(\frac{q_i}{2m_i}\right) = \mu_D + \mu_a \tag{1.4}$$

In Chapter 2 I show the magnitudes of the magnetic moments and dipole charges (anomalous magnetic moments) in consistent units. Of interest, the magnitudes of the dipole charges for the electron, proton and neutron differ by only 15% or so, with the electron dipole charge being *larger* than the proton dipole charge.

The widespread use of g-factors have obscured the relative magnitude of the dipole charges so well that when Rosenbluth (1950) extended Feynman's original minimal coupling work to maximally coupled scattering for electrons off protons, the electron's dipole contribution was ignored: (Rosenbluth 1950, footnote 2)

> "Strictly speaking we should also give the electron an anomalous magnetic moment, but this is quite small and decreases rapidly at high energy"

The Rosenbluth paper (1950) for scattering a minimally coupled electron off a maximally coupled proton had a better agreement with experiment than the original totally minimally coupled analysis at medium to low energies ($\sim$ 200 MeV) and received wide attention. This same paper of Rosenbluth's introduced charge and magnetic form factors for the proton. These form factors were justified by Rosenbluth from considering the action of the proton's cloud of virtual mesons, but he was unable to correctly derive the form factors from this. The mathematical details of the form factors have changed over time, however the underlying assumptions are essentially unchanged.

The form factors are now simply phenomenological functions that adjust the momentum independent (point particle) model to experiment. Many workers have attempted to fit physical charge distributions to them (Kirk et al 1973, Chambers and Hofstadter 1956, Yennie et al 1957, for example). Several aspects of the research presented here relate directly to the validity of this form factor approach and I discuss this more fully in Chapter 5.

My approach in this research is to treat the particles as having ignorable internal structure and deal with only the macroscopically measurable quantities of mass, intrinsic spin, electromagnetic monopole charge (electric charge) and electromagnetic dipole charge (anomalous magnetic moment).

I have been unable to locate any derivation of the maximally coupled vertex first used by Rosenbluth in 1950. I have, therefore, re-derived this vertex in Chapter 3 and found that (apparently) Rosenbluth used an incorrect sign on the maximally coupled contribution to the vertex operator.

The original intent of the research reported on in this thesis, was to extend maximal coupling into a complete second order scattering calculation. Uncovering this seemingly minor sign conflict has meant that I could not ignore its ramifications and the direction of the research has altered somewhat. I discuss several aspects of the effect of this sign difference, and lay the ground work for a further attempt at a full maximally coupled second order scattering analysis in the future.

Chapters 2–4 have been published (Burling–Claridge and Butler, 1989). A copy of this publication is included as Appendix A. They deal with the derivation and the importance of this sign to the first order scattering of electrons off protons.

I re-calculate the full maximally coupled first order scattering for electrons off protons, first calculated by Hubert (1984) using Rosenbluth's vertex. The fully maximally coupled model with our vertex is shown to have good agreement with experiment, the predicted curve lying within experimental uncertainties at 188 MeV (electron beam energy).

With the correct sign in the maximally coupled vertex, the Rosenbluth model (proton only maximally coupled) differs negligibly from simple minimally coupled (Möller) scattering.

In Chapter 5 I extend the published work and investigate the contributions from each of the interactions (monopole-dipole, etc) to first order scattering. The relative sizes of these cross-terms show immediately that omitting the electron's dipole charge can not be justified, for either vertex, in terms of it's 'negligible' contribution. The Rosenbluth model is thus shown to be invalid on its original justification and I discuss the necessary re-interpretation of form factors.

Maximal coupling allows the possibility of a calculation of a decay lifetime for neutral particles, since they have non-zero dipole charges. In Chapter 6 I investigate the application of maximally coupled QED to neutron decay and I calculate the lifetime of the neutron, to first order, with surprisingly close agreement to experiment. The maximally coupled analysis presented is first-order and involves no free parameters. The predicted lifetime with Rosenbluth's sign is found to be several orders of magnitude away from the experimentally determined value.

To calculate the neutron decay lifetime I was obliged to relax the conservation of rest mass along a fermion line and instead assume conservation of dipole charge (see Section 6.2). Effectively, the dipole charge is assumed to be a conserved, quantized property of the particles. Some of the philosophical aspects of this are dealt with in Section 6.7. This latter investigation has also been published, Butler and Burling–Claridge (1989). A copy of this publication is included as Appendix B.

In Chapter 7 I investigate several other first-order maximally coupled scattering possibilities. I evaluate the effect of 'quantizing' the dipole charges for electron-proton scattering and obtain maximally coupled predictions for electron-neutron and neutron-proton scattering. These investigations have mixed success and are discussed in that chapter.

I extend the maximally coupled scattering analysis to two-photon (second order) scattering in Chapter 8. The traces of the matrix elements have been performed, however the resultant expressions are too large to include verbatim in this thesis. In the later sections of the chapter I develop a generalized approach to evaluate the 4-vector integrals required.

The second order maximally coupled matrix elements are enormous algebraic expressions. The completed evaluations (with the integrals left as general as possible) are of the order of 200 kB long (more than 2500 of 80-character lines of computer algebra!). Several days of CPU time are required to evaluate these traces. Furthermore, as shown in Chapter 8, the integrals are themselves non-trivial and sometimes quite long expressions.

These complexities have been compounded by the above mentioned deviation from the original thrust of the research. Thus, while I have made a great deal of progress toward obtaining the full second order maximally scattering expression it has not been possible to complete it for this thesis.

1.2 Definitions

The following conventions are followed throughout this document. Numerical values for the constant are shown in Section 1.3.

1. q_i = Electric monopole charge carried by the ith fermion.
2. m_i = Mass of the ith fermion.
3. α = Fine structure constant.
4. $e = \sqrt{\alpha}$ = Electric monopole charge carried by the proton.
5. $\mu_{\rm B} = \frac{e}{2m_e}$ = Bohr magneton.
6. $\mu_{\rm N} = \frac{e}{2m_p}$ = Nuclear magneton.
7. $\mu_{\rm a}$= Dipole charge (anomalous magnetic moment). We omit the subscript 'a' where convenient. It will be clear from the context that we are refering to the dipole charge.
8. p_x = 4–momentum exchanged between interacting fermions (4–momentum of the photon mediating an electromagnetic interaction).
9. 3–vectors are denoted by bold characters ($\boldsymbol{a}$).
10. When showing vector indices explicitly, we use italic indices (σ_b) for 3–vectors and Greek indices (A_α) for 4–vectors.
11. Repeated indices are always summed over unless otherwise stated.
12. $v_{i\alpha}$ = Minimally coupled vertex for the ith fermion line of a diagram.
13. $V_{i\alpha}(p)$ = Maximally coupled vertex for the ith fermion line of a diagram, 4–momentum p leaving the vertex.
14. The subscripts 'm' ($\rm O_m$) and 'M' ($\rm O_M$) refer to quantities calculated using the minimally or maximally coupled model respectively.
15. The Pauli matrices, σ_a, are defined by their commutation relations:

$$\begin{aligned} [\sigma_a, \sigma_b] &= 2\,i\,\epsilon_{abc}\,\sigma_c\ , \\ \{\sigma_a, \sigma_b\} &= 2\,\delta_{ab}\,I_2\ . \end{aligned}$$

16. We use the Minkowski metric: $g_{\alpha\beta} = \mathrm{diag}(1, -1, -1, -1)$.
17. $\sigma_{\alpha\beta} = \frac{i}{2}(\gamma_\alpha\gamma_\beta - \gamma_\beta\gamma_\alpha)$.
18. A_α = Electromagnetic 4–vector potential.
19. $F_{\alpha\beta} = \partial_\alpha A_\beta - \partial_\beta A_\alpha$ = Electromagnetic tensor.

20. $\not{p}$ = All free indices contracted with γ_α matrices in a symmetric manner, e.g. $\not{p} = p^\alpha \gamma_\alpha$, $\not{F} = \sigma_{\alpha\beta}\ F^{\alpha\beta}$.

21. The Mandelstam invariants are widely used.

$$\begin{aligned} t &= (\text{exchanged momentum})^2 \\ s &= (\text{sum of initial momenta})^2 \end{aligned}$$

1.3 Numerical Values

The constants used throughout this thesis are as follows (CRC 1984, Cohen and Taylor, 1986). The values for the magnetic moments (Dirac and experimental) and the dipole charges (anomalous magnetic moments) for the electron, the proton and the neutron are shown and discussed in Chapter 2.

1. $\alpha = (137.0359895\ \pm\ 61)^{-1}$.
2. $m_e = 0.51099906 \pm 15$ MeV.
3. $m_p = 938.27231 \pm 28$ MeV.
4. $m_n = 939.56563 \pm 28$ MeV.
5. $m_{\overline{\nu}_e} = 0.000000 \pm 35$ MeV.
6. 1 μb = 10^{-34} m^2 = 10^{-30} cm^2

The following conversion factors in natural units are useful.

1. 1 metre = 6.582112×10^{-22} sec
2. 1 $\mu_{\rm B} = \dfrac{m_p}{m_e}\mu_{\rm N} = 1836.15152\ \mu_{\rm N}$

Chapter 2

Anomalous Magnetic Moment

2.1 Introduction

In 1934 Pauli and Weisskopf suggested extending the Dirac operator for spin-$\frac{1}{2}$ particles by including the electromagnetic field tensor, $F_{\alpha\beta}$. Recent work (Sachs, 1982, Barut and McEwan, 1984) has shown that this modified or Pauli-Dirac operator contains all the possible Poincaré invariant terms describing a spin-$\frac{1}{2}$ particle interacting with an electromagnetic field. I have adopted the terminology of referring to the Pauli-Dirac operator and subsequent expressions, derivations, etc, as being 'maximally coupled', since this operator contains the maximum number of (Poincaré invariant) terms and hence includes the maximum coupling of the particle to the electromagnetic field. Further, this serves to distinguish such expressions from those arising from the minimally coupled covariant Dirac operator.

The coupling constant for the Pauli modification is easily identified with the anomalous magnetic moment. In Section 2.2 I show explicitly the identity of and, critically, the sign on the maximal coupling constant. As discussed at the end of that section I adopt the terminology of referring to the maximal coupling constant as the dipole charge.

In Section 2.3 I present the numerical values, in various units, of the magnetic moments (Dirac and experimental) and dipole charges for the electron, the proton and the neutron. Note in particular that while the magnitudes of the magnetic moments (both experimental and Dirac) are quite different, the dipole charges differ by only 10-15%. This was first pointed out to my supervisor by Barut in 1981 (mentioned at his lecture but not published in the proceedings) and forms part of the motivation for this research.

2.2 Identifying the Maximal Coupling Constant

It is well known that the minimally coupled covariant Dirac operator

$$\mathrm{O_m} = \not{p} - q\not{A} - m \tag{2.1}$$

describes the interaction of a fermion of charge q and mass m with an electromagnetic field A_α. This fermion is assumed to be point–like and to interact with the field solely through its electric monopole charge. If we incorporate the addition suggested by Pauli and Weisskopf (1934) (as discussed in Section 1.1) in a general manner, the interaction may be described by the maximally coupled Dirac operator

$$\mathrm{O_M} = \not{p} - q\not{A} - m - \xi\not{F} \tag{2.2}$$

where ξ is the coupling constant associated with the Pauli modification.

Following Messiah (1965, footnote p936) we can find the approximate, non–relativistic Hamiltonian in a weak, magnetic only field case, thus identifying the ξ coupling constant.

For convenience we choose the particular representation

$$\begin{aligned} \gamma_\alpha &= (\beta, \beta\boldsymbol{\alpha}) \\ \boldsymbol{B} &= \nabla \times \boldsymbol{A} \\ \alpha_k &= \begin{pmatrix} 0 & \sigma_k \\ \sigma_k & 0 \end{pmatrix} \\ \beta &= \begin{pmatrix} 1 & 0 \\ 0 & -1 \end{pmatrix} \end{aligned} \tag{2.3}$$

and it may be simply verified that the result obtained will be independent of the choice of representation.

Let us split the maximally coupled operator in two

$$\begin{aligned} \mathrm{O_M} &= T_\mathrm{m} - T_\mathrm{M}\ ; \\ T_\mathrm{m} &= \not{p} - q\not{A} - m, \\ T_\mathrm{M} &= \xi\not{F} \end{aligned} \tag{2.4}$$

Explicitly

$$T_\mathrm{m} = \gamma_\tau(p^\tau - qA^\tau) - m\mathbf{I}_4 \tag{2.5}$$

$$= \begin{pmatrix} p^0 - qA^0 - m & -\boldsymbol{\sigma}.(\boldsymbol{p} - q\boldsymbol{A}) \\ \boldsymbol{\sigma}.(\boldsymbol{p} - q\boldsymbol{A}) & -(p^0 - qA^0) - m \end{pmatrix} \tag{2.6}$$

and $p^0 = E$, $A^0 = \phi$ so

$$T_\mathrm{m} = \begin{pmatrix} E - q\phi - m & -\boldsymbol{\sigma}.(\boldsymbol{p} - q\boldsymbol{A}) \\ \boldsymbol{\sigma}.(\boldsymbol{p} - q\boldsymbol{A}) & -E + q\phi - m \end{pmatrix} \tag{2.7}$$

Similarly

$$\begin{aligned} T_\mathrm{M} &= \xi\sigma_{\alpha\beta}F^{\alpha\beta} \\ &\equiv i\xi\gamma_\alpha\gamma_\beta F^{\alpha\beta} \end{aligned} \tag{2.8}$$

and expanding

$$T_\mathrm{M} = i\xi\left\{\gamma_0\gamma_0 F^{00} - \left(\gamma_0\gamma_k F^{0k} + \gamma_k\gamma_0 F^{k0}\right) + \gamma_i\gamma_j F^{ij}\right\} \tag{2.9}$$

Note that

1. $F^{00} = 0$,

2. $\gamma_0\gamma_k = \begin{pmatrix} 0 & \sigma_k \\ \sigma_k & 0 \end{pmatrix} = -\gamma_k\gamma_0$

   hence ($\boldsymbol{\epsilon}$ = electric field vector)

$$\begin{aligned} \gamma_0\gamma_k F^{0k} + \gamma_k\gamma_0 F^{k0} &= 2\gamma_0\gamma_k F^{0k} \\ &= -2\begin{pmatrix} 0 & \boldsymbol{\sigma}.\boldsymbol{\epsilon} \\ \boldsymbol{\sigma}.\boldsymbol{\epsilon} & 0 \end{pmatrix} \end{aligned}$$

3. $\gamma_i\gamma_j = -\begin{pmatrix} \sigma_i\sigma_j & 0 \\ 0 & \sigma_i\sigma_j \end{pmatrix}$ hence

$$\begin{aligned} \gamma_i\gamma_j F^{ij} &= \tfrac{1}{2}(\gamma_i\gamma_j - \gamma_j\gamma_i)F^{ij} \\ &= -i\begin{pmatrix} \boldsymbol{\sigma}.\boldsymbol{B} & 0 \\ 0 & \boldsymbol{\sigma}.\boldsymbol{B} \end{pmatrix} \end{aligned}$$

Thus

$$T_{\mathrm{M}} = 2\xi\begin{pmatrix} \boldsymbol{\sigma}.\boldsymbol{B} & i\boldsymbol{\sigma}.\boldsymbol{\epsilon} \\ i\boldsymbol{\sigma}.\boldsymbol{\epsilon} & \boldsymbol{\sigma}.\boldsymbol{B} \end{pmatrix} \tag{2.10}$$

and in the non-relativistic limit with zero electric, weak magnetic field we have a maximally coupled Hamiltonian

$$\mathrm{H}_{\mathrm{nr}} = \frac{1}{2m}(\boldsymbol{p} - q\boldsymbol{A})^2 + q\phi - (\frac{q}{2m} + 2\xi)\boldsymbol{\sigma}.\boldsymbol{B} \tag{2.11}$$

where the $\frac{q}{2m}$ term is just the minimally coupled or Dirac magnetic moment, μ_{D}, of equation 1.3.

The coefficient of the spin–dipole term $(\boldsymbol{\sigma}.\boldsymbol{B})$ is the magnetic moment that will be measured experimentally. This is defined to be

$$\mu_{\mathrm{exp}} = \mu_{\mathrm{D}} + \mu_{\mathrm{a}} \tag{2.12}$$

where μ_{a} is the 'anomalous' magnetic moment. For the electron, the proton and their anti–particles

$$|\mu_{\mathrm{exp}}| > |\mu_{\mathrm{D}}| \tag{2.13}$$

so we may deduce that

$$\xi = \frac{\mu_{\mathrm{a}}}{2} \tag{2.14}$$

Thus the general maximally coupled operator is properly

$$\mathrm{O}_{\mathrm{M}} = \not{p} - q\not{A} - m - \frac{\mu_{\mathrm{a}}}{2}\not{F} \tag{2.15}$$

Note that the 'anomalous' magnetic moment arises through $F_{\alpha\beta}$, the spatial derivative of the electromagnetic potential. Thus the maximal coupling constant is associated with

an electromagnetic dipole whereas the Dirac or minimal coupling magnetic moment is related only to a spinning electric charge (Bohm 1979, §9.3). Hence the coefficients of the spin-orbit term, while having the same units, are projections of momentum from different mechanisms. Classically monopoles and dipoles have quite different distance dependecies. In Chapter 5 we show that the contribution from the dipole interactions to electron-proton scattering does indeed have a different distance dependence.

We adopt the terminology of calling the Pauli coupling constant the *dipole charge* rather than the *anomalous magnetic moment*, to distinguish it from the ($g = 2$) spin related minimal coupling moment.

2.3 Magnetic Moment and Dipole Charge Value

The experimentally measured magnetic moments for the electron, the proton and the neutron are known to 9 or 10 significant figures (CRC 1984, Cohen and Taylor 1986). They vary widely in magnitude ($\mu_{\rm B}$ = Bohr magneton, $\mu_{\rm N}$ = Nuclear magneton)

$$\left.\begin{array}{rcrcrcl} \mu_{\exp_e} &=& -1838.2807\ \mu_{\rm N} &=& -1.001596\ \mu_{\rm B} &=& -862.02096\ \frac{\alpha}{2\pi}\mu_{\rm B} \\ \mu_{\exp_p} &=& +2.7928456\ \mu_{\rm N} &=& +0.00152103221\ \mu_{\rm B} &=& +1.3096430\ \frac{\alpha}{2\pi}\mu_{\rm B} \\ \mu_{\exp_n} &=& -1.9159410\ \mu_{\rm N} &=& -0.00104345471\ \mu_{\rm B} &=& -0.8984380\ \frac{\alpha}{2\pi}\mu_{\rm B} \end{array}\right\} \tag{2.16}$$

The minimal coupling or Dirac magnetic moments vary similarly ($\mu_{{\rm D}i} = \frac{q_i}{2m_i}$)

$$\left.\begin{array}{rcrcrcl} \mu_{{\rm D}e} &=& -1836.15152\ \mu_{\rm N} &=& -1.0\ \mu_{\rm B} &=& -861.022516\ \frac{\alpha}{2\pi}\mu_{\rm B} \\ \mu_{{\rm D}p} &=& +1.0\ \mu_{\rm N} &=& +0.000544617\ \mu_{\rm B} &=& +0.46892751\ \frac{\alpha}{2\pi}\mu_{\rm B} \\ \mu_{{\rm D}n} &=& 0.0 & & & & \end{array}\right\} \tag{2.17}$$

Taking the differences between these moments, we see that the dipole charges, in contrast to the above, have very similar magnitudes

$$\left.\begin{array}{rcl} \mu_{{\rm a}_e} &=& -0.99844240\ \frac{\alpha}{2\pi}\mu_{\rm B} \\ \mu_{{\rm a}_p} &=& +0.84071547\ \frac{\alpha}{2\pi}\mu_{\rm B} \\ \mu_{{\rm a}_n} &=& -0.898438\ \frac{\alpha}{2\pi}\mu_{\rm B} \end{array}\right\} \tag{2.18}$$

It is extremely interesting that the dipole charges should be so close in magnitude for the three particles. Chapter 6 follows up a conjecture that the dipole charge may be a property of the particles (much as the monopole charge) rather than a consequence of other properties (as the Dirac magnetic moment).

Chapter 3

Maximally Coupled Vertex

3.1 Introduction

The vertex operator corresponding to the maximally coupled interaction was first quoted by Rosenbluth in his 1950 paper on electron-proton scattering. Unfortunately he gave no reference to the original derivation of this vertex operator. An extensive literature search has also failed to uncover either a prior or subsequent derivation. I am forced to assume that no derivation has been published, although the operator is generally taken for granted to be as Rosenbluth first quoted it (care needs to be taken when comparing expressions, because Rosenbluth used Feynman's metric conventions).

In Section 3.2 I apply the variational techniques of Landau and Lifshitz (1977) on the maximally coupled Hamiltonian density to derive the maximally coupled vertex operator in a consistent manner. The operator so found has a different sign on the maximally coupled addition to that originally used by Rosenbluth, although the two are otherwise identical expressions. This sign difference is enormously important, as I show in my investigations of it in the following chapters.

In Section 3.3 I propose the Feynman rules for maximally coupled interactions, in the Feynman gauge. The only difference from the usual rules (e.g. Aitchison and Hey, 1984) is in the details of the vertex operator.

3.2 Vertex Operator

In Quantum Field Theory the maximally coupled Dirac operator above (equation 2.15) represents the Hamiltonian of a system of fields. We may treat this operator as a (QFT) Hamiltonian density where the maximally coupled (QFT) Hamiltonian is

$$\mathcal{H}_{\mathrm{M}} = \int \langle \mathrm{f}|\mathrm{O}_{\mathrm{M}}|\mathrm{i}\rangle \mathrm{d}^3x \tag{3.1}$$

$$= \int \langle \mathrm{f}|\not{p} - q\not{A} - m - \tfrac{\mu_{\mathrm{a}}}{2}\not{F}|\mathrm{i}\rangle \mathrm{d}^3x \tag{3.2}$$

Following the variational method of Landau & Lifshitz (1977, pp470–471) we may calculate the response of the (QFT) Hamiltonian to an infinitesimal change, $\delta \mathrm{A}^{\alpha}$, in the potential. The vertex is simply related to this response.

Suppose $A^{\alpha} \rightarrow A'_{\alpha} = A^{\alpha} + \delta A^{\alpha}$, then

$$\mathrm{O_M} \rightarrow \mathrm{O_M}' = \mathrm{O_M} + \delta \mathrm{O_M} \tag{3.3}$$

and

$$\mathcal{H}_{\mathrm{M}} \rightarrow \mathcal{H}_{\mathrm{M}}' = \mathcal{H}_{\mathrm{M}} + \delta \mathcal{H}_{\mathrm{M}} \tag{3.4}$$

Using the antisymmetries of $\sigma_{\alpha\beta}$ and $F^{\alpha\beta}$ we find

$$\delta \mathrm{O_M} = (-q\gamma_{\alpha} - \mu_{\mathrm{a}} \partial^{\beta} \sigma_{\beta\alpha}) \delta A^{\alpha} \tag{3.5}$$

and so the variation in the (QFT) Hamiltonian is

$$\delta \mathcal{H}_{\mathrm{M}} = \int \langle \mathrm{f} | (-q\gamma_{\alpha} - \mu_{\mathrm{a}} \partial^{\beta} \sigma_{\beta\alpha}) \delta A^{\alpha} | \mathrm{i} \rangle \mathrm{d}^3 x \tag{3.6}$$

Changing to momentum space ($\delta^{\beta} \rightarrow -ip^{\beta}$)

$$\begin{aligned} \delta \mathcal{H}_{\mathrm{M}} &= \frac{1}{(2\pi)^3} \int \langle \mathrm{f} | (-q\gamma_{\alpha} + i\mu_{\mathrm{a}} p^{\beta} \sigma_{\beta\alpha}) \delta A^{\alpha} | \mathrm{i} \rangle \mathrm{d}^3 p \\ &= \frac{-1}{(2\pi)^3} \int \langle \mathrm{f} | \left(q\gamma_{\alpha} + \tfrac{\mu_{\mathrm{a}}}{2} (\not{p}\gamma_{\alpha} - \gamma_{\alpha}\not{p}) \right) \delta A^{\alpha} | \mathrm{i} \rangle \ \mathrm{d}^3 p \end{aligned} \tag{3.7}$$

The interaction represented by equation 3.7 is that of a single, maximally coupling particle encountering an electromagnetic field, A^{α}. The 4–momentum, p^{β}, of equation 3.7 is the difference between the final and initial momentum of the particle.

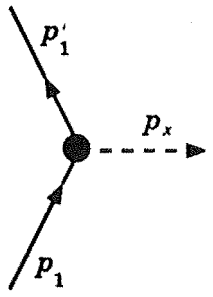

Figure 3.1: Fermion interaction with an electromagnetic field.

Figure 3.1 shows the Feynman diagram of this interaction. Suppose we associate some (unknown) vertex operator, $V_{\alpha}(p)$, corresponding to the vertex shown in Figure 3.1. The amplitude of that diagram is then (following the usual rules, see for example Aitchison & Hey (1984), but leaving the vertex operator general)

$$\mathcal{A}(\alpha : p'_1, p_1, p) = \overline{u}(p'_1) V_{\alpha}(p) u(p_1) \ \varepsilon^{*\alpha}(p, s) \tag{3.8}$$

or, in integral notation

$$\mathcal{A}(\alpha : p_1', p_1, p) = \frac{-i}{(2\pi)^3} \int \langle \mathrm{f}|V_\alpha(p)\varepsilon^{*\alpha}(p,s)|\mathrm{i}\rangle \ \mathrm{d}^3p \tag{3.9}$$

where $\varepsilon^{*\alpha}(p,s)$ is the photon polarization vector (photon leaving the vertex).

Comparing equations 3.9, 3.7 and since $\varepsilon^{*\alpha}(p,s) \equiv \delta A^\alpha$ we can identify the maximally coupled vertex to be

$$V_\alpha(p) = -i\left(q\gamma_\alpha + \frac{\mu_\mathrm{a}}{2}(\not{p}\gamma_\alpha - \gamma_\alpha \not{p})\right) \tag{3.10}$$

Note that the minimally coupled (Dirac) vertex ($-i\,q\gamma_\alpha$) is the simple case of equation 3.10 with $\mu_\mathrm{a} = 0$.

Rosenbluth (1950) calculated the scattering of minimally coupled electrons off maximally coupled protons using a maximally coupled vertex

$$V_\alpha(p)_R = -i\left(q\gamma_\alpha - \frac{\mu_\mathrm{a}}{2}(\not{p}\gamma_\alpha - \gamma_\alpha \not{p})\right) \tag{3.11}$$

which differs from equation 3.10 only in the opposite sign on the anomalous contribution. This is equivalent to a maximally coupled Dirac operator

$$\mathrm{O_M}|_R = \not{p} - q\not{A} - m + \frac{\mu_\mathrm{a}}{2}\not{F} \tag{3.12}$$

3.3 Pauli–Dirac Feynman Rules

A summary of the maximal coupling rules for reading Feynman diagrams describing interactions of spin-$\frac{1}{2}$ particles is shown in Table 3.1. Note that they differ from the usual rules (e.g. Aitchison and Hey 1984) only in the details of the vertex operator.

Symbol	Description	Operator
	particle propagator	$i\frac{\not{p}+m}{p^2-m^2}$
	photon propagator	$\frac{-i}{p_x^2}g_{\alpha\beta}$
	Maximally Coupled Vertex	$-i\left(q\gamma_\alpha+\frac{\mu_a}{2}(\not{p}_x\gamma_\alpha-\gamma_\alpha\not{p}_x)\right)$
	fermion or anti – fermion entering the diagram	$u(p,s)$ or $v(p,s)$
	fermion or anti – fermion leaving the diagram	$\overline{u}(p,s)$ or $\overline{v}(p,s)$
	photon entering or leaving the diagram	$\varepsilon^\alpha(p,\lambda)$ or $\varepsilon^{*\alpha}(p,\lambda)$

Table 3.1: Feynman rules for maximally coupled QED.

Chapter 4

First Order Scattering

4.1 Introduction

In 1949 Feynman first introduced the mathematical tools which have grown to be the 'Feynman' diagram method of describing and analyzing interactions in quantum field theory. His original work on the second order elastic scattering of electrons was extended to cover the non-elastic or Bremstrahlung case in a paper published simultaneously with the first (Schwinger 1949). Feynman's methods have gradually been developed to apply to all quantum fields.

One of the earliest, and spectacularly successful, attempts to extend Feynman's work was by Rosenbluth (1950). Rosenbluth was considering the scattering of energetic electrons off stationary protons at medium energies. Feynman had dealt exclusively with particles interacting via the minimally coupled covariant Dirac operator. Rosenbluth considered the proton to be a particle with some 'intrinsic structure' and so this particle should interact in a way described by the modified Pauli–Dirac or maximally coupled covariant Dirac operator. Practically this meant Rosenbluth introduced a different vertex for the proton, which included this maximally coupled effect.

The results from this work were very important. Not only was a better agreement with experiment available immediately, but since there were now two coupling constants, it was possible to formulate two independent modifiers in such a way that by judicious, if arbitrary, choice of these 'form factors', the bare theoretical prediction could be forced into even better agreement with experiment. These modifiers, after some manipulation and re-combinations have become known as the 'charge' and 'magnetic' form factors. They are fitted phenomenologically to the data, and their interpretation has lead to many insights into the structure and fundamental nature of particles. One of the more obvious early applications was in deriving proton and neutron 'radii' (e.g. Hofstadter et al 1958). They are still in use (see for example Donnelly and Raskin, 1986). I postpone a full discussion of the effect maximally coupled QED has on the use and interpretation of these form factors until Chapter 5.

I showed in Chapter 3 that Rosenbluth began his analysis with a sign error for the maximal

coupling contribution, which must be of critical importance to the interpretation and application of form factors. This aspect also is discussed in Chapter 3, but a full discussion is postponed to Chapter 5 after looking in more detail at the contributions from the various terms to maximally coupled scattering cross-section.

With the advent of computer algebra systems it is now possible to perform a complete first order calculation of the scattering cross-section for both particles maximally coupled to the interaction. This would have been a long and tedious undertaking previously.

I review the general methods required to derive the spin averaged matrix element in Section 4.2. Using these methods and the algebraic processing package REDUCE 3.2, in Section 4.3 I calculate the complete first order maximal coupling matrix element and hence cross-section for two non-identical fermions. The expression I obtain is essentially that obtained previously by Hubert (1984) using Rosenbluth's vertex. The two expressions are identical aside from the sign of the dipole charge. My full expression is compared to experiment in Section 4.4. These results have been published recently (Burling–Claridge and Butler, 1989).

4.2 Spin Averaging

The Feynman diagram Figure 4.1, describing a first order interaction, has a maximally coupled amplitude (following the rules of Table 3.1)

$$\mathcal{A}_{\mathrm{M}} = \frac{-1}{{p_x}^2}\, \overline{u}(p_1')V_{1\alpha}(p_x)u(p_1)\; \overline{u}(p_2')V_2{}^{\alpha}(-p_x)u(p_2) \tag{4.1}$$

where we leave the vertices in their general form for the moment.

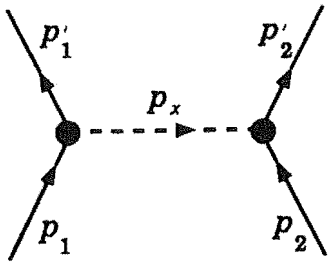

Figure 4.1: Feynman diagram describing first order scattering.

The maximally coupled matrix element is

$$\mathcal{M}_{\mathrm{M}} = \mathcal{A}_{\mathrm{M}}{}^{\dagger}\mathcal{A}_{\mathrm{M}} \equiv \mathcal{A}_{\mathrm{M}}\mathcal{A}_{\mathrm{M}}{}^{\dagger} \tag{4.2}$$

It is simply verified that in general

$$\Big(\overline{u}(p)V_{i\alpha}(p')u(p'')\Big)^{\dagger} \equiv \overline{u}(p'')V_{i\alpha}(-p')u(p) \tag{4.3}$$

and so (the leg 1 variables commute with the leg 2 variables)

$$\begin{aligned}\mathcal{M}_{\rm M} = \frac{1}{{p_x}^4}\, &\overline{u}(p_1')V_{1\alpha}(p_x)u(p_1)\overline{u}(p_1)V_{1\beta}(-p_x)u(p_1') \\ &\times \overline{u}(p_2')V_2{}^{\alpha}(-p_x)u(p_2)\overline{u}(p_2)V_2{}^{\beta}(p_x)u(p_2')\end{aligned} \tag{4.4}$$

Since we are interested in the unpolarised scattering of particles, we assume that we do not know the initial polarizations and we will not measure the final polarizations of the particles. (The spin dependence can be retrieved if desired by using a spin projection operator $(1-\gamma^5)s_i$ to project out the particular spin (s_i) dependencies required.) Hence the cross–section measured will be a sum over the final spin polarization states and an average over the $(2s_1+1)(2s_2+1) = 4$ initial polarization states.

To evaluate the matrix element we employ the spin averaging identities

1. Any products $u(p)\overline{u}(p)$ may be replaced by their projection operators

$$u(p)\overline{u}(p) \to \rho(p) = \tfrac{1}{2}\,(\not{p}+m)$$

2. For any F, (Berestetskii et al, 1971, §29)

$$\sum^{pol} \overline{u}(p)F\,u(p) = tr[(\not{p}+m)F]$$

Thus the matrix element can be expressed as a product of traces

$$\begin{aligned}\mathcal{M}_{\rm M} = \frac{1}{4{p_x}^4}\, &tr\left[(\not{p}_1{}' + m_1)V_{1\alpha}(p_x)(\not{p}_1 + m_1)V_{1\beta}(-p_x)\right] \\ &\times tr\left[(\not{p}_2{}' + m_2)V_2{}^{\alpha}(-p_x)(\not{p}_2 + m_2)V_2{}^{\beta}(p_x)\right]\end{aligned} \tag{4.5}$$

4.3 Electron–Proton Scattering

Let us consider scattering electrons off protons in the laboratory frame. A stationary proton target (denoted as particle 2) is struck by a beam of electrons (particle 1). The electrons are deflected through some angle, θ_1, from their original direction.

In this case

$$\begin{aligned} p_2 &= 0 \quad &\Rightarrow\ E_2 = m_2 \\ {p_1}^2 &= {p_1'}^2 \quad &= {m_1}^2 \\ p_1.p_1' &= E_1E_2 \end{aligned} \tag{4.6}$$

In the rest frame of the proton (laboratory frame), the scattering cross–section is (Aitchison & Hey 1984, Chapter 2 and Appendix E)

$$\left.\frac{{\rm d}\sigma}{{\rm d}\Omega}\right|_{Lab} = \frac{1}{(8\pi)^2}\frac{{E_1'}^2}{{E_1}^2{m_2}^2}\mathcal{M} \tag{4.7}$$

where $\mathcal{M}$ is the matrix element calculated from the Feynman diagram(s) describing the interaction (see Section 4.2). We have in general (Landau & Lifshitz, 1975, §13)

$$E_1' = \frac{(E_1 + m_2)(E_1 m_2 + {m_1}^2) + m_2 \cos\theta_1 ({E_1}^2 - m_1^2)\sqrt{1 - \frac{m_1}{m_2}\sin^2\theta_1}}{(E_1 + m_2)^2 - ({E_1}^2 - {m_1}^2)\cos^2\theta_1} \tag{4.8}$$

At the moment we restrict our attention to the first–order interaction, for which there is the single Feynman diagram of Figure 4.1. The matrix element corresponding to this diagram is derived above (equation 4.5). We perform the traces using the algebraic processing package REDUCE 3.2, first substituting the maximal coupling vertex (equation 3.10) and then simplifying using the Mandelstam invariants (definition 21, Section 1.2).

Thus, finally, the maximally coupled first order elastic scattering matrix element for any two distinguishable fermions, where particle 2 is in the laboratory rest frame, is

$$\begin{aligned}
\mathcal{M}_M = \frac{1}{16t^2}\Big\{ & 2q_1^2 q_2^2 \left(2(s-(m_1^2+m_2^2))^2 + (s+t)^2 - s^2\right) \\
& + \mu_1^2\mu_2^2\, t^2 \left(4(s-(m_1^2+m_2^2))^2 + (2s+t)^2 - 4s^2 + 16m_1^2 m_2^2\right) \\
& + 4\mu_1^2 q_2^2\, t \left((2(m_1^2+m_2^2)-t)s + (2m_1^2+m_2^2)t - s^2 - (m_1^2-m_2^2)^2\right) \\
& + 4\mu_2^2 q_1^2\, t \left((2(m_1^2+m_2^2)-t)s + (m_1^2+2m_2^2)t - s^2 - (m_1^2-m_2^2)^2\right) \\
& - 4\mu_1^2\mu_2 q_2\, t^2 m_2 (8m_1^2 + t) \\
& - 4\mu_1\mu_2^2 q_1\, t^2 m_1 (8m_2^2 + t) \\
& + 48\mu_1\mu_2 q_1 q_2\, t^2 m_1 m_2 \\
& - 8\mu_1 q_1 q_2^2\, t m_1 (2m_2^2 + t) \\
& - 8\mu_2 q_1^2 q_2\, t m_2 (2m_1^2 + t)\Big\}
\end{aligned} \tag{4.9}$$

Note that

1. The Dirac matrix element is simply equation 4.9 with $\mu_1 = \mu_2 = 0$.
2. Rosenbluth's (1950) matrix element can be extracted from equation 4.9 (after the routine struggle of changing parameters and frames) by substituting $m_1 = 0$, $\mu_1 = 0$ and (see Section 3.2) $\mu_2 \to -\mu_2$.
3. Hubert's (1984) expression is just equation 4.9 with $\mu_a \to -\mu_a$ and the Mandelstam invariant $u = (p_2' - p_1)^2$ expressed in terms of the other two Madelstam invariants using the identity $s + t + u = 2(m_1^2 + m_2^2)$.

4.4 Comparison with Experiment

Figures 4.2–4.6 show comparisons between experimental results and several theoretical predictions for the scattering of electrons off stationary (laboratory frame) protons

The experimental results are taken from:

Albrecht et al (1966, 1967); Bartel et al (1966, 1967, 1970); Behrend et al (1967); Berger et al (1968, 1971); Berkelman et al (1963); Bumiller et al (1960, 1961); Chen et al (1963, 1966); Chambers and Hofstadter (1956); Dunning et al (1963); Goiten et al (1970, preliminary results in 1967); Hand (1960); Kirk et al (1973); McAllister and Hofstadter (1956).

The following curves are plotted (NB: these figures have been re–drawn but are essentially just those shown in Burling–Claridge and Butler (1989), Figures 3–7):

1	†	Experimental points showing error estimates, sources as above.
2	————	Maximally coupled scattering: Our vertices
3	—— - ——	Maximally coupled scattering: Rosenbluth's vertices.
4	- - - - - - -	Proton only maximally coupled (Rosenbluth model): Our vertex.
5	—— ——	Rosenbluth model: Rosenbluth's vertex (Duplicates Rosenbluth's original 1950 result).
6	— — — —	Rosenbluth's original results, with form factors.
7	— - - —	Minimally coupled scattering (Möller scattering).

In all of the plots, the original Rosenbluth cross–section (—— ——) is larger than the experimental results. The maximally coupled cross–section (————) has much the same property but is always in better agreement than the Rosenbluth cross–section. Notice that at 188 MeV the maximally coupled cross–section is within two experimental uncertainties.

The original Rosenbluth cross–section, but with form factors to fit this curve to experimental results (— — — —), is still in use, see for example Donnelly and Raskin (1986). Recall that the Rosenbluth model treats only the proton as being maximally coupled in the interaction. We can see immediately from Figures 4.2–4.6, that with our vertex (- - - - - - -) this model deviates only slightly from the Dirac result (— - - —). That is, the interaction between the dipole charge of the proton and the electric monopole charge of the electron is of little importance in this energy range, but see Chapter 5.

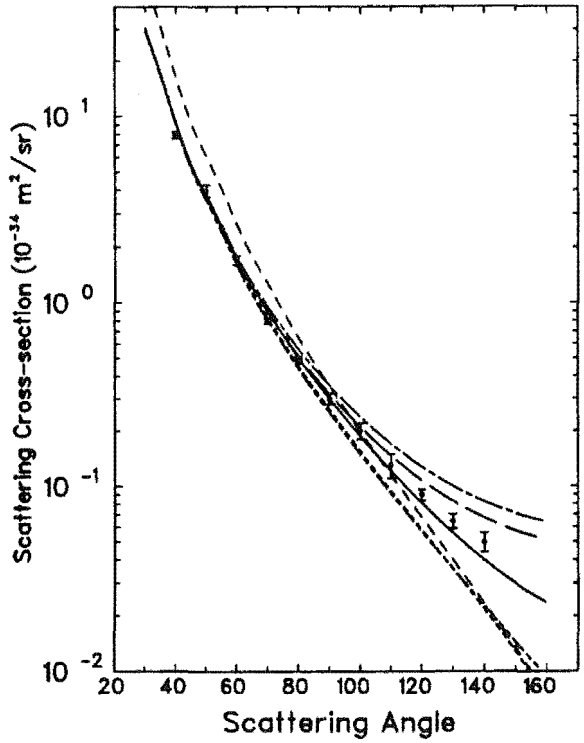

Figure 4.2: First order scattering of electrons off protons: laboratory frame, electron beam energy 188 MeV.

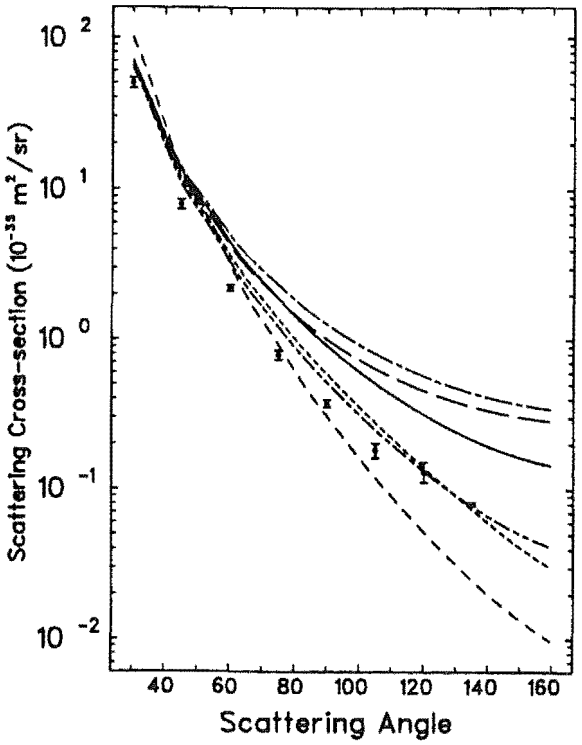

Figure 4.4: First order scattering of electrons off protons: laboratory frame, electron beam energy 400 MeV.

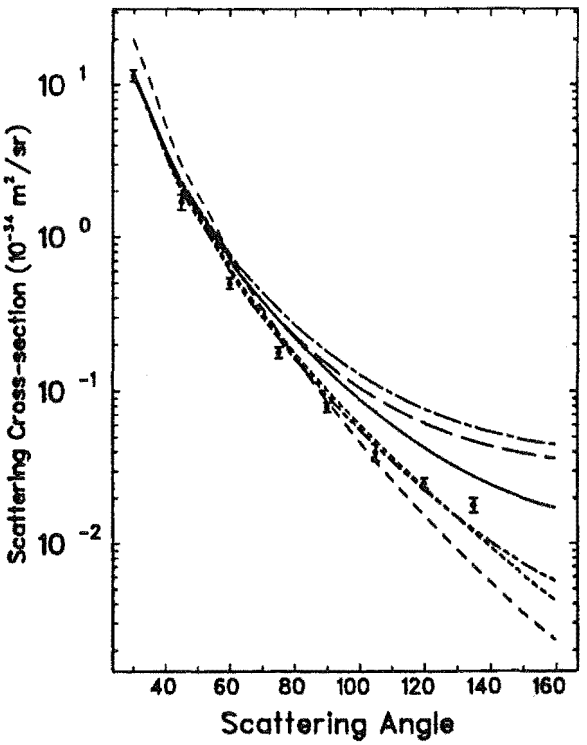

Figure 4.3: First order scattering of electrons off protons: laboratory frame, electron beam energy 300 MeV.

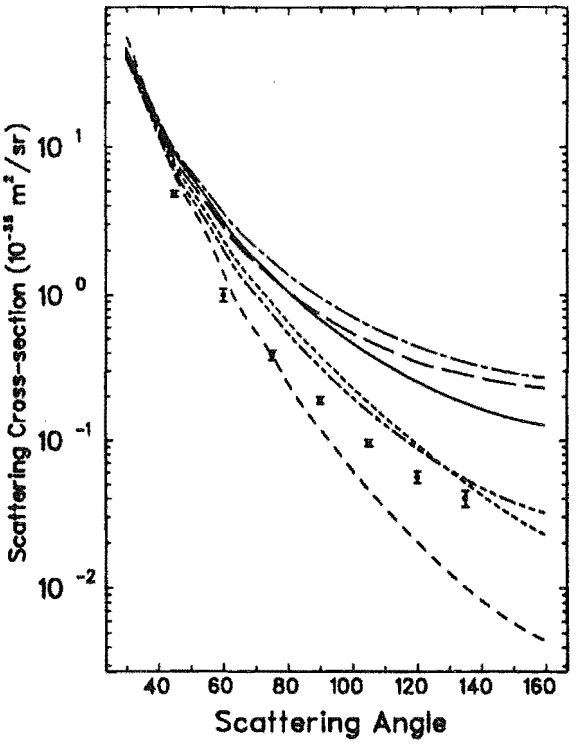

Figure 4.5: First order scattering of electrons off protons: laboratory frame, electron beam energy 500 MeV.

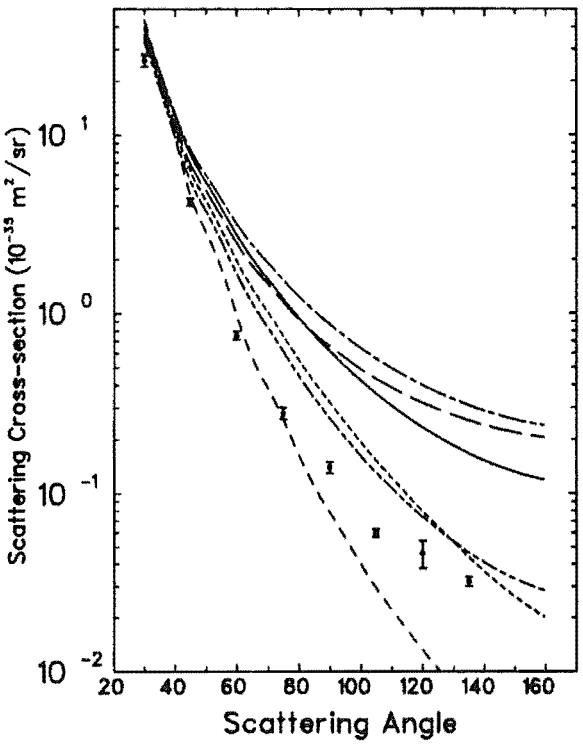

KEY: Figures 4.2–4.6

1 — Experimental Results
2 — Maximally coupled scattering: Our vertices
3 — Maximally coupled scattering: Rosenbluth's vertices
4 — Rosenbluth model: Our vertices
5 — Rosenbluth model: Rosenbluth's vertices
6 — Rosenbluth model: Rosenbluth's vertices with form factors
7 — Minimally coupled scattering

Figure 4.6: First order scattering of electrons off protons: laboratory frame, electron beam energy 550 MeV.

Chapter 5

Energy Dependence and Form Factors

5.1 Introduction

I now take a detailed look at the first-order scattering of Chapter 4. The Rosenbluth model using the maximally coupled vertex derived here has been shown to differ only negligibly from minimal coupling. Including the electron dipole charge (and hence the dipole–dipole and electron dipole–proton monopole terms) leads to a far better agreement with experiment.

In this Chapter I investigate the relative importance of the various cross–terms (monopole–dipole, etc). This gives a direct insight into the underlying mechanism(s) of the interaction itself, and allows me to investigate the validity of the form factor approach to fitting the theoretical predictions to experiment. The data allows me to also test the validity of the Rosenbluth model in general.

Rosenbluth's assumption (for his model which treats only the proton as being maximally coupled) was that the electron's dipole charge could be neglected since its effect was (Rosenbluth 1950, footnote 2) "...quite small and decreases rapidly at high energy". The further analysis in the literature of Rosenbluth's original result has focused on the physical interpretation of the proton's dipole charge. Rosenbluth originally attempted to derive structure constants (form factors) from considering the action of the proton's virtual meson field. This attempt was not altogether successful and the form factors used by later researchers to fit his theoretical curve to the experimental results are phenomenological in nature. The form factors, however, are still assumed to be based, in principle, on the spatially distributed nature of the proton. Implicitly these form factor analyses assume the electron to be a point particle, and to have no contribution to the scattering via it's dipole charge.

The widespread use of these form factors, as discussed above, is justified in terms of a model of an electron with: point monopole (electric) charge; zero dipole charge; point

mass; virtual photon and/or electron-positron pair cloud and a proton with spatially distributed mass; monopole charge and dipole charge; virtual cloud of mesons (or composed of quarks, etc). This has lead to the belief that the dipole charge can only be the result of real monopole charge (and monopole current) distributions. There is an inconsistency with this viewpoint in that both the electron and the proton are considered to be distributed particles, yet only the monopole charge distributions of the proton are considered. Furthermore, as I showed in Chapter 2, the electron dipole charge is slightly larger than the proton.

The electron dipole charge is usually ignored since, among other considerations, there appears to be no physical mechanism that would account for it, e.g. spatially distributed monopole charge or cloud of virtual particles which themselves have dipole charges. This argument can be seen to be somewhat circular. Further, it conflicts with the treatment of the intrinsic angular momentum of point particles. Particles usually regarded as non-composite (e.g. the electron) or both non-composite and massless (e.g. the neutrino), nevertheless have a non-zero moment of their momentum about their centre: their intrinsic spin. Some of the conceptual and philosophical issues raised by this treatment of intrinsic spin are discussed by Biedenharn and Louck (1981, pp1–26), amongst many others.

Chambers and Hofstadter (1956) considered the scattering of electrons off protons at various electron beam energies between 200 and 550 MeV. They showed by transforming from momentum space, that one could derive a charge distribution from the phenomenological form factors required to fit the raw theoretical (Rosenbluth model) curve to experiment. From the charge distribution, one may extract an 'rms radius' and it is not unreasonable to attach this radius to the charge distribution of the real photon. For the energies Chambers and Hofstadter looked at, the best fit to the required form factors was a hollow exponential (re^{-r}) model for the potential with an rms radius 0.78×10^{-13} cm, although very similar accuracy was obtained for Gaussian (e^{-r^2}) and exponential (e^{-r}) distributions with similar rms radii.

At higher energies (see for example Kirk et al (1973), 4–17 GeV electron beam energy) a quite different model from those considered by Chambers and Hofstadter is required. Kirk et al concluded that "...although there is some success in analytic fitting of the data, ...more work is needed before the electromagnetic form factors of the proton are understood at a fundamental level."

Form factors have a wide importance beyond the narrow area of QED electron-proton scattering, and their theoretical interpretation has led to advances in many fields: (Omnès 1971, p380)

> "The development of our present theory of strong interactions has been much influenced by measurement of form factors and their theoretical interpretation."

I show here that Rosenbluth's model can not be justified for either choice of vertex. This has important ramifications for the theoretical basis underlying the approach of developing phenomenological form factors to fit the theoretical expression to the experimental situation. I discuss some of the difficulties in attempting to apply the form factor approach to

maximally coupled interactions in Section 5.3.

5.2 Graphical Comparisons

There are 3 terms that arise from including maximal coupling

- X_1 : Electron monopole charge $\times$ proton dipole charge.
- X_2 : Electron dipole charge $\times$ proton monopole charge.
- X_3 : Electron dipole charge $\times$ proton dipole charge.

We wish to investigate the relative importance of these additional scattering effects, for both choices of vertex. The magnitudes of the various terms vary enormously and some of them change sign over the range of angles we are investigating. Accordingly we have plotted them by first adding the Möller scattering to each. Contrasting the resulting curves to the Möller and the maximally coupled curves will allow us to extract much information about the relative magnitudes and hence importances of the maximally coupled terms. These comparisons are shown in Figures 5.1–5.6

With our vertex, the Rosenbluth model (Möller + X_1) differs little from Möller scattering at any angle (Figures 5.1, 5.4). The other monopole-dipole term (X_2) however, is comparable in magnitude to the Möller scattering at most angles and indeed dominates the scattering for large angles (Figures 5.2, 5.5). This is the opposite behavior from that assumed by the Rosenbluth model, which ignores the X_2 term as being negligible (in comparison to both Möller scattering and the X_1 term).

With Rosenbluth's vertex the two monopole-dipole terms are of comparable magnitude, but importantly they are both of similar or larger magnitude to the Möller scattering terms for large angles.

The reason the dipole-monopole terms dominate at the higher angles is due to the different radial dependence of the dipole and monopole potentials, discussed in Section 1.1. The 'distance of closest approach' is closely related to the scattering angle. At small deflections angles, and hence relatively large approach distances, the scattering is almost entirely monopole-monopole only, whereas for large scattering angles the dipole interactions dominate the scattering.

There is little difference in the magnitude of the dipole-dipole term between the choices of vertex. The dipole-dipole contribution (X_3, Figures 5.3, 5.6) is small at these angles, but there is slightly more effect for the higher beam energy. As can be seen from equation 4.9, for higher exchange momentum (t) the dipole-dipole terms will be increasingly important.

Let us investigate the region where the dipole-dipole terms begin to dominate over the monopole-monopole interaction. The monopole-monopole and dipole-dipole terms of equation 4.9 are very similar, (re-expressing to show this more clearly, $M = m_1^2 + m_2^2$)

$$\begin{aligned} \mathcal{M}_M = \ldots \quad & \Big\{ q_1^2 q_2^2 \left(4s^2 - 8Ms + 4M^2 + 4st + 2t^2\right) \\ + \quad & \mu_1^2 \mu_2^2 t^2 \left(4s^2 - 8Ms + 4M^2 + 4st + t^2 + 16 m_1^2 m_2^2\right) \\ & \ldots \Big\} \end{aligned} \tag{5.1}$$

If we approximate the dipole charges by simply $\frac{\alpha}{2\pi}\mu_{\mathrm{B}}$, and note that $\alpha = e^2$ then (see Section 2.3)

$$\begin{aligned} \mu_{\mathrm{a}} \times m_p &\approx \frac{\alpha}{2\pi} \times \frac{e}{2m_e} m_p \\ &\approx \frac{e^3}{2\pi} m_p \\ &\approx e \end{aligned}$$

and hence when $t \approx m_p^2$

$$q_1^2 q_2^2 \approx \mu_1^2 \mu_2^2 t^2 \tag{5.2}$$

Thus, whenever the exchanged momentum is much larger than the proton rest mass there will be a transition from monopole-monopole to dipole-dipole dominance of the scattering.

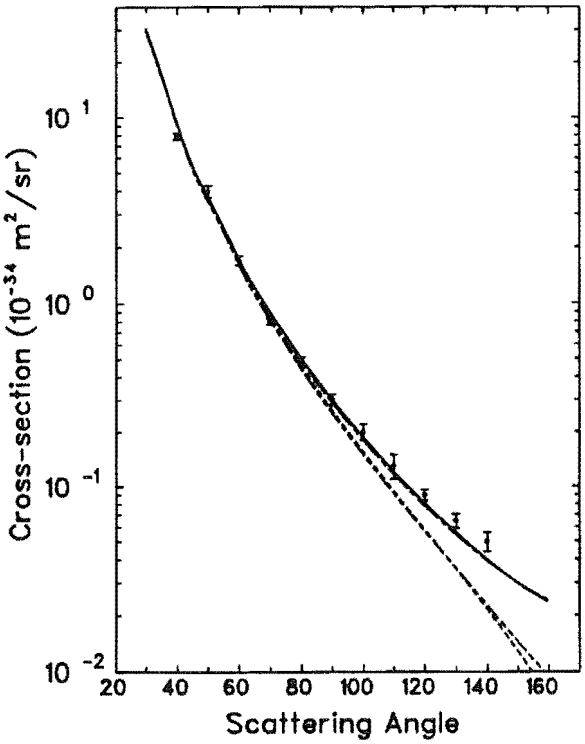

Figure 5.1: Contributions to the scattering from the monopole-dipole terms, our vertex, 188 MeV.

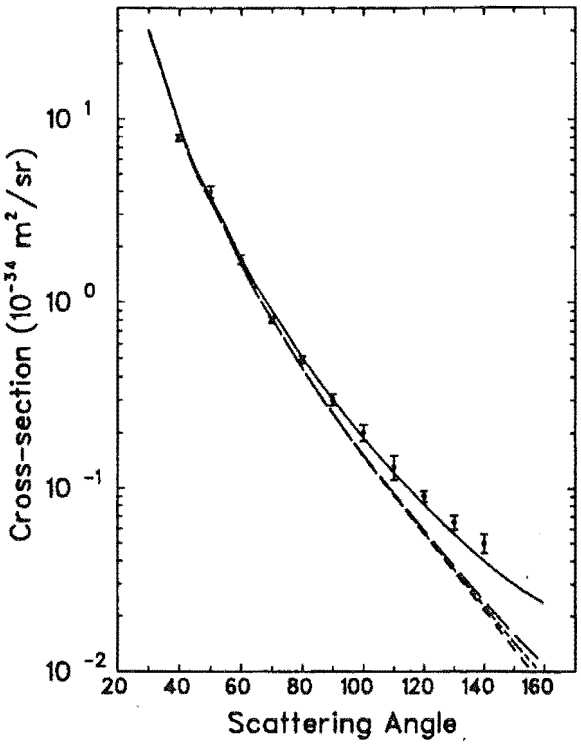

Figure 5.3: Contributions to the scattering from the dipole-dipole terms, 188 MeV.

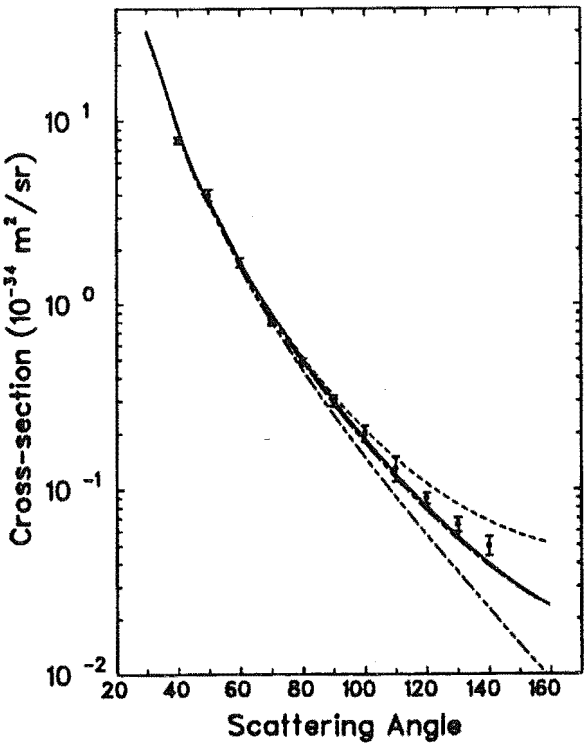

Figure 5.2: Contributions to the scattering from the monopole-dipole terms, Rosenbluth's vertex, 188 MeV.

KEY:

1 † Experimental points with uncertainties.

2 ——— Complete maximally coupled prediction of Section 4.4.

3 - - - - - - - X_1: contributions from $q_e \times \mu_p$.

4 —— - —— X_2: contributions from $\mu_e \times q_p$.

5 —— —— X_3: contributions from $\mu_e \times \mu_p$, our vertex.

6 — — — — X_3: contributions from $\mu_e \times \mu_p$, Rosenbluth's vertex.

7 —— - - —— Minimally coupled scattering, see Section 4.4

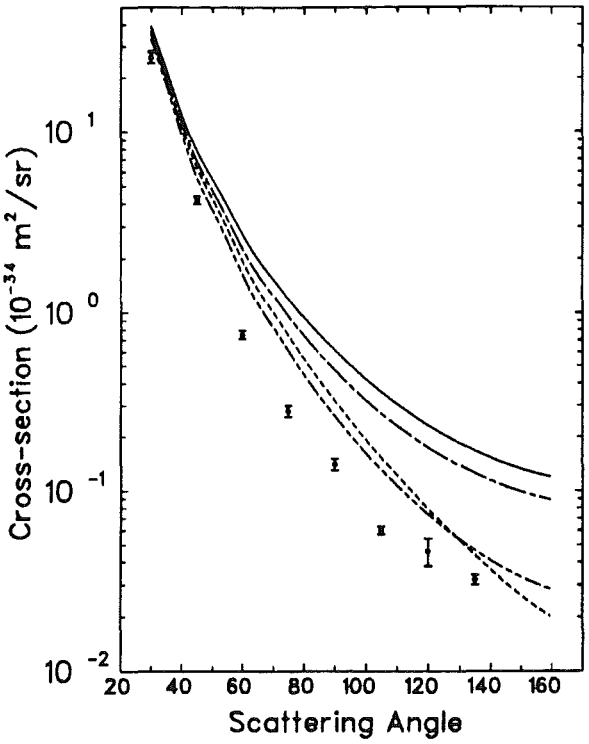

Figure 5.4: Contributions to the scattering from the monopole-dipole terms, our vertex, 550 MeV.

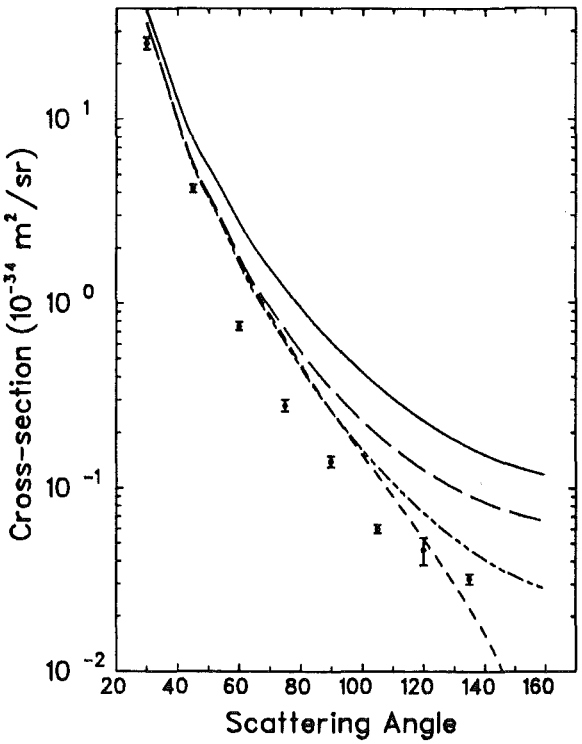

Figure 5.6: Contributions to the scattering from the dipole-dipole terms, 550 MeV.

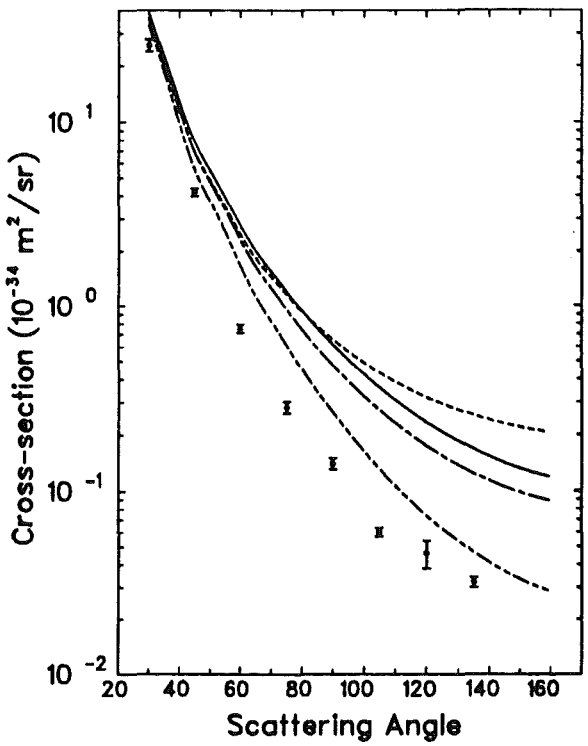

Figure 5.5: Contributions to the scattering from the monopole-dipole terms, Rosenbluth's vertex, 550 MeV.

KEY:

1 — Experimental points with uncertainties.

2 ——— Complete maximally coupled prediction of Section 4.4.

3 - - - - - - X_1: contributions from $q_e \times \mu_p$.

4 —— - —— X_2: contributions from $\mu_e \times q_p$.

5 —— —— X_3: contributions from $\mu_e \times \mu_p$, our vertex.

6 — — — — X_3: contributions from $\mu_e \times \mu_p$, Rosenbluth's vertex.

7 —— - - —— Minimally coupled scattering, see Section 4.4

5.3 Conclusions

The Rosenbluth model (proton only maximally coupled) can not be justified for either choice of vertex. We have shown in Chapter 3 there is serious question as to the accuracy of Rosenbluth's original vertex and hence his scattering cross-section. Further, this chapter has shown that the Rosenbluth model fails in its second assumption: the electron contribution being negligible, and decreasing rapidly at higher energies. Indeed, we have shown that for either sign the dipole-dipole contribution dominates over the monopole-monopole contribution for large exchange momenta.

The relative magnitudes of the terms comprising the maximally coupled addition, along with the above observation, have shown that the dipole interactions, regardless of choice of vertex, have a different angular dependence from the monopole-monopole interaction. This proves that the dipole and monopole interactions have different radial dependencies. The fundamental reasons for this were discussed in Chapter 2.

A re-evaluation of the form factors in the light of this new knowledge may be possible. However, the electron is generally regarded as a non-composite particle of very small size ($\ll$ proton size). A different philosophical justification for form factors applying to the electron would need to be developed.

These results call into question the main precepts of the form factor approach. At the least, the form factor methods will need re-evaluating if they are to remain valid procedures for maximally coupled QED.

Chapter 6

Neutron Decay

6.1 Introduction

The Feynman diagram method can be used to describe particle decay as well as particle interactions. Indeed the diagram technique implicitly deals with decays: at any vertex an incoming particle 'decays' into an outgoing particle and a photon.

The monopole charge of the outgoing particle must be precisely that of the incoming particle since the photon can carry only spin and momentum. The outgoing spin may be either the same as that of the incoming particle, or flipped ($\Delta s_z = 0, \pm 1$).

The other conserved quantity at any vertex is the momentum. In particular the *rest mass* of the incoming particle need not be conserved. In other words, the outgoing and incoming articles need not have the same 'identity'.

Although in minimally coupled QED one can show that gauge invariance implies mass conservation, I have shown in the previous chapters that some of the assumptions and developments that are accepted as valid for minimally couple QED do not transfer well into the extended maximally coupled QED model. The maximally coupled model has the extra coupling constant, the dipole charge. This has been added in a gauge invariant way and it seems reasonable that it might also be conserved. This could allow the possibility of the rest mass not being conserved, while still preserving gauge invariance. Showing this explicitly is beyond the present scope of this research. In this chapter I postulate that maximally coupled QED has an explicit conservation of monopole and dipole charge, but that the rest mass need not be conserved through the interaction.

Thus I may describe a three particle decay (three particles in the final state, none of them the original particle) by the diagram of Figure 6.1, where I then need to identify appropriately the particles corresponding to the legs and I am not constrained to having the 'same' particle on both legs of any vertex.

I now make use of the fact (see Section 2.3) that the dipole charges for the electron, the proton and the neutron have very similar magnitudes. In Section 6.2 I follow the speculation of my supervisor and assume that these values are in fact identical, and equal

to a 'quantized' value. This 'quantization' allows me to apply Figure 6.1 to neutron decay.

If I use the maximally coupled vertices in my analysis of Figure 6.1, I may then perform an analysis of neutron decay which will give a finite lifetime, since the dipole charge of the neutron is non-zero. A minimally coupled analysis must give an infinite lifetime because, the neutron having no electric charge, there will be no coupling of the neutron to its decay products.

The dominant decay mode for the neutron is

$$n \rightarrow p^+ + e^- + \overline{\nu}_e \tag{6.1}$$

Given the 'quantization' of Section 6.2, as discussed above, I may apply Figure 6.1 where the monopole free particles (n, $\overline{\nu}_e$) are on the left leg and the monopole charged particles (p, e) on the right.

This approach views neutron decay as the neutron decaying first into an anti-neutrino and an energetic, virtual, photon which subsequently decays into an electron-proton doublet. The mathematical tools for dealing with such diagrams are well developed.

Experimentally the lifetime of the neutron is determined in one of two ways

1. Measuring the rate of production of β^- particles from a sample.
2. Measuring the remaining amount of neutrons within a sample.

Byrne (1988) reviews this field (see also Wilkinson, 1982) and shows the experimentally determined lifetime steadily decreases to the then most recent value (Last et al, 1988, using the first of the above methods) $\tau_n = 876 \pm 21$ sec. However, more recent work (Mampe et al 1989, using the second method) has found a lifetime $\tau_n = 887 \pm 3$ sec.

In Section 6.7 I discuss the re-evaluation of the Last et al lifetime using a maximally coupled QED model rather than the electro-weak model of Glashow, Salam and Weinberg that was employed. The maximally coupled lifetime is very sensitive to the value chosen in Section 6.2 for the quantized dipole charge. I discuss some of the aspects of this in Section 6.6.

6.2 Quantization

As discussed above, to describe the decay of a single particle into three particles we may use a diagram such as Figure 6.1. We have relaxed the conservation of rest mass along a fermion line and instead we require the dipole charge to be conserved along any fermion line. Hence any two particles connected across a maximal vertex must have the same dipole charge. We are postulating that the dipole charge is an intrinsic property of the particle, and exists only in discrete, quantized values, in a similar sense to the monopole (electric) charge.

As previously shown (Section 2.3) the dipole charges of the electron, the proton and the neutron differ in magnitude by only 10–15%. Let us somewhat arbitrarily assume that each

of these particles (and their anti–particles) have a 'quantized' dipole charge, $\mu_Q = \frac{\alpha}{2\pi}\mu_B$, so that

$$\left.\begin{array}{rcl} \mu_Q & = & \frac{\alpha}{2\pi}\mu_B \\ \mu_{a_e} & = & -\mu_Q \\ \mu_{a_p} & = & +\mu_Q \\ \mu_{a_n} & = & -\mu_Q \\ \mu_{a_{\overline{\nu}_e}} & = & -\mu_Q \end{array}\right\} \tag{6.2}$$

We make this choice since the dipole charge of the electron is the best understood and it can be obtained from the next highest order of a minimally coupled theory to very close agreement with the experimentally measured value.

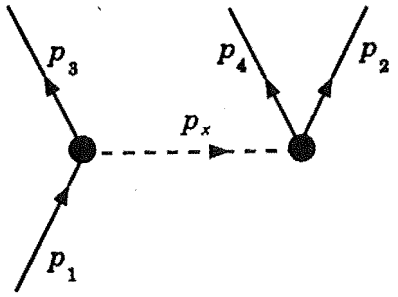

Figure 6.1: Tree diagram of 3–particle decay.

The last dipole charge of equation 6.2, that of the electron anti–neutrino, has not yet been experimentally determined. Our choice of this value for it's dipole charge implies a neutrino g–factor $< 6 \times 10^{-8}$, since $m_{\overline{\nu}_e} \leq 30\ eV$. Solar neutrino models (e.g. Voloshin et al, 1986) argue for a somewhat smaller value ($\mu_{a_{\overline{\nu}_e}} \sim 10^{-11} - 10^{-10}\mu_B$), but that work relies on a long series of assumptions and is, at present, unconfirmed by any more direct measurements.

6.3 Phase Space

The decay rate, Γ, for any channel, c, is defined most generally as

$$\Gamma_c = \frac{1}{2m_1}\int \mathcal{M}\ \mathrm{dLips}(s : p_2, p_3, p_4) \tag{6.3}$$

where m_1 = mass of the initial particle,
$\mathcal{M}$ = the matrix element of the decay, calculated from the Feynman amplitude(s), $\mathcal{A}_n$, of the diagram(s) describing the decay and
dLips(...) = Lorentz invariant element of phase space.

Pilkuhn (1979) gives detailed examples of calculating the general decay rate for the decay of a single particle into three particles. In Section 4.6 of his text he evaluates dLips(s : p_2, p_3, p_4) in the rest frame of the initial particle ($s = m_1^2$) to be

$$\mathrm{dLips}(s : p_2, p_3, p_4) = \frac{1}{\pi(4\pi)^4}\mathrm{d}E_2\mathrm{d}E_3\mathrm{d}E_4\delta(m_1 - E_2 - E_3 - E_4)\mathrm{d}\Omega_4\mathrm{d}\phi \tag{6.4}$$

The angle ϕ and the solid angle Ω_4 define the orientation of the momentum plane formed by the 3–vectors of the decay product particles: $\boldsymbol{p}_2$, $\boldsymbol{p}_3$, $\boldsymbol{p}_3$. The evaluation is in the rest frame of the decay particle, where

$$\boldsymbol{p}_2 + \boldsymbol{p}_3 + \boldsymbol{p}_3 = 0 \tag{6.5}$$

The spin averaged matrix element is independent of ϕ, Ω_4, hence the ϕ, Ω_4 integrals may be trivially performed

$$\int \mathrm{d}\phi \; \mathrm{d}\Omega_4 = \int_0^{\pi} \mathrm{d}\phi \int_0^{4\pi} \mathrm{d}\Omega = 4\pi^2 \tag{6.6}$$

The δ function, describing the physical constraint of overall energy conservation, may be used to remove any of the three energy integrals as convenient. We choose to perform the integration over E_4 (the proton energy) first and so

$$\mathrm{dLips}(s : p_2, p_3, p_4) = \frac{1}{(4\pi)^3} \mathrm{d}E_2 \mathrm{d}E_3 \tag{6.7}$$

with the constraint that $E_4 = m_1 - E_2 - E_3$. The decay rate is now an integral over the energies E_2, E_3.

The limiting values of E_2, E_3 occur when $\boldsymbol{p}_2$, $\boldsymbol{p}_3$, $\boldsymbol{p}_4$ are co–linear,

$$|\boldsymbol{p}_2| \pm |\boldsymbol{p}_3| \pm |\boldsymbol{p}_4| = 0 \tag{6.8}$$

Successive squaring of equation 6.8 and a little manipulation shows that this limiting condition is equivalent to

$$(p_2^2)^2 + (p_3^2)^2 + (p_4^2)^2 - 2p_2^2p_3^2 - 2p_2^2p_4^2 - 2p_3^2p_4^2 = 0 \tag{6.9}$$

Since $p^2 = E^2 - m^2$ and using the constraint $E_4 = m_1 - E_2 - E_3$ we may express the limits on E_2, E_3 as solutions to

$$\begin{aligned} 0 \;=\; & -8m_1(E_2^2E_3 + E_2E_3^2) \\ & +4E_2^2(m_1^2 + m_3^2) + 4E_3^2(m_1^2 + m_2^2) \\ & +4E_2E_3(3m_1^2 + m_2^2 + m_3^2 + m_4^2) \\ & -4m_1(E_2 + E_3)(m_1^2 + m_2^2 + m_3^2 + m_4^2) \\ & +[m_1^2 + (m_2 + m_3)^2 - m_4^2][m_1^2 + (m_2 - m_3)^2 - m_4^2] \end{aligned} \tag{6.10}$$

Thus the decay rate is

$$\Gamma = \frac{1}{2(4\pi)^3 \, m_1^2} \int \mathcal{M} \; \mathrm{d}E_2 \mathrm{d}E_3 \tag{6.11}$$

where the limits of the energy integrals are the solutions for E_2, E_3 of equation 6.10.

6.4 Calculation

The Feynman amplitude for one particle decaying into three particles (from Figure 6.1, following the rules of Table 3.1) is

$$\mathcal{A}_{1\to3} = \frac{-1}{{p_x}^2} \; \overline{u}(p_3) V_{1\alpha}(p_x) u(p_1) \;\; \overline{u}(p_2) V_2{}^{\alpha}(-p_x) \overline{u}(p_4) \tag{6.12}$$

so that, using the trace identities of Section 4.2

$$\begin{aligned}\mathcal{M}_{1\to 3} &= \frac{1}{4{p_x}^4}\ tr\left[(\not{p}_3+m_3)V_{1\alpha}(p_x)(\not{p}_1+m_1)V_{1\beta}(-p_x)\right]\\ &\times\ tr\left[(\not{p}_2+m_2)V_2{}^{\alpha}(-p_x)(\not{p}_4+m_4)V_2{}^{\beta}(p_x)\right]\end{aligned} \tag{6.13}$$

Following essentially the same evaluation as for the first order electron–proton scattering matrix element (Section 4.3), with the necessary alterations to the simplifications, we find that the maximally coupled 1→3 particle decay is

$$\begin{aligned}\mathcal{M}_{1\to 3} = \frac{1}{16t^2}\Big\{\ & 2q_1^2q_2^2\ \ [2(t-4m_4^2-m_2^2+4m_2m_4)m_1m_3\\ &-2(m_1^2+m_2^2+m_3^2+m_4^2-t)s\\ &+(m_2^2-2m_2m_4+2m_3^2+m_4^2-t)m_1^2+(m_3^2+2m_4^2-t)m_2^2\\ &+(m_4^2-t)m_3^2+2s^2-2m_3^2m_4+2m_2m_4t-m_4^2t+t^2]\\ &+\mu_1^2\mu_2^2\ \ [4((m_2^2-m_4^2-t)m_1^2-(m_3^2+t)m_2^2\\ &+(m_4^2-t)m_3^2-m_4^2t+t^2)st+((8m_3^2m_4^2+3t^2)m_2^2\\ &+2(4m_3^2+t)m_2m_4t-2(2m_3^2+t)m_2^2-4(m_4^4-t^2)m_3^2\\ &+2m_4^4t-m_4^2t^2-t^3)m_1^2-2((2m_4^2+t)m_2^2-m_2^4\\ &+2m_2m_4t-m_4^4-m_4^2t)m_1^4\\ &-(2(2m_4^2-t)m_3^4-3m_4^2t^2)m_2^2\\ &-2(2(m_2+m_4)^2+t)((m_2-m_4)^2-t)m_1m_2t\\ &+(2m_3^4+2m_3^2t-t^2)m_2^4-2(2m_3^4-t^2)m_2m_4t\\ &-2(m_4^2-t)^2m_3^2t+2(m_4^2-t)m_3^4m_4^2+4s^2t^2\\ &+2m_2^3m_4t^2-m_4^2t^3+t^4]\\ &-\mu_1^2q_2^2\ \ [4((m_2^2-m_4^2-t)m_1^2-(m_3^2+t)m_2^2\\ &+(m_4^2-t)m_3^2-m_4^2t+t^2)s\\ &-(2(4m_3^2+t)m_2m_4+(2m_4^2-3t)m_2^2+m_2^4-3m_4^4\\ &+m_4^2t+2t^2)m_1^2\\ &+2((m_2+m_4)^2+2t)((m_2-m_4)^2-t)m_1m_3\\ &-2(m_2^2-2m_2m_4-m_4^2-t)m_1^4+(2m_3^4+m_4^4+m_4^2t-t^2)m_2^2\\ &+2(2m_3^4-t^2)m_2m_4+2(m_3^2-m_4^2)m_2^4\\ &-2(m_4^2-t)^2m_3^2-2(m_4^2-t)m_3^4+4s^2t\\ &+m_2^6-2m_2^3m_4t+m_4^4t-m_4^2t^2]\\ &-\mu_2^2q_1^2\ \ [4(m_2^2-m_4^2-t)m_1^2-(m_3^2+t)m_2^2\\ &+(m_4^2-t)m_3^2-m_4^2t+t^2)s\\ &-(2(2m_3^2-t)m_2m_4+(2m_3^2-3t)m_2^2+2(m_4^2-t)m_3^2\\ &+2m_2^4-2m_4^4+m_4^2t+t^2)m_1^2\\ &+2(2(m_2+m_4)^2+t)((m_2-m_4)^2-t)m_1m_3\\ &-(m_2^2-2m_2m-4-3m_4^2-t)m_1^4\\ &+(3m_3^4-m_4^2t-t^2)m_2^2+2(m_3^4-2t^2)m_2m_4\\ &+(2m_3^2+t)m_2^4-2(m_4^2-t)^2m_3^2-(m_4^2-t)m_3^4\\ &+4s^2t+2m_2^3m_4t+2m_4^4t-2m_4^2t^2]\end{aligned} \tag{6.14}$$

$$
\begin{aligned}
&- 2\mu_1^2\mu_2 q_2 \quad (2(m_1^2-m_3^2)^2 - m_1^2 t - 6m_1 m_3 t \\
&\qquad -m_2^2 t - t^2)((m_2-m_4)^2 - t)(m_2+m_4) \\
&- 2\mu_1\mu 2^2 q_1 \quad ((m_1-m_3)^2 - t)(m_1+m_3)(2(m_2+m_4)^2 \\
&\qquad +t)((m_2-m_4)^2 - t) \\
&+ 2\mu_1\mu_2 q_1 q_2 \quad [(((5m_4^2+7t)m_3^2 + 7m_4^2 t + 5t^2)m_2 \\
&\qquad -5(m_2-m_4)(m_3^2+t)m_2^2 - 5(m_4^2-t)m_3^2 m_4 \\
&\qquad -7m_4^3 t + 7m_4 t^2)m_1 \\
&\qquad -((5m_4^2-7t)m_4 - 5(m_4^2+t)m_2 + 5m_2^3 - 5m_2^2 m_4)m_1^2 m_3 \\
&\qquad -(5(m_4^2+t)m_2 - 5m_2^3 + 5M - 2^2 m_4 - 5m_4^3 + 7m_4 t)m_1^3 \\
&\qquad -2(m_1-m_3)(m_2-m_4)st + (m_2-m_4)(5m_3^2-7t)m_2^2 m_3 \\
&\qquad -(m_3^2-t)(5m_4^2+7t)m_2 m_3 + 5(m_3^2-t)(m_4^2-t)m_3 m_4] \\
&- 4\mu_1 q_1 q_2^2 \quad [(m_2^2-m_3^2)(m_4^2-t) + 3(m_3^2+t)m_2 m_4 \\
&\qquad -m_4^4 + t^2)m_1 \\
&\qquad +(m_1-m_3)(m_2^2 - 3m_2 m_4 - t)m_1^2 - (m_1-m_3)(m_2^2-m_4^2)s \\
&\qquad +(m_3^2-t)(m_4^2-t)m_3 - 3(m_3^2-t)m_2 m_3 m_4 + m_2^2 m_3 m_4^2] \\
&- 2\mu_2 q_1^2 q_2 \quad [2((m_3^2-t)m_2 + m_2^3 - m_2^2 m_4 + m_3^2 m_4)m_1^2 \\
&\qquad -((m_4^2-t)m_3^2 + 2m_3^4 - 2m_4^2 t - 2t^2)m_2 \\
&\qquad -2(m_1^2-m_3^2)(m_2-m_4)s - 6((m_2-m_4)^2 - t)(m_2+m_4)m_1 m_3 \\
&\qquad -(m_3^2+m_4^2+3t)m_2^3 + (m_3^2+m_4^2+t)m_2^2 m_4 \\
&\qquad +(m_4^2-t)m_3^2 m_4 - 2m_1^4 m_4 + m_2^5 - m_2^4 m_4 \\
&\qquad -2m_4^3 t + 2m_4 t^2] \Big)
\end{aligned}
$$

Either of the two integrations that need to be performed on this expression (with respect to E_2 and E_3) may be performed analytically by REDUCE. Substitution of the limits from equation 6.10 into the resultant expression, integrating with respect to the other energy and finally substituting the limits for this energy causes problems because of the sheer size of the algebraic expression. Both integrals, therefore, were evaluated numerically using the REDUCE program shown in Appendix B.

6.5 Lifetime

Applying equation 6.14 with

$$
\left.
\begin{aligned}
m_1 &= m_n \\
m_2 &= m_e \\
m_3 &= m_{\overline{\nu}_e} \approx 0 \\
m_4 &= m_p \\
q_1 &= 0 \\
q_2 &= q_p \\
\mu_1 &= -\mu_Q \\
\mu_2 &= +\mu_Q
\end{aligned}
\right\} \qquad (6.15)
$$

and performing both of the E_2, E_3 integrals numerically (see Appendix B) we find a neutron lifetime

$$\tau_n = 1015 \text{ sec} \tag{6.16}$$

This theoretically predicted value is startlingly close to experimental values. When we published this investigation (Butler and Burling–Claridge, 1989) the most recent experiment (Last et al 1988) gave $\tau_n = 876 \pm 21$ sec. Other, earlier, experiments claiming similar accuracy (see Byrne (1988) for a brief review, also Wilkinson (1982)) give a range of values, several about or above 1000 sec, however the large values date from the 1960's. A recent publication (Mampe et al 1989) calculates the lifetime by measuring the remaining neutrons in a storage device. They find $\tau_n = 887 \pm 3$ sec. There seems to be some agreement among experimentalists that this last value is reliable (Last, 1990, private correspondence).

Using Rosenbluth's vertex (equation 3.11) to describe the maximal coupling results in a predicted lifetime $\tau_n = 1.1$ sec.

6.6 β^- Decay Spectrum

In the experiment of Last et al, the β^- particles are emitted with a spectrum of energies, ranging in principle from zero to (almost) the difference in rest energies. Only those β^- particles within a certain energy range were detected because of the need to exclude low energy background particles. The experimentally measured spectrum was thus extrapolated to the full emission spectrum using an appropriate model.

Last et al found that the useful limit of their detector system was $K_e \geq 363.7$ keV. That is, they could not reliably detect (or rather, calibrate their detector for) β^- particles with $K_e < 363.7$ keV. They used the electro–weak model of Glashow, Salam and Weinberg, to deduce the proportion of emitted particles they were able to measure. We understand the GSW model to predict that 45.7% of the β^- particles will be emitted with a larger energy than this 363.7 keV cutoff. The actual detection proportion is obtained by convolving this predicted distribution with the detector sensitivity. Last et al thus deduced that their experimental configuration detected 34.85% of the β^- particles emitted.

Our maximally coupled expression of equation 6.14 can be used to find the β^- decay energy spectrum as well as the neutron lifetime. The β^- decay spectrum is simply the number of β^- particles with energy in the range E_2 to $E_2 + \mathrm{d}E_2$, or

$$\mathrm{d}n_e = \frac{\int \mathcal{M}(E_2, E_3)\, \mathrm{d}E_3}{\mathrm{d}E_2} \tag{6.17}$$

Which may be evaluated either numerically or algebraically by REDUCE. The maximally coupled decay spectrum, as a function of the kinetic energy of the β^- particles, is shown in Figure 6.2.

We find that a maximally coupled model predicts 49.5% of the β^- particles will have kinetic energies $K_e \geq 363.7 keV$. Without convolving this distribution with Last et al's

detector sensitivity, we may naively re-evaluate the Last et al results using the ratio of the two (maximal coupling, GSW) predicted distributions. This suggests that their published data corresponds to a neutron lifetime, using a maximally coupled QED model,

$$\begin{aligned} \tau &= \tfrac{49.5}{45.7} \times \tau_{\text{Last}} \\ &= 949 \pm 22 \text{ sec} \end{aligned} \tag{6.18}$$

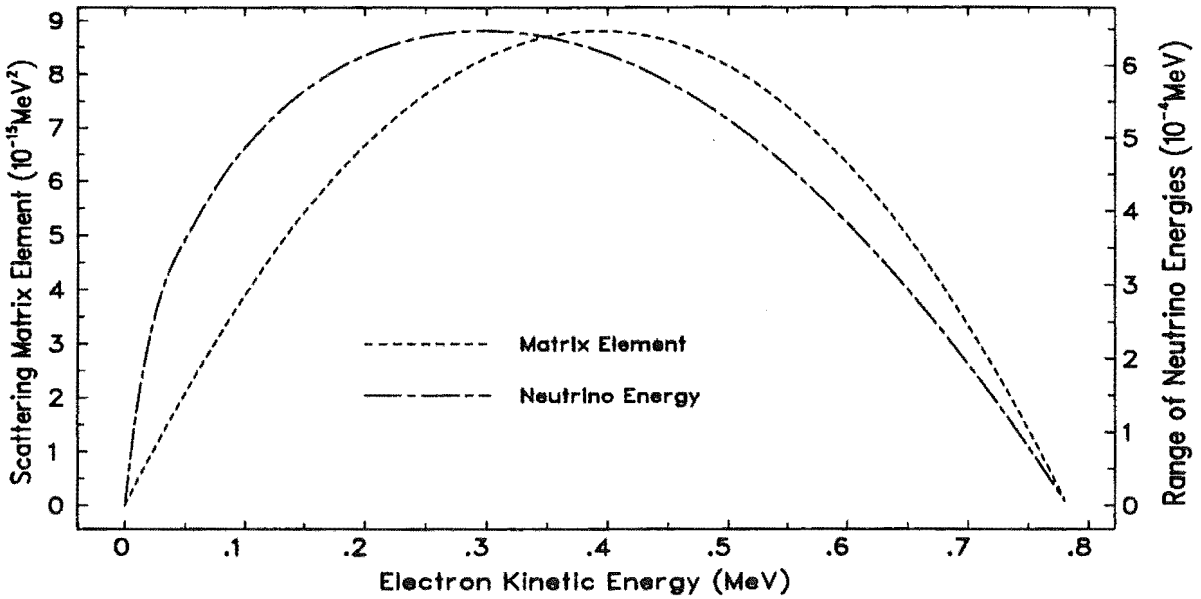

Figure 6.2: β^- decay spectrum.

We have exchanged correspondence with Last and we look forward to hearing if the use of the maximally coupled β^- spectrum when correctly convolved with the detector sensitivity will bring the two experimental results (Last et al and Mampe et al) into agreement.

We note that our calculated value for the life time is extremely sensitive to the value chosen for μ_Q. If we choose the 'quantized' dipole charge to be the electron dipole charge rather than exactly $\frac{\alpha}{2\pi}\mu_B$ (an alteration of less than 0.2%), we find a predicted lifetime of $\tau_n = 1068$, 5% larger than our first estimate. By judicious choice of the value for μ_Q, we can obtain either Mampe et al's result or Last et al's result. However, we feel that there is little merit in pursuing this 'phenomenological fitting' approach, given that this is a first order calculation. The exchanged momenta is of the order of 1 GeV (proton mass) and at these energies it is reasonable to expect second order effects to become important.

6.7 Discussion

The results of this chapter are quite startling. We have obtained a sensible prediction for the neutron lifetime from a first order analysis with no free parameters.

These results raise the question of whether weak field phenomenon are a direct manifestation of maximally coupled electromagnetism and if the GSW model is in some sense phenomenologically equivalent to maximally coupled QED.

Chapter 7

Other First Order Scattering

7.1 Introduction

The success of first order maximally coupled QED, using our vertex, to predict electron-proton scattering and even a neutron lifetime is startling. Several other possible applications for maximally coupled QED present themselves. In this chapter I look at a few such possibilities.

In Section 7.2, I extend the assumption first made in the previous chapter, and investigate electron-proton scattering with a 'quantized' dipole charge.

I briefly investigate two other possible scatterings: electron-neutron (Section 7.3) and neutron-proton (Section 7.4) scattering, using the usual values for the dipole charges. The validity of the minimally coupled model employed to obtain the electron-neutron scattering from electron-deuteron scattering (which is the experimentally measured cross-section) is also discussed in Section 7.3.

7.2 Quantized e-p Scattering

In Chapter 6 we showed that the assumption that the dipole charge is an intrinsic property of a particle, and occurs in only discrete, 'quantized' values leads to a surprisingly good agreement with experiment for a particular decay channel ($n \rightarrow p + e + \overline{\nu}_e$). The success of this prediction leads us to question whether we should not be treating the dipole charge in this fashion at all times. To this end we re-evaluate the electron-proton scattering of Chapter 4, but use the quantized dipole charges of Chapter 5 in place of the electron and proton dipole charges.

We simply substitute

$$\begin{aligned} \mu_e &= -\mu_Q \\ \mu_p &= +\mu_Q \end{aligned} \tag{7.1}$$

into equation 4.9 and otherwise follow exactly the analysis of Section 4.3. Comparison

with experiment is shown in Figures 7.1, 7.2, for electron beam energies of 188 MeV and 550 MeV respectively.

We note there is very little difference between the 'quantized' result and that using the normal dipole charge values. This is to be expected, since we are increasing the size of the proton and neutron dipole moments by only about 10–15%. The size of the dipole moment is not nearly as critical for particle scattering as it was for the neutron decay of Chapter 6. In the latter case there were many near cancellations by subtraction, where the exact magnitude of the dipole charge became critically important.

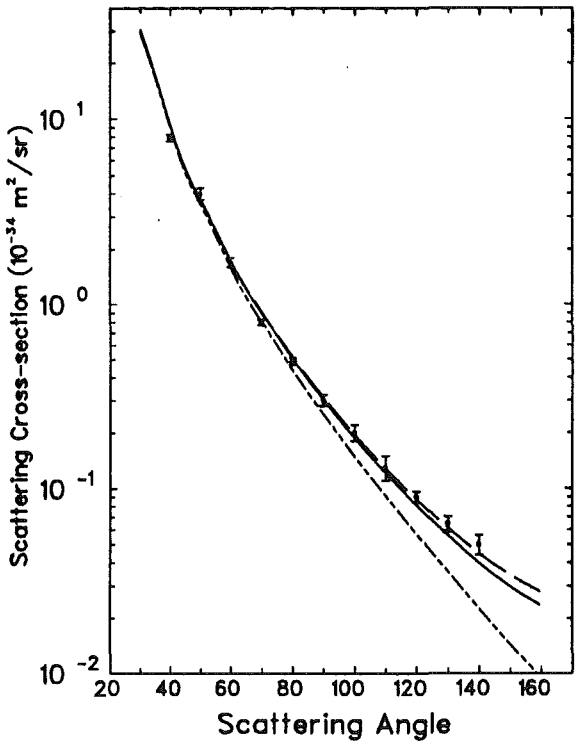

Figure 7.1: Quantized scattering of electrons off protons: laboratory frame, electron beam energy 188 MeV.

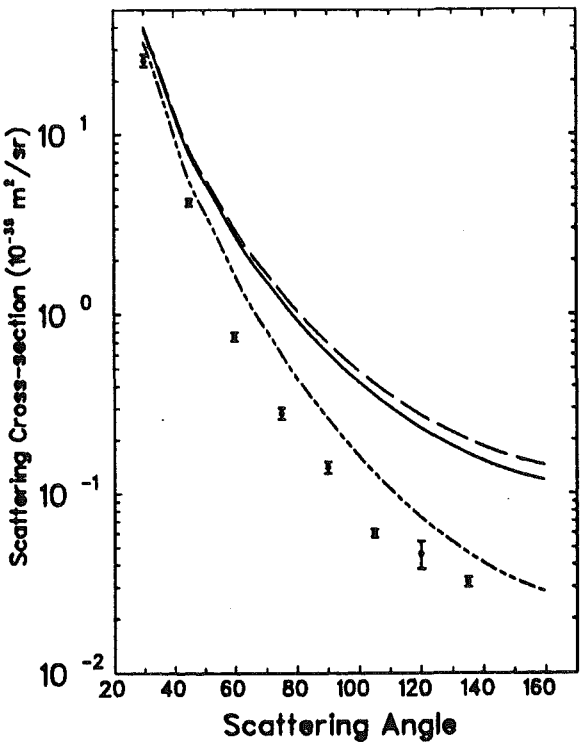

Figure 7.2: Quantized scattering of electrons off protons: laboratory frame, electron beam energy 550 MeV.

KEY:

1 — Experimental points with uncertainties.

2 — Maximally coupled prediction as in Section 4.4.

3 — Quantized maximally coupled prediction.

4 — Minimally coupled (Dirac) scattering.

7.3 Electron–Neutron Scattering

The electron–neutron scattering cross-section is calculated experimentally by scattering electrons off deuterium. Using a model of deuteron structure, the electron–proton contribution is 'subtracted' from the electron–deuteron scattering cross–section. The experimental methods used to calculate this cross–section are reviewed by Budnitz et al (1968), which also presents some results.

To calculate a theoretical prediction for electron–neutron scattering we may use (as a first attempt) the first order analysis of Section 4.3 with

$$\left.\begin{array}{rcl} q_2 & = & 0 \\ \mu_2 & = & \mu_n \end{array}\right\} \tag{7.2}$$

but all other quantities unchanged. The electron-neutron scattering cross-section is (from equations 4.7 and 4.9)

$$\begin{aligned} \left.\frac{\mathrm{d}\sigma}{\mathrm{d}\Omega}\right|_{\mathrm{en}} = \frac{E_e'^{\,2}}{(32\pi E_e m_n t)^2} \Big\{ & \\ & \mu_e^2\mu_n^2\, t^2 \left(4(s-(m_e^2+m_n^2))^2 + (2s+t)^2 - 4s^2 + 16m_e^2m_n^2\right) \\ & +4\mu_n^2 q_e^2\, t \left((2(m_e^2+m_n^2)-t)s + (m_e^2+2m_n^2)t - s^2 - (m_e^2-m_n^2)^2\right) \\ & -4\mu_e\mu_n^2 q_e\, t^2 m_e(8m_n^2+t) \Big\} \end{aligned} \tag{7.3}$$

Following Section 7.2 and Chapter 6 we also may investigate the effect of 'quantizing' the dipole moments with the substitution

$$\begin{array}{rcl} \mu_e & = & \pm\mu_{\mathrm{Q}} \\ \mu_n & = & \pm\mu_{\mathrm{Q}} \end{array} \tag{7.4}$$

the negative case being for our vertex and the positive for Rosenbluth's vertex.

The experimental data are taken from Hofstadter et al (1958) and Yearian and Hofstadter (1958). This data is for electrons scattering off deuterium. For our first comparison (Table 7.1) we have assumed that the total cross-section is simply the sum of the electron-proton and the electron-neutron spin-averaged cross-sections

$$\left.\frac{\mathrm{d}\sigma}{\mathrm{d}\Omega}\right|_{\mathrm{D}} = \left.\frac{\mathrm{d}\sigma}{\mathrm{d}\Omega}\right|_{\mathrm{en}} + \left.\frac{\mathrm{d}\sigma}{\mathrm{d}\Omega}\right|_{\mathrm{ep}} \tag{7.5}$$

This is not valid exactly but Jankus (1956) and Blankenbecler (1957) have shown that for standard (Rosenbluth model) QED it is a reasonable first approximation, with correction terms of around 5% at most (see for example Hofstadter et al, 1958, for more discussion on this aspect). Since the experimental data for 500 MeV electron-proton scattering is available, our comparison was to use equation 7.5 and add the experimental electron-proton cross-section to our calculated electron-neutron cross-section, giving a direct comparison. This comparison is shown in Table 7.1 for a few indicative scattering angles at 500 MeV electron beam energy.

There is no significant difference between the choices of our vertex or Rosenbluth's vertex for maximally coupled electron-neutron scattering at these energies.

It would appear that the maximally coupled electron-neutron scattering prediction is in poor agreement with experiment. However, we should not accept these results at face value. We have shown previously that derivations and assumptions that are valid for minimally coupled interactions are not so for maximally coupled interactions. We should like to perform a complete maximally coupled analysis of electron-deuteron scattering explicitly including the relative spins of the proton and neutron. (Remember that dipole charge is the projection of dipole moment and the direction associated with the dipole moment is related to the particle spin.) This calculation is beyond the scope of the research being reported and is left for future work.

Angle	Cross-section (m^2/sr)	
(deg)	Measured	Max. Coupl.
75	$(4.60 \pm 0.49) \times 10^{-36}$	$(8.66 \pm 0.3) \times 10^{-36}$
90	$(2.36 \pm 0.40) \times 10^{-36}$	$(5.07 \pm 0.1) \times 10^{-36}$
105	$(1.50 \pm 0.30) \times 10^{-37}$	$(3.22 \pm 0.05) \times 10^{-36}$
120	$(9.06 \pm 1.98) \times 10^{-37}$	$(2.27 \pm 0.05) \times 10^{-36}$
135	$(7.58 \pm 1.23) \times 10^{-37}$	$(1.78 \pm 0.04) \times 10^{-36}$

Table 7.1: Comparison of predicted and experimental electron–deuteron scattering, electron beam energy 500 MeV.

7.4 Neutron–Proton Scattering

The neutron and proton interact via both the electromagnetic and the strong nuclear forces, although the interaction is dominated by the latter. In particular any purely electromagnetic analysis of, e.g., neutron-proton scattering should show that the electromagnetic contribution to the scattering is negligible.

The minimally coupled and Rosenbluth (considering the dipole charge of the proton only) models for n-p scattering both give identically zero predictions, which trivially fit the above criteria. The maximally coupled model, on the other hand, will give a non-zero prediction.

It behooves us to evaluate maximally coupled neutron-proton scattering, and show explicitly the contribution this electromagnetic interaction makes to the scattering cross-section.

Relatively recent data is available for neutron–proton scattering, e.g. Evans et al (1982). In these experiments a proton beam impacts on a target to produce a neutron beam whose energy must be measured. This neutron beam is incident on a target of liquid hydrogen, the scattered neutrons subsequently being detected and the scattering angles being determined to high accuracy.

Thus we have a massive, chargeless particle (neutron, particle 1) incident onto a stationary,

massive, charged particle (proton, particle 2). We again use the analysis of Section 4.3 but with

$$\left.\begin{array}{rcl} q_1 & = & 0 \\ \mu_1 & = & \mu_n \\ m_1 & = & m_n \end{array}\right\} \tag{7.6}$$

The neutron-proton cross-section is commonly measured in the centre of momentum frame. Aitchison and Hey (1984, §2) show the centre of momentum cross-section to be

$$\left.\frac{\mathrm{d}\sigma}{\mathrm{d}\Omega}\right|_{\mathrm{CM}} = \frac{\mathcal{M}}{(8\pi(E_1+E_2))^2} \tag{7.7}$$

and so, from equation 4.9, the maximally coupled centre of momentum cross-section for neutron-proton scattering is

$$\begin{aligned} \left.\frac{\mathrm{d}\sigma}{\mathrm{d}\Omega}\right|_{np} = \frac{1}{(32\pi(E_n+E_p)t)^2} \Big\{ & \\ & \mu_n^2\mu_p^2\, t^2 \left(4(s-(m_n^2+m_p^2))^2+(2s+t)^2-4s^2+16m_n^2m_p^2\right) \\ & +4\mu_n^2 q_p^2\, t \left((2(m_n^2+m_p^2)-t)s+(2m_n^2+m_p^2)t-s^2-(m_n^2-m_p^2)^2\right) \\ & -4\mu_n^2\mu_p q_p\, t^2 m_p(8m_n^2+t) \Big\} \end{aligned} \tag{7.8}$$

Table 7.2 shows the comparison of this maximal coupling prediction with experiment. The experimental results are taken from Evans et al (1982) and Bersbach et al (1976).

The maximally coupled QED prediction is much less than the experimentally measured cross-sections, accounting for less than 0.01% of the scattering measured. This is precisely the result that we had expected and indicates that the maximally coupled QED model does not conflict with the Standard Model of particle theory.

CM energy (MeV)	θ_{CM} (deg)	Cross-section		
		Measured (mb/sr)	Maximally coupled* (μb/sr) Our vertex	Ros. Vertex
58.8	11.8	15.13 ± 1.70	2.03	2.107
	31.0	11.75 ± 0.63	0.2926	0.3696
	42.3	11.27 ± 0.37	0.1563	0.2334
86.5	11.9	12.72 ± 1.42	1.997	2.073
	31.1	8.87 ± 0.49	0.289	0.3658
	49.7	4.82 ± 0.30	0.113	0.1897
130.5	11.0	8.89 ± 0.42	2.338	2.413
	31.5	6.14 ± 0.46	0.2841	0.36
	50.2	3.55 ± 0.30	0.1113	0.1871
181.8	11.1	6.54 ± 0.39	2.297	2.371
	31.9	3.56 ± 0.25	0.278	0.3525
	50.8	2.16 ± 0.22	0.1096	0.1839
239.5	11.3	5.40 ± 0.52	2.218	2.29
	32.3	3.31 ± 0.36	0.2727	0.3451
	51.4	2.31 ± 0.38	0.1083	0.1806
390.2	11.7	7.16 ± 0.98	2.075	2.141
	33.4	3.59 ± 0.66	0.261	0.3265
	53.0	3.84 ± 0.86	0.1072	0.1721
647.5	51.1	3.16 ± 0.12	0.1306	0.1808
	130.9	1.21 ± 0.05	0.0254	0.06754
	178.2	9.06 ± 0.06	0.01714	0.05713

*Assuming the dipole charges to have the 'quantized' value μ_Q makes a negligible difference to the data shown

Table 7.2: Comparison of predicted and experimental neutron–proton scattering for several angles and energies.

7.5 Discussion

We have shown that for first order scattering of protons, neutrons and electrons 'quantizing' the dipole moment increases only slightly the size of the cross-section calculated. We conclude there to be insufficient phenomenological evidence to decide whether or not the dipole charges are intrinsically quantized.

When we evaluated neutron-proton scattering, the prediction was found to have a negligible contribution to the scattering cross-section. This is in accordance with the scattering being dominated by the strong nuclear interaction, and justifies the standard assumption of ignoring the electromagnetic contribution.

The poor agreement of maximally coupled QED with experiment for electron-neutron scattering was argued to be mostly due to the basically minimally coupled model commonly used to extract the electron-neutron contribution from electron-deuteron scattering. We discussed, but did not calculate, an alternative model which incorporates the dipole charges and moments explicitly.

Chapter 8

Two-Photon Exchange Processes

8.1 Introduction

It is well known that the dipole moment of the electron may be calculated from the next higher order in a minimally coupled QED model. I have shown in Chapter 5 that the dipole-dipole terms dominate if $p_x > m_p$. Thus to investigate the maximally coupled model at higher energies (> 1 GeV) I need to calculate the second order or two-photon maximally coupled scattering.

There is some question as to the renormalizability of the maximally coupled model. Naive power counting would state that the maximally coupled interaction is non-renormalizable (see for example Itzykson and Zuber, §8.1). However, this takes no account of the intrinsically antisymmetric nature of the dipole moments (remember the dipole charge is the coefficient of the antisymmetic electromagnetic field tensor, $F_{\alpha\beta}$). The two-photon analysis presented here is not completed, but I do not seem to have any renormalization problems.

In evaluating two-photon scattering we require the diagrams of Table 8.1 in addition to the simple tree graph scattering diagram. These other diagrams all have one further photon than the tree level diagram. This additional photon may have any momentum, and we need to sum or integrate over all of the possible values it may take.

Feynman (1949) and Schwinger (1949) evaluated some of the integrals required for minimally coupled two-photon scattering. Redhead (1953) extended these calculations deriving the integrals for two-photon exchange.

Maximal coupling requires more integrals than minimal coupling, and I re-derive the earlier minimal coupling results to standardize the notation. The more general approach of Aitchison and Hey (1984) and Ramond (1981) is adopted here.

8.2 The Matrix Elements

To describe the two-photon interaction of two distinguishable fermions we need the 9 elastic and 4 inelastic diagrams of Figure 8.1.

The total second order Feynman amplitude may be expressed as

$$\mathcal{A}_T = \mathcal{A}_0 + \mathcal{A}_E + \mathcal{A}_I \tag{8.1}$$

where $\mathcal{A}_0$ = the first order interaction amplitude (equation 4.1)

$\mathcal{A}_E = \sum_{n=5}^{9} \mathcal{A}_n$, the elastic diagrams

$\mathcal{A}_I = \sum_{n=10}^{13} \mathcal{A}_n$, the inelastic diagrams

When considering first order scattering (Chapter 4) we evaluated the scattering as coefficients for the various terms of $(q_1 + \mu_{a1})^2 \times (q_2 + \mu_{a2})^2$. For first order, minimally coupled scattering this simplifies to the single term $q_1^2 q_2^2$. We might identify first order maximally coupled scattering as being to order α'^2 ($\alpha' \sim (q + \mu_a)^2$) in the same sense as first order scattering is often identified to be to order α^2 ($\alpha \sim q^2$, see Section 1.2).

The next order in the expansion series for maximally coupled scattering then is α'^3, following from second order minimal coupled scattering. We therefore limit ourselves to such combinations of the amplitudes (when calculating the matrix element) that are no larger than $O(\alpha'^3)$.

A further constraint is that $\mathcal{A}_n^\dagger \mathcal{A}_m \neq 0$ iff D_n, D_m have the same final and initial states, i.e. the interaction detail is indistinguishable away from the immediate interaction region. Thus, for example, $\mathcal{A}_{10}^\dagger \mathcal{A}_1 \equiv 0$ but $\mathcal{A}_{10}^\dagger \mathcal{A}_{11} \neq 0$.

The second order matrix element, $\mathcal{M}_2$, is

$$\begin{aligned} \mathcal{M}_2 &= \mathcal{A}_T^\dagger \mathcal{A}_T & (8.2)\\ &= \mathcal{A}_0^\dagger \mathcal{A}_0 + \mathcal{A}_0^\dagger \mathcal{A}_E + \mathcal{A}_I^\dagger \mathcal{A}_I + \mathcal{A}_E^\dagger \mathcal{A}_0 + O(\alpha'^4) & (8.3) \end{aligned}$$

and since $\mathcal{M}_2$ must be real

$$\begin{aligned} \mathcal{M}_2^\dagger &\equiv \mathcal{M}_2 \\ \Rightarrow \mathcal{A}_E^\dagger \mathcal{A}_0 &\equiv \mathcal{A}_0^\dagger \mathcal{A}_E \end{aligned}$$

and so

$$\mathcal{M}_2 = \mathcal{M} + 2\mathcal{M}_E + \mathcal{M}_I \tag{8.4}$$

where $\mathcal{M}$ = the first order scattering matrix element of equation 4.9,

$\mathcal{M}_E = \mathcal{A}_0^\dagger \mathcal{A}_E$, the elastic matrix element,

$\mathcal{M}_I = \mathcal{A}_I^\dagger \mathcal{A}_I$, the inelastic matrix element.

Explicitly

$$\mathcal{M}_E = \mathcal{A}_0^\dagger\mathcal{A}_1 + \mathcal{A}_0^\dagger\mathcal{A}_2 + \mathcal{A}_0^\dagger\mathcal{A}_3 + \mathcal{A}_0^\dagger\mathcal{A}_4 + \mathcal{A}_0^\dagger\mathcal{A}_5 \quad (8.5)$$

$$+\mathcal{A}_0^\dagger\mathcal{A}_6 + \mathcal{A}_0^\dagger\mathcal{A}_7 + \mathcal{A}_0^\dagger\mathcal{A}_8 + \mathcal{A}_0^\dagger\mathcal{A}_9 \quad (8.6)$$

$$\mathcal{M}_I = \mathcal{A}_{10}^\dagger\mathcal{A}_{10} + 2\mathcal{A}_{10}^\dagger\mathcal{A}_{11} + \mathcal{A}_{11}^\dagger\mathcal{A}_{11} \quad (8.7)$$

$$+\mathcal{A}_{12}^\dagger\mathcal{A}_{12} + 2\mathcal{A}_{12}^\dagger\mathcal{A}_{13} + \mathcal{A}_{13}^\dagger\mathcal{A}_{13} \quad (8.8)$$

These amplitudes are shown in detail in Table 8.1 and the resultant matrix elements in Tables 8.2, 8.3.

All of the matrix elements must be integrated over the extra, arbitrary momentum photon, k. This is dealt with in the following sections.

Evaluation of these traces was performed using REDUCE 3.2, an algebraic processing package. Some of the traced matrix elements run to more than 2000 kB of output (more than 2500 of 80 character lines) and required more than 120 hours of CPU time (Acorn Cambridge Workstation) to evaluate. The resultant expressions are obviously too large to include in this report, but if particularly required they can be supplied on electronic media.

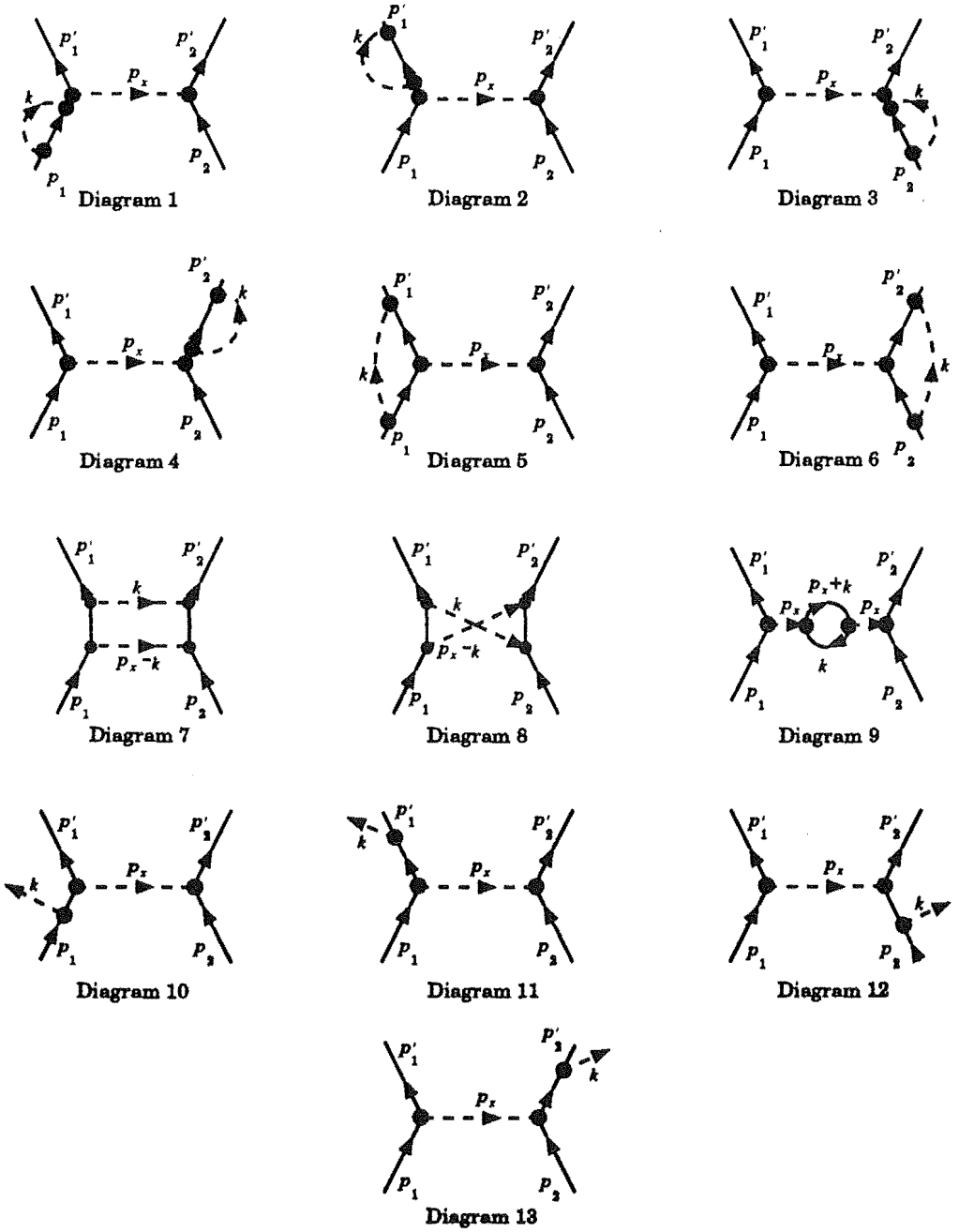

Figure 8.1: The two photon diagrams.

Diagram	Amplitude
D_1	$\mathcal{A}_1 = \overline{u}(p_1')V_{1\beta}(p_x)(\not{p}_1 + m_1)V_{1\alpha}(-k)(\not{p}_1 - \not{k} + m_1)V_1{}^{\alpha}(k)u(p_1)$ $\overline{u}(p_2')V_2{}^{\beta}(-p_x)u(p_2)/[k^2p_x^2(p_1^2 - m1^2)(k^2 - 2p_1.k)]$
D_2	$\mathcal{A}_2 = \overline{u}(p_1')V_{1\alpha}(-k)(\not{p}_1' - \not{k} + m_1)V_1{}^{\alpha}(k)(\not{p}_1' + m_1)V_{1\beta}(p_x)u(p_1)$ $\overline{u}(p_2')V_2{}^{\beta}(-p_x)u(p_2)/[k^2p_x^2(k^2 - 2p_1'.k)(p_1'^2 - m_1^2)]$
D_3	$\mathcal{A}_3 = \overline{u}(p_1')V_{1\beta}(p_x)u(p_1)\overline{u}(p_2')V_2{}^{\beta}(-p_x)(\not{p}_2 + m_2)V_{2\alpha}(-k)$ $(\not{p}_2 - \not{k} + m_2)V_2{}^{\alpha}(k)u(p_2)/[k^2p_x^2(p_2^2 - m_2^2)(k^2 - 2p_2.k)]$
D_4	$\mathcal{A}_4 = \overline{u}(p_1')V_{1\beta}(p_x)u(p_1)\overline{u}(p_2')V_{2\alpha}(-k)(\not{p}_2' - \not{k} + m_2)$ $V_2{}^{\alpha}(k)(\not{p}_1' + m_1)V_2{}^{\beta}(-p_x)u(p_2)/[k^2p_x^2(k^2 - 2p_1'.k)(p_2^2 - m_2^2)]$
D_5	$\mathcal{A}_5 = \overline{u}(p_1')V_{1\alpha}(-k)(\not{p}_1' - \not{k} + m_1)V_{1\beta}(p_x)(\not{p}_1 - \not{k} + m_1)V_1{}^{\alpha}(k)u(p_1)$ $\overline{u}(p_2')V_2{}^{\beta}(-p_x)u(p_2)/[k^2p_x^2(k^2 - 2p_1'.k)(k^2 - 2p_1.k)]$
D_6	$\mathcal{A}_6 = \overline{u}(p_1')V_{1\alpha}(p_x)u(p_1)\overline{u}(p_2')V_{2\beta}(-k)(\not{p}_2' - \not{k} + m_2)$ $V_2{}^{\alpha}(-p_x)(\not{p}_2 - \not{k} + m_2)V_2{}^{\beta}(k)u(p_2)/[k^2p_x^2(k^2 - 2p_2'.k)(k^2 - 2p_2.k)]$
D_7	$\mathcal{A}_7 = \overline{u}(p_1')V_{1\alpha}(k)(\not{p}_1' + \not{k} + m_1)V_{1\beta}(p_x - k)u(p_1)\overline{u}(p_2')V_2{}^{\alpha}(-k)$ $(\not{p}_2' - \not{k} + m_2)V_2{}^{\beta}(k - p_x)u(p_2)/[k^2(k - p_x)^2(k^2 - 2p_1'.k)(k^2 - 2p_2'.k)]$
D_8	$\mathcal{A}_8 = \overline{u}(p_1')V_{1\alpha}(k)(\not{p}_1' + \not{k} + m_1)V_{1\beta}(p_x - k)\overline{u}(p_2')V_2{}^{\beta}(k - p_x)$ $(\not{p}_2 + \not{k} + m_2)V_2{}^{\alpha}(-k)u(p_2)/[k^2(k - p_x)^2(k^2 + 2p_1'.k)(k^2 - 2p_2.k)]$
D_9	$\mathcal{A}_9 = \overline{u}(p_1')V_{1\alpha}(p_x)u(p_1)V_{3\beta}(-p_x)(\not{p}_x + \not{k} + m_3)V_3{}^{\beta}(p_x)(\not{k} + m_3)$ $\overline{u}(p_2')V_2{}^{\alpha}(-p_x)u(p_2)/[p_x^2(k^2 - m_3^2)(k^2 + 2p_x.k + p_x^2 - m_3^2)]$
D_{10}	$\mathcal{A}_{10} = \overline{u}(p_1')V_{1\alpha}(p_x)(\not{p}_1 - \not{k} + m_1)V_{1\beta}(k)u(p_1)$ $\overline{u}(p_2')V_2{}^{\alpha}(-p_x)u(p_2)\varepsilon^{*\tau}/[p_x^2(k^2 - 2p_1.k)]$
D_{11}	$\mathcal{A}_{11} = \overline{u}(p_1')V_{1\beta}k(\not{p}_1' + \not{k} + m_1)V_{1\alpha}(p_x)u(p_1)$ $\overline{u}(p_2')V_2{}^{\alpha}(-p_x)u(p_2)\varepsilon^{*\tau}/[p_x^2(k^2 + 2p_1'.k)]$
D_{12}	$\mathcal{A}_{12} = \overline{u}(p_1')V_{1\alpha}(p_x)u(p_1)\overline{u}(p_2')V_2{}^{\alpha}(-p_x)(\not{p}_2 - \not{k} + m_2)$ $V_{2\beta}(k)u(p_2)\varepsilon^{*\tau}/[p_x^2(k^2 - 2p_2.k)]$
D_{13}	$\mathcal{A}_{13} = \overline{u}(p_1')V_{1\alpha}(p_x)u(p_1)\overline{u}(p_2')V_{2\beta}(k)(\not{p}_2' + \not{k} + m_2)$ $V_2{}^{\alpha}(-p_x)u(p_2)\varepsilon^{*\tau}\ [p_x^2(k^2 - 2p_2'.k)]$

Table 8.1: Two-photon diagram amplitudes.

Matrix Element	Amplitudes	Expression
$\mathcal{M}_1$	$\mathcal{A}_0^\dagger \mathcal{A}_1$	$(\not{p}_1' + m_1)V_{1\sigma}(p_x)(\not{p}_1 + m_1)V_{1\alpha}(-k)(\not{p}_1 - \not{k} + m_1)V_1{}^\alpha(k)$ $(\not{p}_1' + m_1)V_{1\tau}(-p_x)(\not{p}_2' + m_2)V_2{}^\sigma(-p_x)(\not{p}_2 + m_2)$ $V_2{}^\tau(p_x)/[p_x^4 k^2(p_1^2 - m_1^2)(k^2 - 2p_1.k)]$
$\mathcal{M}_2$	$\mathcal{A}_0^\dagger \mathcal{A}_2$	$(\not{p}_1' + m_1)V_{1\alpha}(-k)(\not{p}_1' - \not{k} + m_1)V_1{}^\alpha(k)(\not{p}_1' + m_1)V_{1\sigma}(p_x)$ $(\not{p}_1' + m_1)V_{1\tau}(-p_x)(\not{p}_2' + m_2)V_2{}^\sigma(-p_x)(\not{p}_2 + m_2)$ $V_2{}^\tau(p_x)/[p_x^4 k^2(k^2 - 2p_1'.k)(p_1'^2 - m_1^2)]$
$\mathcal{M}_3$	$\mathcal{A}_0^\dagger \mathcal{A}_3$	$(\not{p}_1' + m_1)V_{1\sigma}(-p_x)(\not{p}_1 + m_1)V_{1\tau}(p_x)(\not{p}_2' + m_2)V_2{}^\sigma(p_x)$ $(\not{p}_2 + m_2)V_{2\alpha}(-k)(\not{p}_2 - \not{k} + m_2)V_2{}^\alpha(k)(\not{p}_2' + m_2)$ $V_2{}^\tau(-p_x)/[p_x^4 k^2(p_2^2 - m_2^2)(k^2 - 2p_2.k)]$
$\mathcal{M}_4$	$\mathcal{A}_0^\dagger \mathcal{A}_4$	$(\not{p}_1' + m_1)V_{1\sigma}(-p_x)(\not{p}_1 + m_1)V_{1\tau}(p_x)(\not{p}_2' + m_2)V_{2\alpha}(-k)$ $(\not{p}_2' - \not{k} + m_2)V_2{}^\alpha(k)(\not{p}_2' + m_2)V_2{}^\sigma(p_x)(\not{p}_2' + m_2)$ $V_2{}^\tau(-p_x)/[p_x^4 k^2(k^2 - 2p_2'.k)(p_2'^2 - m_2^2)]$
$\mathcal{M}_5$	$\mathcal{A}_0^\dagger \mathcal{A}_5$	$(\not{p}_1' + m_1)V_{1\alpha}(-k)(\not{p}_1' - \not{k} + m_1)V_{1\sigma}(p_x)(\not{p}_1 - \not{k} + m_1)V_1{}^\alpha(k)$ $(\not{p}_1' + m_1)V_{1\tau}(-p_x)(\not{p}_2' + m_2)V_2{}^\sigma(-p_x)(\not{p}_2 + m_2)$ $V_2{}^\tau(p_x)/[p_x^4 k^2(k^2 - 2p_1'.k)(k^2 - 2p_1.k)]$
$\mathcal{M}_6$	$\mathcal{A}_0^\dagger \mathcal{A}_6$	$(\not{p}_1' + m_1)V_{1\sigma}(-p_x)(\not{p}_1 + m_1)V_{1\tau}(p_x)(\not{p}_2' + m_2)$ $V_{2\alpha}(-k)(\not{p}_2' - \not{k} + m_2)V_2{}^\sigma(p_x)(\not{p}_2 - \not{k} + m_2)V_2{}^\alpha(k)(\not{p}_2' + m_2)$ $V_2{}^\tau(-p_x)/[p_x^4 k^2(k^2 - 2p_2'.k)(k^2 - 2p_2.k)]$
$\mathcal{M}_7$	$\mathcal{A}_0^\dagger \mathcal{A}_7$	$(\not{p}_1' + m_1)V_{1\sigma}(k)(\not{p}_1' + \not{k} + m_1)V_{1\alpha}(p_x - k)(\not{p}_1 + m_1)V_{1\beta}(-p_x)$ $(\not{p}_2' + m_2)V_2{}^\sigma(-k)(\not{p}_2' - \not{k} + m_2)V_2{}^\alpha(k - p_x)(\not{p}_2 + m_2)$ $V_2{}^\beta(p_x)/[p_x^2 k^2(p_x - k)^2(k^2 + 2p_1'.k)(k^2 - 2p_2'.k)]$
$\mathcal{M}_8$	$\mathcal{A}_0^\dagger \mathcal{A}_8$	$(\not{p}_1' + m_1)V_{1\sigma}(k)(\not{p}_1' + \not{k} + m_1)V_{1\alpha}(p_x - k)(\not{p}_1 + m_1)V_{1\beta}(-p_x)$ $(\not{p}_2' + m_2)V_2{}^\alpha(k - p_x)(\not{p}_2 + \not{k} + m_2)V_2{}^\sigma(-k)(\not{p}_2 + m_2)$ $V_2{}^\beta(p_x)/[p_x^2 k_x^2(p_x - k)^2(k^2 + 2p_1'.k)(k^2 + 2p_2.k)]$
$\mathcal{M}_9$	$\mathcal{A}_0^\dagger \mathcal{A}_9$	$(\not{p}_1' + m_1)V_{1\tau}(p_x)(\not{p}_1 + m_1)V_{1\alpha}(-p_x)(\not{p}_2' + m_2)V_{2\sigma}(-p_x)$ $(\not{p}_2 + m_2)V_2{}^\alpha(p_x)(\not{p}_x + \not{k} + m_3)V_3{}^\tau(-p_x)(\not{k} + m_3)$ $V_3{}^\sigma(p_x)/[p_x^6(k^2 - m_3^2)(k^2 + 2p_x.k + 2p_x^2 - m_3^2)]$

Table 8.2: Matrix elements required for two-photon elastic scattering.

Matrix Element	Amplitudes	Expression
$\mathcal{M}_{10}$	$\mathcal{A}_{10}^{\dagger}\mathcal{A}_{10}$	$(\not{p}_1{}' + m_1)V_{1\sigma}(k)(\not{p}_1{}' + \not{k} + m_1)V_{1\tau}(p_x)(\not{p}_1 + m_1)V_{1\alpha}(-px)$ $(\not{p}_1{}' + \not{k} + m_1)V_1{}^{\sigma}(-k)(\not{p}_2{}' + m_2)V_2{}^{\tau}(-p_x)(\not{p}_2 + m_2)$ $V_2{}^{\alpha}(p_x)/[k^2p_x^2(k^2 + 2p_1{}'.k)^2]$
$\mathcal{M}_{11}$	$\mathcal{A}_{11}^{\dagger}\mathcal{A}_{11}$	$(\not{p}_1{}' + m_1)V_{1\tau}(p_x)(\not{p}_1 - \not{k} + m_1)V_{1\sigma}(k)(\not{p}_1 + m_1)V_1{}^{\sigma}(-k)$ $(\not{p}_1 - \not{k} + m_1)V_{1\alpha}(-p_x)(\not{p}_2{}' + m_2)V_2{}^{\tau}(-p_x)(\not{p}_2 + m_2)$ $V_2{}^{\alpha}(p_x)/[k^2p_x^4(k^2 - 2p_1.k)^2]$
$\mathcal{M}_{12}$	$\mathcal{A}_{12}^{\dagger}\mathcal{A}_{12}$	$(\not{p}_1{}' + m_1)V_{1\tau}(px)(\not{p}_1 + m_1)V_{1\alpha}(-p_x)(\not{p}_2{}' + m_2)V_{2\sigma}(k)$ $(\not{p}_2{}' + \not{k} + m_2)V_2{}^{\tau}(-px)(\not{p}_2 + m_2)V_2{}^{\alpha}(p_x)(\not{p}_2{}' + \not{k} + m_2)$ $V_2{}^{\sigma}(-k)/[k^2p_x^4(k^2 - 2p_2{}'.k)^2]$
$\mathcal{M}_{13}$	$\mathcal{A}_{13}^{\dagger}\mathcal{A}_{13}$	$(\not{p}_1{}' + m_1)V_{1\tau}(p_x)(\not{p}_1 + m_1)V_{1\alpha}(-p_x)(\not{p}_2{}' + m_2)V_2{}^{\tau}(-p_x)$ $(\not{p}_2 - \not{k} + m_2)V_{2\sigma}(k)(\not{p}_2 + m_2)V_2{}^{\sigma}(-k)(\not{p}_2 - \not{k} + m_2)$ $V_2{}^{\alpha}(p_x)/[k^2p_x^4(k^2 - 2p_2.k)^2]$
$\mathcal{M}_{14}$	$\mathcal{A}_{10}^{\dagger}\mathcal{A}_{11}$	$(\not{p}_1{}' + m_1)V_{1\tau}(p_x)(\not{p}_1 - \not{k} + m_1)V_{1\alpha}(k)(\not{(p)}_1 + m_1)V_{1\sigma}(-p_x)$ $(\not{p}_1{}' + \not{k} + m_1)V_1{}^{\alpha}(-k)(\not{p}_2 + m_2)V_2{}^{\tau}(-p_x)(\not{p}_2 + m_2)$ $V_2{}^{\sigma}(p_x)/[k^2p_x^4(k^2 - 2p_1.k)(k^2 + 2p_1{}'.k)]$
$\mathcal{M}_{15}$	$\mathcal{A}_{12}^{\dagger}\mathcal{A}_{13}$	$(\not{p}_1{}' + m_1)V_{1\tau}(p_x)(\not{p}_1 + m_1)V_{1\sigma}(-p_x)(\not{p}_2{}' + m_2)V_2{}^{\tau}(-p_x)$ $(\not{p}_2 - \not{k} + m_2)V_{2\alpha}(k)(\not{p}_2 + m_2)V_2{}^{\sigma}(p_x)(\not{p}_2{}' + \not{k} + m_2)$ $V_2{}^{\alpha}(-k)/[k^2p_x^2(k^2 - 2p_2.k)(k^2 + 2p_2{}'.k)]$

Table 8.3: Matrix elements required for two-photon inelastic scattering.

8.3 General Form of the Integrals

We can classify the required integrals over the internal momentum, k_α, into three types:

$$\mathcal{I}_1(1 : \alpha : \alpha\beta : \alpha\beta\tau),$$

$$\mathcal{I}_2(1 : \alpha : \alpha\beta : \alpha\beta\tau : \alpha\beta\tau\sigma),$$

$$\mathcal{I}_3(1 : \alpha : \alpha\beta : \alpha\beta\tau : \alpha\beta\tau\sigma).$$

where the abbreviations $(1 : \alpha : \alpha\beta : \ldots)$ denote the various valid numerators:
$(1 : k_\alpha : k_\alpha k_\beta : \ldots)$

The matrix elements from the simple fermion self–interaction diagrams, D_1–D_4, have two k–dependent vertices, one k–dependent fermion propagator and one k–dependent photon propagator. The numerators of the required k–dependent integrals will include a 'k_α' term from each of the vertices and one from the fermion propagator. Thus the numerator will have terms up to $k_\alpha k_\beta k_\tau$ and the denominator will include the two k-dependent propagator terms,

$$\mathcal{I}_1(1 : \alpha : \alpha\beta : \alpha\beta\tau) = \int \frac{(1 : k_\alpha : k_\alpha k_\beta : k_\alpha k_\beta k_\tau)\ \mathrm{d}^4k}{k^2(k^2 - 2p_a.k - D_a)} \tag{8.9}$$

The generalized p_a, D_a are specifically

$$\begin{array}{lllll} \mathcal{M}_1: & p_a = p_1'; & D_a & = -({p_1'}^2 - m_1^2) & = 0 \\ \mathcal{M}_2: & p_a = p_1; & D_a & = -({p_1}^2 - m_1^2) & = 0 \\ \mathcal{M}_3: & p_a = p_2'; & D_a & = -({p_2'}^2 - m_2^2) & = 0 \\ \mathcal{M}_4: & p_a = p_2; & D_a & = -({p_2}^2 - m_2^2) & = 0 \end{array}$$

The matrix elements from the more complicated fermion self interaction diagrams, D_5, D_6, and those from the inelastic scattering diagrams, D_{10}–D_{13} have two k–dependent fermion propagators, two k–dependent vertices and one k–dependent photon propagator. Thus the numerators of the required integrals will include terms to a maximum of $k_\alpha k_\beta k_\tau k_\sigma$ and the denominator will contain the three k–dependent propagator terms,

$$\mathcal{I}_2(1 : \alpha : \alpha\beta : \alpha\beta\tau : \alpha\beta\tau\sigma) = \int \frac{(1 : k_\alpha : k_\alpha k_\beta : k_\alpha k_\beta k_\tau : k_\alpha k_\beta k_\tau k_\sigma)\ \mathrm{d}^4k}{k^2(k^2 - 2p_a.k - D_a)(k^2 - 2p_b.k - D_b)} \tag{8.10}$$

The generalized p_a, p_b, D_a, D_b are specifically

$$\begin{array}{lllll}
\mathcal{M}_5: & p_a = p_1'; & D_a & = -({p_1'}^2 - m_1^2) & = 0 \\
& p_b = p_1; & D_b & = -(p_1^2 - m_1^2) & = 0 \\
\mathcal{M}_6: & p_a = p_2'; & D_a & = -({p_2'}^2 - m_2^2) & = 0 \\
& p_b = p_2; & D_b & = -(p_2^2 - m_2^2) & = 0 \\
\mathcal{M}_{10}: & p_a = -p_1'; & D_a & = -({p_1'}^2 - m_1^2) & = 0 \\
& p_b = -p_1'; & D_b & = -({p_1'}^2 - m_1^2) & = 0 \\
\mathcal{M}_{11}: & p_a = p_1; & D_a & = -(p_1^2 - m_1^2) & = 0 \\
& p_b = p_1; & D_b & = -(p_1^2 - m_1^2) & = 0 \\
\mathcal{M}_{12}: & p_a = -p_2'; & D_a & = -({p_2'}^2 - m_2^2) & = 0 \\
& p_b = -p_2'; & D_b & = -({p_2'}^2 - m_2^2) & = 0 \\
\mathcal{M}_{13}: & p_a = p_2; & D_a & = -(p_2^2 - m_2^2) & = 0 \\
& p_b = p_2; & D_a & = -(p_2^2 - m_2^2) & = 0 \\
\mathcal{M}_{14}: & p_a = -p_1'; & D_a & = -({p_1'}^2 - m_1^2) & = 0 \\
& p_b = p_1; & D_a & = -(p_1^2 - m_1^2) & = 0 \\
\mathcal{M}_{15}: & p_a = -p_2'; & D_a & = -({p_2'}^2 - m_2^2) & = 0 \\
& p_b = p_2; & D_a & = -(p_2^2 - m_2^2) & = 0
\end{array}$$

The last integral type we need consider are those arising in calculating the matrix elements for the two–photon exchange diagrams, D_7, D_8. These matrix elements include two k–dependent fermion propagators, two k–dependent vertices and two k–dependent photon propagators. Thus the numerators of the required integrals will contain terms to a maximum of $k_\alpha k_\beta k_\tau k_\sigma$ and the denominator will contain the four propagator terms,

$$\mathcal{I}_3(1:\alpha:\alpha\beta:\alpha\beta\tau:\alpha\beta\tau\sigma) = \int \frac{(1:k_\alpha:k_\alpha k_\beta:k_\alpha k_\beta k_\tau:k_\alpha k_\beta k_\tau k_\sigma)\ \mathrm{d}^4k}{k^2(k^2-2p_a.k-D_a)(k^2-2p_b.k-D_b)(k^2-2p_c.k-D_c)} \tag{8.11}$$

The generalized p_a, D_a, etc are specifically

$$\begin{array}{lllll}
\mathcal{M}_7: & p_a = p_1; & D_a & = -(p_1^2 - m_1^2) & = 0 \\
& p_b = -p_2; & D_b & = -(p_2^2 - m_2^2) & = 0 \\
& p_c = p_x; & D_c & = -p_x^2 & = -t \\
\mathcal{M}_8: & p_a = p_1; & D_a & = -(p_1^2 - m_1^2) & = 0 \\
& p_b = -p_2'; & D_b & = -({p_2'}^2 - m_2^2) & = 0 \\
& p_c = p_x; & D_c & = -p_x^2 & = -t
\end{array}$$

8.4 Simplification of Integrals Required

The integrals $\mathcal{I}_1, \mathcal{I}_2, \mathcal{I}_3$ of Section 8.3 need to be modified to allow their evaluation. We first simplify the denominators by re-expressing the several terms as a series of integrals of one single termed denominator.

For simplification let us refer to the integrals as

$$\begin{aligned} \mathcal{I}_1(\ldots) &= \int \frac{(\ldots)\mathrm{d}^4k}{(k)(a)} \\ \mathcal{I}_2(\ldots) &= \int \frac{(\ldots)\mathrm{d}^4k}{(k)(a)(b)} \\ \mathcal{I}_3(\ldots) &= \int \frac{(\ldots)\mathrm{d}^4k}{(k)(a)(b)(c)} \end{aligned} \tag{8.12}$$

where

$$\begin{aligned} (k) &= k^2 \\ (a) &= k^2 - 2p_a.k - D_a \\ (b) &= k^2 - 2p_b.k - D_b \\ (c) &= k^2 - 2p_c.k - D_c \end{aligned} \tag{8.13}$$

In the manner of Feynman (1949) we introduce an arbitrary cutoff parameter, λ

$$\frac{1}{k^2} = -\lim_{\lambda^2\to\infty}\int_0^{\lambda^2} \frac{\mathrm{d}L}{(k^2-L)^2} \tag{8.14}$$

or, in terms of the simplification, equation 8.13, above

$$(k) = k^2 \to -(k^2 - L)^2 \tag{8.15}$$

and an extra integral is added to each of $\mathcal{I}_1, \mathcal{I}_2, \mathcal{I}_3$.

The identity (Feynman, 1949)

$$\frac{1}{AB} = \int_0^1 \frac{\mathrm{d}x}{(Ax + B(1-x))^2} \tag{8.16}$$

allows multiple term denominators to be re-expressed as a single term. Successively differentiating with respect to A generates the further identities

$$\frac{1}{A^2B} = \int_0^1 \frac{2x\ \mathrm{d}x}{(Ax + B(1-x))^3} \tag{8.17}$$

$$\frac{1}{A^3B} = \int_0^1 \frac{3y^2\ \mathrm{d}y}{(Ay + B(1-y))^4} \tag{8.18}$$

$$\frac{1}{A^4B} = \int_0^1 \frac{4z^3\ \mathrm{d}z}{(Az + B(1-z))^5} \tag{8.19}$$

which are sufficient for our evaluations.

Applying equation 8.17 to $\mathcal{I}_1$ and setting $A \to (k)$, $B \to (a)$ we find

$$\mathcal{I}_1(\ldots) = -\int_0^{\lambda^2} \mathrm{d}L \int_0^1 2x\ \mathrm{d}x \int_{all\ space} \frac{(\ldots)\ \mathrm{d}^4k}{(k^2 - 2R_1.k - D_1)^3} \tag{8.20}$$

with

$$\begin{aligned} R_1 &= (1-x)p_a \\ D_1 &= (1-x)D_a + xL \quad = xL \end{aligned} \tag{8.21}$$

Similarly, if we apply equation 8.17 to $\mathcal{I}_2$ then equation 8.18 to that result

$$\mathcal{I}_2(\ldots) = -\int_0^{\lambda^2} \mathrm{d}L \int_0^1 2x \,\mathrm{d}x \int_0^1 3y^2 \,\mathrm{d}y \int_{all\ space} \frac{(\ldots)\,\mathrm{d}^4k}{(k^2 - 2R_2.k - D_2)^4} \tag{8.22}$$

with

$$\begin{aligned} R_2 &= (1-y)p_b + yR_1 \\ D_2 &= (1-y)D_b + yD_1 = yD_1 \quad = yxL \end{aligned} \tag{8.23}$$

Finally we apply equation 8.17 to $\mathcal{I}_3$, equation 8.18 to the results and equation 8.19 to those results and obtain

$$\mathcal{I}_3(\ldots) = -\int_0^{\lambda^2} \mathrm{d}L \int_0^1 2x \,\mathrm{d}x \int_0^1 3y^2 \,\mathrm{d}y \int_0^1 4z^3 \,\mathrm{d}z \int_{all\ space} \frac{(\ldots)\,\mathrm{d}^4k}{(k^2 - 2R_3.k - D_3)^5} \tag{8.24}$$

with

$$\begin{aligned} R_3 &= (1-z)p_c + zR_2 \\ D_3 &= (1-z)D_c + zD_2 \quad = (1-z)D_c + zyxL \end{aligned} \tag{8.25}$$

Let us further simplify our notation and define integrals $\mathcal{I}_{R_i}(\ldots)$, $i = 1,2,3$ in the following manner

$$\left.\begin{aligned} \mathcal{I}_1(\ldots) &= -\int_0^{\lambda^2} \mathrm{d}L \int_0^1 2x \,\mathrm{d}x \,\mathcal{I}_{R_1}(\ldots) \\ \mathcal{I}_2(\ldots) &= -\int_0^{\lambda^2} \mathrm{d}L \int_0^1 2x \,\mathrm{d}x \int_0^1 3y^2 \,\mathrm{d}y \,\mathcal{I}_{R_2}(\ldots) \\ \mathcal{I}_3(\ldots) &= -\int_0^{\lambda^2} \mathrm{d}L \int_0^1 2x \,\mathrm{d}x \int_0^1 3y^2 \,\mathrm{d}y \int_0^1 4z^3 \,\mathrm{d}z \,\mathcal{I}_{R_3}(\ldots) \end{aligned}\right\} \tag{8.26}$$

In general then

$$\mathcal{I}_{R_i}(\ldots) = \int \frac{(\ldots)\,\mathrm{d}^4k}{(k^2 - 2R_i.k - D_i)^{i+2}} \tag{8.27}$$

contain the k-dependence of the required integrals. The composition of R_i may be ignored and substituted after integrating with respect to k, for the subsequent (x, y, z, L) integrations, since R_i is not a function of k.

The integrals of equation 8.27 may be simplified to the single group of integrals

$$\mathcal{I}_R(\ldots) = \int \frac{(\ldots)\,\mathrm{d}^4k}{(k^2 - 2R.k - D)^A} \tag{8.28}$$

where we are interested in the particular cases $A = 3, 4, 5$.

Having simplified the denominators let us turn our attention to the numerators of the integrands.

The composite vector R is independent of k and so we may differentiate the integrand of equation 8.28 through the integral with respect to (for example) R_α,

$$\begin{aligned} \frac{\partial}{\partial R_\alpha}\left(\int \frac{\mathrm{d}^4k}{(k^2 - 2R.k - D)^A}\right) &\equiv \int \frac{\partial}{\partial R_\alpha}\left(\frac{\mathrm{d}^4k}{(k^2 - 2R.k - D)^A}\right) \\ &= 2A\int \frac{k_\alpha\,\mathrm{d}^4k}{(k^2 - 2R.k - D)^{A+1}} \end{aligned} \tag{8.29}$$

which 'generates' a k_α in the numerator.

This differentiation procedure may be repeated as many times as is necessary, thus generating the numerators $(k_\alpha, k_\alpha k_\beta, \ldots)$ required from the simpler, constant numerator integral. In principle this method will allow us to re–express all of the required integrals in terms of a series of consecutive differentiations of more simple ones.

For brevity let us define one further integral, the base of the differentiation chain and the simplest case of equation 8.28

$$\mathcal{I}_{RA} = \mathcal{I}_R(1) = \int \frac{\mathrm{d}^4k}{(k^2 - 2R.k - D)^A} \tag{8.30}$$

With each subsequent differentiation of $\mathcal{I}_{RA}$ a further k_α is added to the numerator and the exponent of the denominator increases in magnitude. To arrive at the integral $\int \frac{k_\alpha k_\beta k_\tau k_\sigma \ \mathrm{d}^4k}{(k^2 - 2R.k - D)^4}$ (required to evaluate $\mathcal{I}_2(\alpha\beta\tau\sigma)$), for example, we will require to differentiate four times. This implies the original $\mathcal{I}_{RA}$ integral has $A = 0$. Rather, since $\frac{d}{dx}(\ln f(x)) = \frac{f'(x)}{f(x)}$, we define the special case

$$\mathcal{I}_{R0} = \int \ln\left(k^2 - 2R.k - D\right) \mathrm{d}^4k \tag{8.31}$$

so that

$$\frac{\partial}{\partial R_\alpha}\mathcal{I}_{R0} = -2\int \frac{k_\alpha \ \mathrm{d}^4k}{(k^2 - 2R.k - D)} \tag{8.32}$$

8.5 Chain Solutions

We will show in detail the construction of the differentiation chain for one integral, the others follow in a similar manner.

For the integral $\mathcal{I}_3(\alpha\beta\tau)$ we require the 4-vector integral

$$\mathcal{I}_{R_3}(\alpha\beta\tau) = \int \frac{k_\alpha k_\beta k_\tau \ \mathrm{d}^4k}{(k^2 - 2R_z.k - D_z)^5} \tag{8.33}$$

In general the first differentiation of $\mathcal{I}_{RA}$ is

$$\begin{aligned} \frac{\partial}{\partial R_\alpha}\mathcal{I}_{RA} &= \int \frac{\partial}{\partial R_\alpha}\left(\frac{1}{(k^2 - 2R.k - D)^A}\right)\mathrm{d}^4k \\ &= 2A\int \frac{k_\alpha \ \mathrm{d}^4k}{(k^2 - 2R.k - D)^{(A+1)}} \end{aligned} \tag{8.34}$$

Differentiating equation 8.34 with respect to R_β

$$\frac{\partial}{\partial R_\beta}\left(\frac{\partial}{\partial R_\alpha}\mathcal{I}_{RA}\right) = 2^2A(A+1)\int \frac{k_\alpha k_\beta \ \mathrm{d}^4k}{(k^2 - 2R.k - D)^{(A+2)}} \tag{8.35}$$

and differentiating again, with respect to R_τ

$$\frac{\partial}{\partial R_\tau}\left(\frac{\partial}{\partial R_\beta}\left(\frac{\partial}{\partial R_\alpha}\mathcal{I}_{RA}\right)\right) = 2^3 A(A+1)(A+2)\int \frac{k_\alpha k_\beta k_\tau \, \mathrm{d}^4k}{(k^2 - 2R.k - D)^{(A+3)}} \tag{8.36}$$

Comparing equation 8.33 with equation 8.36, substituting for A, etc, and solving for the integral we have

$$\mathcal{I}_{R_3}(\alpha\beta\tau) = \frac{1}{192}\frac{\partial}{\partial R_\tau}\frac{\partial}{\partial R_\beta}\frac{\partial}{\partial R_\alpha}\mathcal{I}_{R2} \tag{8.37}$$

The chains of differentiations for all the required integrals are constructed in a similar manner. The complete chain of solutions is as follows

$$\left.\begin{array}{lllll}
(1) & (\alpha) & (\alpha\beta) & (\alpha\beta\tau) & (\alpha\beta\tau\sigma) \\
\mathcal{I}_{R0} & & & & \\
\mathcal{I}_{R1} & -\frac{1}{2}\frac{\partial}{\partial R_\alpha}\mathcal{I}_{R0} & & & \\
\mathcal{I}_{R2} & \frac{1}{2}\frac{\partial}{\partial R_\alpha}\mathcal{I}_{R1} & -\frac{1}{4}\frac{\partial}{\partial R_\beta}\frac{\partial}{\partial R_\alpha}\mathcal{I}_{R0} & & \\
\mathcal{I}_{R3} & \frac{1}{4}\frac{\partial}{\partial R_\alpha}\mathcal{I}_{R2} & \frac{1}{8}\frac{\partial}{\partial R_\beta}\frac{\partial}{\partial R_\alpha}\mathcal{I}_{R1} & -\frac{1}{16}\frac{\partial}{\partial R_\tau}\frac{\partial}{\partial R_\beta}\frac{\partial}{\partial R_\alpha}\mathcal{I}_{R0} & \\
\mathcal{I}_{R4} & \frac{1}{6}\frac{\partial}{\partial R_\alpha}\mathcal{I}_{R3} & \frac{1}{24}\frac{\partial}{\partial R_\beta}\frac{\partial}{\partial R_\alpha}\mathcal{I}_{R2} & \frac{1}{48}\frac{\partial}{\partial R_\tau}\frac{\partial}{\partial R_\beta}\frac{\partial}{\partial R_\alpha}\mathcal{I}_{R1} & -\frac{1}{96}\frac{\partial}{\partial R_\sigma}\frac{\partial}{\partial R_\tau}\frac{\partial}{\partial R_\beta}\frac{\partial}{\partial R_\alpha}\mathcal{I}_{R0} \\
\mathcal{I}_{R5} & \frac{1}{8}\frac{\partial}{\partial R_\alpha}\mathcal{I}_{R4} & \frac{1}{48}\frac{\partial}{\partial R_\beta}\frac{\partial}{\partial R_\alpha}\mathcal{I}_{R3} & \frac{1}{192}\frac{\partial}{\partial R_\tau}\frac{\partial}{\partial R_\beta}\frac{\partial}{\partial R_\alpha}\mathcal{I}_{R2} & \frac{1}{384}\frac{\partial}{\partial R_\sigma}\frac{\partial}{\partial R_\tau}\frac{\partial}{\partial R_\beta}\frac{\partial}{\partial R_\alpha}\mathcal{I}_{R1}
\end{array}\right\} \tag{8.38}$$

where the last three rows of this chain ($\mathcal{I}_{R3}\ldots$, $\mathcal{I}_{R4}\ldots$, $\mathcal{I}_{R5}\ldots$) are the integrals we require for $\mathcal{I}_1, \mathcal{I}_2, \mathcal{I}_3$ to evaluate second order maximally coupled scattering.

Hence, we have simplified the problem to requiring six integrals, with constant numerators, and evaluating a differentiation chain from these, rather than requiring fourteen individual integrals eleven of which have complicated 4–vector numerators.

8.6 4-space Integrals

Now

$$\mathcal{I}_{RA} = \int_{all\ space} \frac{\mathrm{d}^4k}{(k^2 - 2R.k - D)^A}$$

so if we move our origin

$$\kappa_\alpha = k_\alpha - R_\alpha \tag{8.39}$$

then

$$\begin{aligned} \mathrm{d}^4\kappa &= \mathrm{d}^4k \\ k^2 - 2R.k - D &= \kappa^2 - D_\kappa \end{aligned}$$

where $D_\kappa = D + R^2$, and

$$\mathcal{I}_{RA} = \int_{all\ space} \frac{d^4\kappa}{(\kappa^2 - D_\kappa)^A} \tag{8.40}$$

We are free to choose any suitable co-ordinate system to evaluate these integrals. Since the integral is now in the form $\int f(r)$, we choose the spherical polar co-ordinate system where

$$\mathrm{d}^4\kappa = \kappa^3 \,\mathrm{d}\kappa \,\mathrm{d}\phi \,\sin\theta_1 \,\mathrm{d}\theta_1 \,\sin^2\theta_2 \,\mathrm{d}\theta_2$$

and

$$0 < \kappa < \infty \quad ; \quad 0 < \phi < 2\pi \quad ; \quad 0 < \theta_1, \theta_2 < \pi$$

Thus

$$\mathcal{I}_{RA} = \int_0^{2\pi} \mathrm{d}\phi \int_0^{\pi} \sin\theta_1 \,\mathrm{d}\theta_1 \int_0^{\pi} \sin^2\theta_2 \,\mathrm{d}\theta_2 \int_0^{\infty} \frac{\kappa^3 \,\mathrm{d}\kappa}{(\kappa^2 - D_\kappa)^A} \tag{8.41}$$

the angular integrals may be trivially evaluated

$$\mathcal{I}_{RA} = 2\pi^2 \int_0^{\infty} \frac{\kappa^3 \,\mathrm{d}\kappa}{(\kappa^2 - D_\kappa)^A} \tag{8.42}$$

Let us substitute $\zeta = \kappa^2 \Rightarrow \mathrm{d}\zeta = 2\kappa \,\mathrm{d}\kappa$ so that

$$\mathcal{I}_{RA} = \pi^2 \int_0^{\infty} \frac{\zeta \,\mathrm{d}\zeta}{(\zeta - D_\kappa)^A} \tag{8.43}$$

which is trivially integrable by parts for $A > 2$,

$$\mathcal{I}_{RA}\Big|_{A>2} = \frac{\pi^2}{(A-1)(A-2)} \,\frac{1}{(-D_\kappa)^{(A-2)}} \tag{8.44}$$

The integral for $A = 2$ $(\zeta = \kappa^2)$

$$\begin{aligned} \mathcal{I}_{R2} &= \pi^2 \int_0^{\infty} \frac{\zeta \,\mathrm{d}\zeta}{(\zeta - D_\kappa)^2} \\ &= \pi^2 \lim_{\chi\to\infty} \int_0^{\chi} \frac{\zeta \,\mathrm{d}\zeta}{(\zeta - D_\kappa)^2} \\ &= \pi^2 \lim_{\chi\to\infty} \ln\left(\frac{\chi - D_\kappa}{-D_\kappa}\right) - 1 \end{aligned} \tag{8.45}$$

The limit $(\chi \to \infty)$ may be dealt with at any time. It is convenient to retain the solution in this limit form since differentiating such an expression with respect to R_α $(D_\kappa = D + R^2)$ will reduce it to a form where the limit may be simply applied.

When $A = 1$, as above (using REDUCE)

$$\begin{aligned} \mathcal{I}_{R1} &= \pi^2 \lim_{\chi\to\infty} \int_0^{\chi} \frac{\zeta \,\mathrm{d}\zeta}{(\zeta - D_\kappa)} \\ &= \pi^2 D_\kappa \lim_{\chi\to\infty} \left[\ln\left(\frac{\chi - D_\kappa}{-D_\kappa}\right) + \chi\right] \end{aligned} \tag{8.46}$$

Finally we need $A = 0$ (again, using REDUCE)

$$\begin{aligned} \mathcal{I}_{R0} &= \pi^2 \lim_{\chi\to\infty} \int_0^{\chi} \zeta \ln(\zeta - D_\kappa) \,\mathrm{d}\zeta \\ &= \frac{\pi^2}{4} \lim_{\chi\to\infty} \left[2\chi^2 \ln(\chi - D_\kappa) - 2D_\kappa^2 \ln\left(\frac{\chi - D_\kappa}{-D_\kappa}\right) - 2\chi D_\kappa - \chi^2\right] \end{aligned} \tag{8.47}$$

8.7 Differentiation

The integrals $\mathcal{I}_{RA}$, $A = 0, 1, \ldots, 5$ must now be differentiated as per the chain of solutions shown in equation 8.38. Simplifying, we require

$$\left.\begin{array}{lcl}
\mathcal{I}_1(1) & : & \mathcal{I}_{R3} \\
\mathcal{I}_1(\alpha) & : & \frac{1}{4}\frac{\partial}{\partial R_\alpha}\mathcal{I}_{R2} \\
\mathcal{I}_1(\alpha\beta) & : & \frac{1}{8}\frac{\partial}{\partial R_\beta}\frac{\partial}{\partial R_\alpha}\mathcal{I}_{R1} \\
\mathcal{I}_1(\alpha\beta\tau) & : & -\frac{1}{16}\frac{\partial}{\partial R_\tau}\frac{\partial}{\partial R_\beta}\frac{\partial}{\partial R_\alpha}\mathcal{I}_{R0} \\
 & & \\
\mathcal{I}_2(1) & : & \mathcal{I}_{R4} \\
\mathcal{I}_2(\alpha) & : & \frac{1}{6}\frac{\partial}{\partial R_\alpha}\mathcal{I}_{R3} \\
\mathcal{I}_2(\alpha\beta) & : & \frac{1}{24}\frac{\partial}{\partial R_\beta}\frac{\partial}{\partial R_\alpha}\mathcal{I}_{R2} \\
\mathcal{I}_2(\alpha\beta\tau) & : & \frac{1}{48}\frac{\partial}{\partial R_\tau}\frac{\partial}{\partial R_\beta}\frac{\partial}{\partial R_\alpha}\mathcal{I}_{R1} \\
\mathcal{I}_2(\alpha\beta\tau\sigma) & : & -\frac{1}{96}\frac{\partial}{\partial R_\sigma}\frac{\partial}{\partial R_\tau}\frac{\partial}{\partial R_\beta}\frac{\partial}{\partial R_\alpha}\mathcal{I}_{R0} \\
 & & \\
\mathcal{I}_3(1) & : & \mathcal{I}_{R5} \\
\mathcal{I}_3(\alpha) & : & \frac{1}{8}\frac{\partial}{\partial R_\alpha}\mathcal{I}_{R4} \\
\mathcal{I}_3(\alpha\beta) & : & \frac{1}{48}\frac{\partial}{\partial R_\beta}\frac{\partial}{\partial R_\alpha}\mathcal{I}_{R3} \\
\mathcal{I}_3(\alpha\beta\tau) & : & \frac{1}{192}\frac{\partial}{\partial R_\tau}\frac{\partial}{\partial R_\beta}\frac{\partial}{\partial R_\alpha}\mathcal{I}_{R2} \\
\mathcal{I}_3(\alpha\beta\tau\sigma) & : & \frac{1}{384}\frac{\partial}{\partial R_\sigma}\frac{\partial}{\partial R_\tau}\frac{\partial}{\partial R_\beta}\frac{\partial}{\partial R_\alpha}\mathcal{I}_{R1}
\end{array}\right\} \tag{8.48}$$

The differentiations are algebraically tedious but relatively straight forward. The solution set for these 4-vector integrals is as follows (after extensive simplification using REDUCE, where appropriate, and evaluating the limit ($\chi \to \infty$) wherever possible.)

$$\begin{aligned}
\mathcal{I}_{R_1}(1) &= \mathcal{I}_{R3} \\
&= \frac{\pi^2}{2(-D-R^2)}
\end{aligned} \tag{8.49}$$

$$\begin{aligned}
\mathcal{I}_{R_1}(\alpha) &= \frac{1}{4}\frac{\partial}{\partial R_\alpha}\mathcal{I}_{R2} \\
&= \frac{\pi^2 R_\alpha}{2(-D-R^2)}
\end{aligned} \tag{8.50}$$

$$\begin{aligned}
\mathcal{I}_{R_1}(\alpha\beta) &= \frac{1}{8}\frac{\partial}{\partial R_\beta}\frac{\partial}{\partial R_\alpha}\mathcal{I}_{R1} \\
&= \frac{\pi^2}{4}\delta_{\alpha\beta}\lim_{\chi\to\infty}\ln\left(\frac{\chi-D-R^2}{-D-R^2}\right) - \frac{\pi^2\delta_{\alpha\beta}}{4} + \frac{\pi^2 R_\alpha R_\beta}{2(-D-R^2)}
\end{aligned} \tag{8.51}$$

$$\begin{aligned}\mathcal{I}_{R_1}(\alpha\beta\tau) &= -\tfrac{1}{16}\frac{\partial}{\partial R_\tau}\frac{\partial}{\partial R_\beta}\frac{\partial}{\partial R_\alpha}\mathcal{I}_{R1} \\ &= -\frac{\pi^2}{4}\left[\delta_{\alpha\beta}R_\tau + \delta_{\alpha\tau}R_\beta + \delta_{\beta\tau}R_\alpha\right]\lim_{\chi\to\infty}\left[2 - \ln\left(\frac{\chi - D - R^2}{-D - R^2}\right)\right] \\ &\quad -\frac{\pi^2 R_\alpha R_\beta R_\tau}{2(-D-R^2)}\end{aligned} \tag{8.52}$$

$$\begin{aligned}\mathcal{I}_{R_2}(1) &= \mathcal{I}_{R4} \\ &= \frac{\pi^2}{6(-D-R^2)^2}\end{aligned} \tag{8.53}$$

$$\begin{aligned}\mathcal{I}_{R_2}(\alpha) &= \tfrac{1}{6}\frac{\partial}{\partial R_\alpha}\mathcal{I}_{R3} \\ &= \frac{\pi^2 R_\alpha}{6(-D-R^2)^2}\end{aligned} \tag{8.54}$$

$$\begin{aligned}\mathcal{I}_{R_2}(\alpha\beta) &= \tfrac{1}{24}\frac{\partial}{\partial R_\beta}\frac{\partial}{\partial R_\alpha}\mathcal{I}_{R2} \\ &= \frac{\pi^2\delta_{\alpha\beta}}{12(-D-R^2)} + \frac{\pi^2 R_\alpha R_\beta}{6(-D-R^2)^2}\end{aligned} \tag{8.55}$$

$$\begin{aligned}\mathcal{I}_{R_2}(\alpha\beta\tau) &= \tfrac{1}{48}\frac{\partial}{\partial R_\tau}\frac{\partial}{\partial R_\beta}\frac{\partial}{\partial R_\alpha}\mathcal{I}_{R1} \\ &= \frac{\pi^2}{12(-D-R^2)}\left[\delta_{\alpha\beta}R_\tau + \delta_{\alpha\tau}R_\beta + \delta_{\beta\tau}R_\alpha\right] + \frac{\pi^2 R_\alpha R_\beta R_\tau}{6(-D-R^2)^2}\end{aligned} \tag{8.56}$$

$$\begin{aligned}\mathcal{I}_{R_2}(\alpha\beta\tau\sigma) &= -\tfrac{1}{96}\frac{\partial}{\partial R_\sigma}\frac{\partial}{\partial R_\tau}\frac{\partial}{\partial R_\beta}\frac{\partial}{\partial R_\alpha}\mathcal{I}_{R0} \\ &= -\frac{\pi^2}{24}\left(\delta_{\alpha\beta}\delta_{\sigma\tau} + \delta_{\alpha\tau}\delta_{\sigma\beta} + \delta_{\beta\tau}\delta_{\sigma\alpha}\right)\left[1 - \lim_{\chi\to\infty}\ln\left(\frac{\chi - D - R^2}{-D-R^2}\right)\right] \\ &\quad -\frac{\pi^2}{12(-D-R^2)}\left[\delta_{\alpha\beta}R_\sigma R_\tau + \delta_{\alpha\tau}R_\sigma R_\beta + \delta_{\beta\tau}R_\sigma R_\alpha\right. \\ &\quad \left.+\delta_{\alpha\sigma}R_\beta R_\tau + \delta_{\beta\sigma}R_\alpha R_\tau + \delta_{\sigma\tau}R_\alpha R_\beta\right] \\ &\quad +\frac{\pi^2}{6(-D-R^2)^2}R_\alpha R_\beta R_\tau R_\sigma\end{aligned} \tag{8.57}$$

$$\begin{aligned}\mathcal{I}_{R_3}(1) &= \mathcal{I}_{R5} \\ &= \frac{\pi^2}{12}\frac{1}{(-D_\kappa)^3}\end{aligned} \tag{8.58}$$

$$\begin{aligned}\mathcal{I}_{R_3}(\alpha) &= \tfrac{1}{8}\frac{\partial}{\partial R_\alpha}\mathcal{I}_{R4} \\ &= \frac{\pi^2 R_\alpha}{12(-D-R^2)^3}\end{aligned} \tag{8.59}$$

$$\begin{aligned}
\mathcal{I}_{R_3}(\alpha\beta) &= \tfrac{1}{48}\frac{\partial}{\partial R_\beta}\frac{\partial}{\partial R_\alpha}\mathcal{I}_{R3} \\
&= \frac{\pi^2\delta_{\alpha\beta}}{48(-D-R^2)^2} + \frac{\pi^2 R_\alpha R_\beta}{12(-D-R^2)^3}
\end{aligned} \tag{8.60}$$

$$\begin{aligned}
\mathcal{I}_{R_3}(\alpha\beta\tau) &= \tfrac{1}{192}\frac{\partial}{\partial R_\tau}\frac{\partial}{\partial R_\beta}\frac{\partial}{\partial R_\alpha}\mathcal{I}_{R2} \\
&= \frac{\pi^2}{48(-D-R^2)^2}\left[\delta_{\alpha\beta}R_\tau + \delta_{\alpha\tau}R_\beta + \delta_{\beta\tau}R_\alpha\right] + \frac{\pi^2 R_\alpha R_\beta R_\tau}{12(-D-R^2)^3}
\end{aligned} \tag{8.61}$$

$$\begin{aligned}
\mathcal{I}_{R_3}(\alpha\beta\tau\sigma) &= -\tfrac{1}{384}\frac{\partial}{\partial R_\sigma}\frac{\partial}{\partial R_\tau}\frac{\partial}{\partial R_\beta}\frac{\partial}{\partial R_\alpha}\mathcal{I}_{R1} \\
&= -\frac{\pi^2}{96(-D-R^2)}\left[\delta_{\alpha\beta}\delta_{\sigma\tau} + \delta_{\alpha\tau}\delta_{\sigma\beta} + \delta_{\beta\tau}\delta_{\alpha\sigma}\right] \\
&\quad -\frac{\pi^2}{48(-D-R^2)^2}\left[\delta_{\alpha\beta}R_\sigma R_\tau + \delta_{\alpha\tau}R_\sigma R_\beta + \delta_{\beta\tau}R_\sigma R_\alpha\right. \\
&\quad \left. + \delta_{\alpha\sigma}R_\beta R_\tau + \delta_{\beta\sigma}R_\alpha R_\tau + \delta_{\sigma\tau}R_\alpha R_\beta\right] \\
&\quad -\frac{\pi^2}{12(-D-R^2)^3}R_\alpha R_\beta R_\tau R_\sigma
\end{aligned} \tag{8.62}$$

We now need to substitute for the appropriate R_i 4-vector and perform the integrations over x, y, z, L.

8.8 Integration Over the Dummy Variables

The 4-vector integrals of Section 8.7, equations 8.49 – 8.62, must be integrated as shown in equation 8.26. The R_i 4-vectors and the D_i are given in equations 8.21, 8.23 and 8.25. As an example of the method let us evaluate the x, y, z, L integrals of $\mathcal{I}_2(\alpha\beta)$.

For this integral $R = R_2$ and (from equations 8.12 and 8.55)

$$\begin{aligned}
\mathcal{I}_2\alpha\beta &= -\int_0^{\lambda^2} \mathrm{d}L \int_0^1 3y^2\mathrm{d}y \int_0^1 2x\mathrm{d}x\ \mathcal{I}_{R_2}(\alpha\beta) \\
&= -\int_0^{\lambda^2} \mathrm{d}L \int_0^1 3y^2\mathrm{d}y \int_0^1 2x\mathrm{d}x \left[\frac{\pi^2\delta_{\alpha\beta}}{12(-D-R^2)} + \frac{\pi^2 R_\alpha R_\beta}{6(-D-R^2)^2}\right]
\end{aligned} \tag{8.63}$$

We split this expression in the obvious way

$$\mathcal{I}_2\alpha\beta = T_1 + T_2 \tag{8.64}$$

with

$$\begin{aligned}
T_1 &= -\int_0^{\lambda^2} \mathrm{d}L \int_0^1 3y^2\mathrm{d}y \int_0^1 2x\mathrm{d}x\ \frac{\pi^2\delta_{\alpha\beta}}{12(-D-R^2)} \\
T_2 &= -\int_0^{\lambda^2} \mathrm{d}L \int_0^1 3y^2\mathrm{d}y \int_0^1 2x\mathrm{d}x\ \frac{\pi^2 R_\alpha R_\beta}{6(-D-R^2)^2}
\end{aligned} \tag{8.65}$$

Looking firstly at the integral on x, we substitute the expression for R_2 from equation 8.23 to find

$$\begin{aligned} T_1 &= -\frac{\pi^2\delta_{\alpha\beta}}{12}\int_0^{\lambda^2} \mathrm{d}L \int_0^1 3y^2\mathrm{d}y \int_0^1 \frac{2x\ \mathrm{d}x}{a_2x^2+a_1x+a_0} \\ T_2 &= -\frac{\pi^2}{6}\int_0^{\lambda^2} \mathrm{d}L \int_0^1 3y^2\mathrm{d}y \int_0^1 \frac{b_2x^2+b_1x+b_0}{(a_2x^2+a_1x+a_0)^2}\ 2x\mathrm{d}x \end{aligned} \tag{8.66}$$

where

$$\begin{aligned} a_2 &= -p_a^2y^2 \\ a_1 &= 2y^2(pa^2 - p_a.p_b) + y(2p_a.p_b - L) \\ a_0 &= -y^2(p_a-p_b)^2 - 2yp_b.(p_a-p_b) - p_a^2 \\ b_2 &= y^2p_{a\alpha}p_{b\beta} \\ b_1 &= y^2(p_{a\alpha}p_{b\beta} - 2p_{a\alpha}p_{a\beta} + p_{a\alpha}p_{b\alpha}) - y(p_{a\alpha}p_{b\beta} + p_{a\beta}p_{b\alpha}) \\ b_0 &= (yp_{a\alpha} - yp_{b\alpha} + p_{b\alpha})(yp_{a\beta} - yp_{b\beta} + p_{b\beta}) \end{aligned} \tag{8.67}$$

These expressions are integrable, and the definite integrals on x are (using REDUCE 3.2)

$$\begin{aligned} T_1 = \frac{\pi^2\delta_{\alpha\beta}}{2}\int_0^{\lambda^2} \mathrm{d}L \int_0^1 \mathrm{d}y \frac{y^2\sqrt{4a_2a_0-a_1^2}}{(4a_2a_0-a_1^2)a_2} \\ \times\left\{ a_1\left[\arctan\left(\frac{2a_2+a_1}{\sqrt{4a_2a_0-a_1^2}}\right) - \arctan\left(\frac{a_1}{\sqrt{4a_2a_0-a_1^2}}\right)\right]\right. \\ \left. -(4a_2a_0-a_1^2)\log\left(\frac{a_2+a_1+a_0}{a_0}\right)\right\} \end{aligned} \tag{8.68}$$

and

$$\begin{aligned} T_2 = \frac{\pi^2}{2}\int_0^{\lambda^2} \mathrm{d}L \int_0^1 \frac{-y^2\ \mathrm{d}y}{(4a_2a_0-a_1^2)^2(a_2+a_1+a_0)a_2^2} \\ \times\left\{ 2\left[2(3b_2+b_1)a_1a_0 + (b_1-b_0)a_1^2 + 4a_0^2b_2\right]a_2^2a_1\right. \\ -4\left[4(b_2+b_1)a_0^2 + 2(b_1-b_0)a_1a_0 + a_1^2b_0\right]a_2^3 \\ -2\left(2a_2^2a_1b_0 - 4a_2^2a_0b_1 + 6a_2a_1a_0b_2 - a_1^3b_2\right)\left(a_2+a_1+a_0\right)\sqrt{4a_2a_0-a_1^2} \\ \times\left[\arctan\left(\frac{2a_2+a_1}{\sqrt{4a_2a_0-a_1^2}}\right) - \arctan\left(\frac{a_1}{\sqrt{4a_2a_0-a_1^2}}\right)\right] \\ +\log\left(\frac{a_2+a_1+a_0}{a_0}\right)(4a_2a_0-a_1^2)^2(a_2+a_1+a_0)b_2 \\ \left. -2(a_1+a_0)a_2a_1^3b_2 + 16a_2^4a_0b_0\right\} \end{aligned} \tag{8.69}$$

Substituting the values for a_2, etc from equation 8.67 into either of these two expressions results in a long (>100 lines), extremely complicated expression to further integrate.

Indeed, we have been unable to develop a method to suitably integrate such terms. All of the integrals over these dummy variables have this or similar problem, regardless of which variable is chosen to commence the integration sequence.

Due to the altered thrust of the research from our original intention (after finding Rosenbluth's sign error), although this method has been successful up to this point, we have been unable to complete the integration over the dummy variables for any of these integrals. Further research is indicated to complete this aspect.

8.9 Discussion

We have obtained the traces of the matrix elements required for two-photon scattering. The integration of these matrix elements with respect to the extra 4-momentum (k) is extremely difficult. The change in the thrust of the research from its original direction, due to our discovery of Rosenbluth's possible sign error (as discussed earlier), has meant that the complete solution of these integrals is beyond the scope of this report.

Significant progress has been made in developing a systematic approach to the integration of the traces. Solutions to all of the spatial integrations have been found, although some are not yet in a closed form. This should allow the complete solution of the integrals to be performed in later work.

Chapter 9

Conclusion

The original thrust of the research reported here was to extend maximally coupled QED to second order and, along the way, to investigate a few interesting first order phenomena to which the maximally coupled model might be expected to apply.

Being unable to find any derivation in the literature, I have re-derived the maximally coupled vertex. My resultant vertex disagrees with that used by Rosenbluth (and hence all subsequent workers in the field). Discovering this discrepancy caused a major change in direction for the research, extending the maximally coupled model to second order became less important than investigating the wide ranging implications of the discrepancy.

Using the vertex derived here I have shown that the full maximally coupled scattering cross-section to first order for electron-proton scattering to be in far better agreement with experiment than the commonly employed Rosenbluth model prediction. Further, at around 200 MeV the prediction developed here agrees with experiment to within the experimental uncertainties. At higher energies (and hence exchange momenta) this agreement falls away, however it is always in better agreement than the bare Rosenbluth expression.

Through an investigation of the relative magnitudes for the various terms contributing to the maximally coupled cross-section I have shown that Rosenbluth's second assumption (ignoring the electron dipole charge) can not be justified. Rosenbluth's model, but using the vertex developed here, differs little from the minimally coupled result. Further, I have shown that for exchanged momentum around the proton rest mass, the dipole-dipole terms are comparable to or larger than the monopole-monopole terms. Hence the dipole terms become more important as the exchanged energy increases, which is the opposite to the assumptions originally made by Rosenbluth and implicitly applied by all subsequent workers. These observations have removed the main justifications on which form factor fitting of Rosenbluth's expression to experiment is based, and I have discussed the difficulty of trying to re-develop such a method to fit the full maximally coupled predictions to experiment.

I discussed the application of maximally coupled QED to particle decays. In the case investigated here I obtained a neutron lifetime within 15% of the latest experimental value from a first order analysis involving no free parameters.

I have shown that maximally coupled QED neutron-proton scattering accounts for about 10^{-4} of the measured scattering. This is as expected since these particles interact via both the electromagnetic and strong nuclear forces, the latter dominating the interaction.

I found poor agreement between the maximally coupled QED model and experiment for electron-neutron scattering. However, the usual model for extracting electron-neutron scattering from the experimentally measured electron-deuteron scattering data is based on a minimally coupled model. I have seriously questioned the application of this to a maximally coupled calculation. The minimally coupled model takes no account of either the neutron and proton spins nor their dipole charges. The development of a new model reflecting the fundamental importance of the dipole moments and dipole charges to the interaction was beyond the scope of the research reported here and is left for future research.

All of the two-photon scattering matrix elements for any two non-identical fermions have been calculated, up to the integrations over the extra 4-momentum (k). These integrals have been partially completed here, and all of the 4-space integrations have been performed and are presented. Due to the complexity of the intermediate expressions, I have not however been able to solve the integrations over the dummy variables employed to complete the evaluation of the required integrals for two-photon scattering. This is one of the consequences of the change in direction of the research. The development, as reported here, of a systematic approach to these integrals will allow their solution in later research.

Much of the research reported here has been of a speculative nature, testing the application and validity of the maximally coupled QED model. I believe we have shown the superiority of this conceptually simple (if somewhat more mathematically complicated) extension of minimally coupled QED. The model applies to and gives sensible predictions for the usual QED interactions and also for neutron decay, which could not previously be addressed using solely electromagnetic considerations. Much work in this field remains, and the ground work is laid here for the extension of maximally coupled QED into second order interactions.

Aknowledgements

I would like to thank Dr Philip H. Butler for his enormous help with many aspects of the research reported here, for his enthusiasm and support; Mrs Jennifer D. Allan for her understanding and Mr Hughan J. Ross for his helpful discussions and clarification of several obscure mathematical details.

Bibliography

Aitchison I.J.R. and Hey A.J.G, 1984, *Gauge Theories in Particle Physics*, Adam Hilger, Bristol.

Albrecht W., Behrend H.J., Braise F.W., Flauger W., Hultschig H., Steffen K.G., 1966, *Elastic Electron–Proton Scattering at Momentum Transfers up to* $245F^{-2}$, Phys. Rev. Lett., **17**, 1192.

Albrecht W., Behrend H.J., Dorner H., Flauger W., Hultschig H., 1967, *Some Recent Measurements of Proton Form Factors*, Phys. Rev. Lett., **18**, 1014.

Bartel W., Dudelzak B., Krehbeil H., M^{c}Elroy J.M., Meyer–Berkhout U., Morrison R.J, Nguyen–Nyoc H., Schmidt W., Webber G., 1966, *Small–angle Electron–Proton Elastic Scattering Cross–Section for Squared Momentum Transfers Between* 10 *and* $105F^{-2}$, Phys. Rev. Lett., **17**, 608.

Bartel W., Dudelzak B., Krehbeil H., M^{c}Elroy J.M., Meyer–Berkhout U., Morrison R.J, Nguyen–Nyoc H., Schmidt W., Webber G., 1967, *The Charge Form Factor of the Proton at a Momentum Transfer of* $75fm^{-2}$, Phys. Lett., **25B**, 236.

Bartel W. Büszer W., Div R., Felst R. Harms D., Krehbeil H., Kuhlmann P.E., M^{c}Elroy J.M., Webber G., 1970, *Electromagnetic Proton Form Factors at Squared Four–Momentum Transfer Between* 1 *and* $3(GeV/c)^2$, Phys. Lett., **33B**, 245.

Barut A.O., 1981, *Magnetic Interactions of Stable Particles and Magnetic Resonances*, p73–108, in Selegman T.H. (Ed), *Group Theory and it's Applications in Physics–1980*, Am. Inst. Phys., New York, 1981.

Barut A.O. and McEwan J., 1984, *A Generalized Local U(1) Gauge Invariance for both Standard and Pauli Couplings of QED*, Phys. Lett., **135**, 172.

Behrend H.J., Brasse F.W., Engler J., Hiltshig H., Galster S., Hartwig G., Schopper H., Ganssauge E., 1967, *Elastic Electron–Proton Scattering at Momentum Transfers up to* $110fermi^{-2}$, N. Cim., **A48**, 140.

Berestetskii V.B., Lifshitz E.M., Pitaevskii L.P., 1971, *Relativistic Quantum Theory, Part 1*, Permagon Press, Oxford, England.

Berger C., Gersing E., Knop G., Langenbeck B., Rith K., Schumaker F., 1968, *Electromagnetic Form Factors of the Proton Between* 15 *and* $50fm^{-2}$, Phys. Lett., **28B**, 276.

Berger C., Berket V., Knop G., Langenbeck B., Rith K., 1971, *Electromagnetic Form Factor of the Proton at squared Four–Momentum Transfer* 15 *and* $50fm^{-2}$, Phys. Lett., **35B**, 87.

Berkelman K., Feldman M., Littauer R.M. Roose G., Wilson R.R., 1963, *Electron–Proton Scattering at High–Momentum Transfer*, Phys. Rev., **130**, 2061.

Bersbach A.J., Mischke R.E, Reiman A.H., 1976, *Neutron–Proton Forward Elastic Scattering From* 58 *to* $391MeV$, Phys. Rev., **D13**, 535.

Biedenharn L.C. and Louck J.D., 1981, *Angular Momentum in Quantum Physics, Theory and Application*, Encyclopedia of Mathematics and its Applications, **V8**, Addison Wesley, Reading, Mass..

Blankenbecler R., 1957, *Improved Sum Rule for Electron-Deuteron Scattering*, Bull. Am. Phys. Soc. Ser. II, **2**, 389.

Bohm A., 1979, *Quantum Mechanics*, Springer–Verlag, New York.

Budnitz R.J., Appel J., Carrol L., Chen J., Dunning J.R. Jr., Goiten M., Hanson K., Imrie D., Mistretta C., Walker J.K., Wilson R., 1968, *Neutron Form factors from Quasi–Elastic Electron–Deuteron Scattering*, Phys.Rev., **173**, 1357.

Bumiller F., Croissaux M., Hofstadter R., 1960, *Electron Scattering from the Proton*, Phys. Rev. Lett., **5**, 261.

Bumiller F., Croissaux M., Dally E., Hofstadter R., 1961, *Electromagnetic Form Factors of the Proton*, Phys. Rev., **124**, 1623.

Burling–Claridge G.R. and Butler P.H., 1989, *Rosenbluth Scattering and Pauli's Approach to Anomalous Magnetic Moments*, J. Phys. G., **15**, 571.

Butler P.H. and Burling–Claridge G.R., 1989, *Neutron β Decay From Maximally Coupled Quantum Electrodynamics*, J. Phys. G., **15**, L201.

Byrne J., 1988, *Half Life Defies Measurement*, Nature, **333**, 398.

Chambers E.E. and Hofstadter R., 1956, *Structure of the Proton*, Phys. Rev., **103**, 1454.

Chen K.W., Cone A.A, Dunning J.R. Jr., Frank S.G.F., Ramsey N.F., Walker J.K., Wilson R., 1963, *Electron–Proton Scattering at High Momentum Transfers*, Phys. Rev. Lett., **11**, 561.

Chen K.W., Dunning J.R. Jr., Cone A.A, Ramsey N.F., Walker J.K., Wilson R. , 1966, *Measurement of Proton Electromagnetic Form Factors at High Momentum Transfers*, Phys. Rev., **141**, 1267.

Cohen E.R. and Taylor B.N, 1986, *The 1986 Adjustment of the Fundamental Physical Constants*, CODATA Bulletin, **No.63**, Permagon, Oxford (reprinted 1987, *Rev. Mod. Phys.*, **59**, 1121).

Corben H.C, 1968, *Classical and Quantum Mechanics of Spinning Particles*, Holden-Day, San Francisco.

CRC Handbook of Chemistry and Physics, 64th Ed, 1983, CRC Press.

Donnelly T.W., Raskin A.S., 1986, *Considerations of Polarization in Inclusive Electron Scattering from Nuclei*, Ann. Phys., **169**, 247.

Dunning J.R., Chen K.W., Ramsey N.F., Res J.R., Shlaer W., Walker J.K., Wilson R., 1963, *Electron–Proton Elastic Scattering at* 1 *and* $4BeV$, Phys. Rev. Lett., **10**, 500.

Evans M.L., Glass G., Hiebert J.C., .Jain M., Kenefick R.A., Northcliffe L.C., Bonner B.E., Simmons J.E., Bjork C.W., Riley P.J., Bryant H.C., Gassapakis C.G., Dierterle B., Leavitt C.P., Wolfe D.M., Warren D.W., 1982, *Differential Cross–Section for n–p Elastic Scattering in the Angular Range* $51^0 < \theta^* < 180^0$ *at* $647.5MeV$, Phys. Rev., **C26**, 2525.

Feynman R.P., 1949, *Space-Time Approach to Quantum Electrodynamics*, Phys. Rev., **76**, 769.

Goiten M., Budnitz R.J., Carroll L., Chen J., Dunning J.R. Jr., Hanson K., Imrie D., Mistretta C., Walker J.K., Wilson R., Dell G.F., Fotino M., Paterson J.M., Winick H., 1967, *Measurements of Elastic Electron–Proton Scattering at High Momentum Transfer by a Coincidence Technique*, Phys. Rev. Lett., **18**, 1016.

Goiten M., 1970, *Elastic Electron–Proton Scattering Cross–Sections Measured by a Coincidence Technique*, Phys. Rev., **D1**, 2449.

Hand L.N., 1960, *Electron–Proton Scattering at* $900MeV$ *and* 135^0, Phys. Rev. Lett., **5**, 168.

Hofstadter R., Bumiller F., Yearian M.R., 1958, *The Electromagnetic Structure of the Proton and Neutron*, Rev. Mod. Phys., **30**, 482.

Hubert A.H., 1984, *Radiative Corrections to Electron–Proton Scattering*, MSc Thesis, University of Canterbury.

Itzykson C. and Zuber J.-B., 1980, *Quantum Field Theory*, McGraw–Hill, New York.

Jankus V.Z., 1956, *Calculation of Electron-Deuteron Scattering Cross-sections*, Phys. Rev., **102**, 1956.

Kirk P.N., Breidenbach M., Friedman J.I., Hartman G.C., Kendall H.W. Buschborn G., Coward D.H., DeStaebler H., Early R.A., Litt J., Minten A., Mo L.W., Panofsky W.K.H., Taylor R.E., Barish B.C., Loken S.C., Mar J., Pine J., 1973, *Elastic Electron-Proton Scattering at Large Four Momentum Transfers*, Phys. Rev., **D8**, 63.

Landau L.D. and Lifshitz E.M., 1975, *The Classical Theory of Fields*, Permagon Press, Oxford, England.

Landau L.D. and Lifshitz E.M., 1977, *Quantum Mechanics*, Permagon Press, Oxford, England.

Last J., Arnold M., Döhner J., Dubbers D. and Freedman S.J., 1988, *Pulsed–Beam Neutron Lifetime Measurement*, Phys. rev. Lett., **60**, 995.

McAllister R.W. and Hofstadter R., 1956, *Elastic Scattering of* $188MeV$ *Electrons from*

the Proton and the Alpha Particle, Phys. Rev., **102**, 851.

Mampe W., Ageron P., Bates C., Pendlebury J.M., Steyerl A., 1989, *Neutron Lifetime Measured with Stored Ultracold Neutrons*, Phys. Rev. Lett., **63**, 593.

Messiah A., 1965, *Quantum Mechanics Volume II*, North-Holland, Amsterdam.

Omnès R.,1971,*Introduction to Particle Physics*, Transl. by G. Barton (French ed., 1970), Wiley and Sons, New York.

Pauli W. and Weisskopf V., 1934, *Über die Quantisierung der skalaren relativistischen Wellengleichung*, Helv. Phys. Acta, **7**, 709.

Pilkuhn H., 1979, *Relativistic Particle Physics*, Springer Verlag, New York.

Ramond P., 1981, *Field Theory A Modern Primer*, Benjamin Cummins, Reading.

Redhead M.L.G., 1953, *Radiative Corrections to the Scattering of Electrons and Positrons by Electrons*, Proc. Roy. Soc., **220**, 219.

Rosenbluth M.N., 1950, *High-Energy Elastic Scattering of Electrons on Protons*, Phys. Rev., **79**, 615.

Sachs M., 1982, *A Generalized e-p Interaction at Small Distances from a New Approach to Electrodynamics*, Nouv. Cim., **70A**, 229.

Schwinger J., 1949, *Quantum Electrodynamics III. The Electromagnetic Properties of the Electron - Radiative Corrections to Scattering*, Phys. Rev., **76**, 790.

Voloshin M.B., Vysotsky M.I. and Okun L.B., 1986, *Electrodynamics of the Neutrino and Possible Effects for Solar Neutrinos*, Sov. Phys. JETP, **64**, 446.

Yearian M.R. and Hofstadter R., 1958, *Magnetic Form Factor of the Neutron*, Phys. Rev., **110**, 552.

Yennie D.R., Levy M.M., Ravenhall D.G., 1957, *Electromagnetic Structure of Nucleons*, Rev. Mod. Phys., **29**, 144.

Wilkinson D.H., 1982, *Analysis of Neutron β-Decay*, Nuclear Physics A, **377**, 474.

Appendix A

Rosenbluth Scattering and Pauli's Approach to Anomalous Magnetic Moments

The following pages are a photocopy of the article *Rosenbluth Scattering and Pauli's Approach to Anomalous Magnetic Moments* (Butler and Burling-Claridge 1989).

J. Phys. G: Nucl. Part. Phys. 15 (1989) 571–582. Printed in the UK

Rosenbluth scattering and Pauli's approach to anomalous magnetic moments

G Robert Burling-Claridge and Philip H Butler
Physics Department, University of Canterbury, Christchurch 1, New Zealand

Received 23 May 1988

Abstract. In standard QED particle interactions are evaluated using minimal coupling, coupling the particles solely through their (electric monopole) charges. The Dirac Hamiltonian is used to describe the interaction of a single spin-$\frac{1}{2}$ particle with an electromagnetic field. Pauli suggested the addition of a further gauge-invariant term to the Dirac Hamiltonian where the coupling constant for this extra term should not be directly linked to the particle's electric charge. We study some of the effects of this additional term and show that for the scattering of electrons off protons, the first-order Pauli–Dirac analysis has at least as good agreement with experiment as previous analyses based on the Dirac Hamiltonian. We show that Rosenbluth used the incorrect sign on the anomalous magnetic moment of the proton. Using Rosenbluth's prescription of considering only the proton's anomalous magnetic moment but correcting the sign, we find only a negligible difference from a completely Dirac analysis. Any proton form factors, and thus any charge distributions, deduced from the Rosenbluth result will be incorrect.

1. Introduction

The Dirac Hamiltonian is used to describe the interaction of a single spin-$\frac{1}{2}$ particle with an electromagnetic field. The particle is assumed to be coupled minimally to the field through the $q\not{A}$ term, which is dependent solely on the electric monopole charge, q. Pauli (Pauli and Weisskopf 1934) suggested appending a further gauge-invariant term to the Dirac Hamiltonian of the form $\not{F} = \sigma_{\alpha\beta}F^{\alpha\beta}$, where the coupling constant for this extra term is not connected with the particle's electric charge. It is well known that one can evaluate Pauli's extended Hamiltonian in a weak-field approximation to show that the coupling constant of the Pauli term gives a means of treating the anomalous magnetic moment of a spin-$\frac{1}{2}$ particle.

Rosenbluth (1950) and many others have used the Pauli–Dirac Hamiltonian—the Dirac Hamiltonian with Pauli's additional term—to describe an internal electromagnetic structure for the proton. However, many texts decry this modification on the grounds that the Pauli–Dirac Hamiltonian fails the power-counting definition of renormalisability (see, for example, Itzykson and Zuber 1980, p 381).

Problems in QED are commonly treated using a perturbative expansion in terms of the fine structure constant α. Barut (1981) awakened our interest in the Pauli modification by pointing out that the magnitudes of the anomalous magnetic moments of the electron, proton and neutron are nearly equal.

0954-3889/89/050571 + 12 $02.50

The rest of this paper is arranged as follows. In §2 we consider the Pauli modification to the Dirac Hamiltonian and show how the sign of this modification is fixed by consistency with experimental results. In §3 we find the vertex operator corresponding to this Pauli–Dirac Hamiltonian. The variational techniques of Landau and Lifshitz (1977) are used to obtain the conserved current, which is then equated to the vertex operator. The vertex operator that we derive has a different sign for the anomalous magnetic moment to that used by Rosenbluth (1950).

In §4 we use our Pauli–Dirac vertex and REDUCE III, an algebraic computational language, to calculate the complete first-order Pauli–Dirac scattering cross section for two non-identical fermions. Our result can be converted to that found by Rosenbluth if we take the incorrect sign on the anomalous magnetic moment and simplify the equation by setting one of these moments to zero. The standard Dirac result may also be extracted from ours by setting both of the anomalous moments to zero.

In §5 the results of §4 are compared graphically for elastic scattering of electrons off protons at beam energies of 188 MeV, 300 MeV, 400 MeV, 500 MeV and 550 MeV. Several interesting features are apparent. Finally in §6 we draw some conclusions about the validity of previous calculations in this field.

Throughout this paper we adopt the system of units where

$$c = \hbar = 1 \tag{1}$$

$$e = |q_e| \tag{2}$$

$$\alpha = e^2 \approx \tfrac{1}{137} \tag{3}$$

and adopt the Minkowski metric

$$g_{\alpha\beta} = \mathrm{diag}(1, -1, -1, -1). \tag{4}$$

3-vectors are denoted by bold characters. When showing indices explicitly we use italic subscripts (σ_b) for 3-vectors and greek (A_α) for 4-vectors.

The Pauli matrices, σ_a, are needed only via their commutation relations:

$$\begin{aligned} [\sigma_a, \sigma_b] &= 2i\varepsilon_{abc}\sigma_c \\ \{\sigma_a, \sigma_b\} &= 2\delta_{ab} I_2. \end{aligned} \tag{5}$$

2. The Pauli–Dirac Hamiltonian

The usual form of the Dirac Hamiltonian for a single fermion interacting with an electromagnetic field is

$$H_D = \not{p} - q\not{A} - m. \tag{6}$$

This electromagnetic potential interaction takes account only of the contribution of the particle's electric monopole charge, q.

The Dirac magnetic moment

$$\mu_D = q/2m \tag{7}$$

where q is the particle charge and m the particle mass, is a direct result of the particle's spin and charge (see for example Jackson 1975, §11.8).

In order to take account of the particle's anomalous magnetic moment, we use the additional term as suggested by Pauli

$$\xi \not{F} = \xi \sigma_{\alpha\beta} F^{\alpha\beta} \tag{8}$$

where $F^{\alpha\beta} = \partial^\alpha A^\beta - \partial^\beta A^\alpha$, $\sigma_{\alpha\beta} = \frac{1}{2}\mathrm{i}(\gamma_\alpha\gamma_\beta - \gamma_\beta\gamma_\alpha)$ and ξ is the coupling constant associated with this particular interaction.

The Dirac Hamiltonian H_D is thus modified to the Pauli–Dirac Hamiltonian:

$$H_{PD} = \not{p} - q\not{A} - m - \xi\not{F}. \tag{9}$$

Following Messiah (1965, footnote p 936) we can find the approximate, non-relativistic Hamiltonian in a weak magnetic field case, thus identifying the ξ coupling constant with the anomalous magnetic moment.

For convenience we choose the particular representation

$$\begin{aligned} &\gamma_\mu = (\beta, \beta\boldsymbol{\alpha}) \\ &\boldsymbol{B} = \nabla \times \boldsymbol{A} \\ &\alpha_k = \begin{pmatrix} 0 & \sigma_k \\ \sigma_k & 0 \end{pmatrix} \\ &\beta = \begin{pmatrix} 1 & 0 \\ 0 & -1 \end{pmatrix} \end{aligned} \tag{10}$$

and obtain

$$H_{nr} = \frac{1}{2m}(\boldsymbol{p} - q\boldsymbol{A})^2 + q\varphi - \left(\frac{q}{2m} + 2\xi\right)\boldsymbol{\sigma}\cdot\boldsymbol{B}. \tag{11}$$

The coefficient of the spin–dipole ($\boldsymbol{\sigma}\cdot\boldsymbol{B}$) term will be the experimentally measured magnetic moment. This experimental value is

$$\mu_{exp} = \mu_D + \mu_a, \tag{12}$$

where the Dirac magnetic moment, μ_D, is given by equation (7) and $\mu_a = 2\xi$ is the anomalous contribution to the magnetic moment.

For electrons, protons and their antiparticles we have

$$|\mu_{exp}| > |\mu_D|. \tag{13}$$

We deduce that given our choice in equation (9), μ_D and 2ξ have the same algebraic sign for these particles.

The Pauli–Dirac Hamiltonian of equation (9) is then

$$H_{PD} = \not{p} - q\not{A} - m - \tfrac{1}{2}\mu_a\not{F} \tag{14}$$

the '$-$' being forced by consistency to experimental results.

The familiar Dirac moments, equation (7), of the electron, proton and neutron are of quite different sizes. Expressed in terms of the Bohr magneton,

$$\mu_B = \frac{e}{2m_e} = 9.274 \times 10^{-24}\ \mathrm{J\,T^{-1}} \tag{15}$$

they are

$$\begin{aligned} &\text{electron: } \mu_{\mathrm{De}} = -\mu_{\mathrm{B}} \\ &\text{proton: } \mu_{\mathrm{Dp}} \simeq 0.001\,521\mu_{\mathrm{B}} \\ &\text{neutron: } \mu_{\mathrm{Dn}} = 0 \end{aligned} \tag{16}$$

since $m_e/m_p \approx 0.001\,521$ and $q_n = 0$.

The anomalous magnetic moments of these three particles have very similar magnitudes. If we express the anomalous magnetic moments in terms of $(\alpha/2\pi)\mu_B$, the leading term of the QED expansion for the anomalous moment of the electron, we find

$$\begin{aligned} &\text{electron: } \mu_{\mathrm{ae}} \simeq -0.998(\alpha/2\pi)\mu_{\mathrm{B}} \\ &\text{proton: } \mu_{\mathrm{ap}} \simeq 0.841(\alpha/2\pi)\mu_{\mathrm{B}} \\ &\text{neutron: } \mu_{\mathrm{an}} \simeq -0.898(\alpha/2\pi)\mu_{\mathrm{B}}. \end{aligned} \tag{17}$$

Observe that $(\alpha/2\pi) \approx 0.001\,162 \approx 0.76(m_e/m_p)$. Hence the anomalous and Dirac moments contribute almost equally to the experimental magnetic moment of the proton, whereas for the electron the anomalous contribution is three orders of magnitude less than the Dirac. For the neutron, the anomalous magnetic moment is the only contribution to the experimental moment.

3. The Pauli–Dirac vertex operator

The above derivation is in quantum mechanical operator notation, consistent with Messiah (1965). However we wish to change to quantum field theory notation. The Pauli–Dirac Hamiltonian of equation (14) represents the Hamiltonian of a system of fields. In a quantum field theory approach, we treat this Hamiltonian operator as a Hamiltonian density where the quantum field Pauli–Dirac Hamiltonian is

$$\begin{aligned} \mathcal{H}_{\mathrm{PD}} &= \int \langle \mathrm{f}|H_{\mathrm{PD}}|\mathrm{i}\rangle \, \mathrm{d}^3x \\ &= \int \langle \mathrm{f}|\not{p} - q\not{A} - m - \tfrac{1}{2}\mu_{\mathrm{a}}\not{F}|\mathrm{i}\rangle \, \mathrm{d}^3x. \end{aligned} \tag{18}$$

We calculate the response of the Hamiltonian density to a change in the potential, δA_a, and then define the current, J_a, as the coefficient of δA_a in the Hamiltonian (see Landau and Lifshiftz 1977, pp 470–1).

Suppose $A_a \rightarrow A'_a = A_a + \delta A_a$, then

$$H_{PD} \rightarrow H'_{PD} = H_{PD} + \delta H_{PD} \tag{19}$$

and

$$\mathcal{H}_{PD} \rightarrow \mathcal{H}'_{PD} = \mathcal{H}_{PD} + \delta\mathcal{H}_{PD}. \tag{20}$$

Using the antisymmetry of $\sigma_{\alpha\beta}$ and of $F_{\alpha\beta}$ we find

$$\begin{aligned} \delta H_{PD} &= -q\delta A_a \gamma^a - \mu_a \partial_\beta \sigma^{\beta a} \delta A_a \\ &= (-q\gamma^a - \mu_a \partial_\beta \sigma^{\beta a})\delta A_a \end{aligned} \tag{21}$$

and thus we have

$$\begin{aligned} \delta\mathcal{H}_{PD} &= \int \langle f|\delta H_{PD}|i\rangle \, d^3x \\ &= \int \langle f|(-q\gamma^a - \mu_a \partial_\beta \sigma^{\beta a})\delta A_a|i\rangle \, d^3x. \end{aligned} \tag{22}$$

Changing to the conjugate variables

$$\partial_a \rightarrow -ip_a \tag{23}$$

and thus changing the integral to momentum space, we find

$$\delta\mathcal{H}_{PD} = \frac{1}{(2\pi)^3} \int \langle f|(-q\gamma^a + i\mu_a p_\beta \sigma^{\beta a})\delta A_a|i\rangle \, d^3p. \tag{24}$$

The 4-vector current, J_a, is defined as

$$\delta\mathcal{H}_{PD} = \frac{1}{(2\pi)^3} \int (-qJ_a)\delta A^a \, d^3p. \tag{25}$$

Comparing equations (24) and (25) we deduce

$$\begin{aligned} qJ_a &= q\gamma_a - i\mu_a p^\beta \sigma_{\beta a} \\ &= q\gamma_a + \tfrac{1}{2}\mu_a(\not{p}\gamma_a - \gamma_a \not{p}). \end{aligned} \tag{26}$$

The interaction represented by equation (26) is that of the current of a single particle encountering an electromagnetic field, A_a, either an external field or a field due to a second particle. The 4-momentum, p, of equation (26) is the difference between the initial and final momenta of the particle and hence is equal to the 4-momentum of the electromagnetic field. Figure 1 shows the Feynman diagram representation of this vertex.

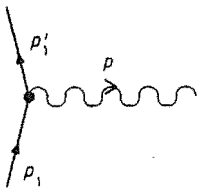

Figure 1. Interaction of a free particle with an electromagnetic field.

The usual Feynman rules may be applied to read this diagram. Figure 1 gives the Feynman amplitude

$$\begin{aligned} A(a: p_1', p_1, p) &= \bar{u}(p_1') V_a(p) u(p_1) \\ &= \int \langle \mathrm{f}| V_a(p) |\mathrm{i}\rangle \, \mathrm{d}^3 p \\ &= \int \langle \mathrm{f}| q J_a |\mathrm{i}\rangle \, \mathrm{d}^3 p. \end{aligned} \tag{27}$$

The above analysis has shown that the vertex for the Pauli–Dirac interaction of a spin-$\frac{1}{2}$ particle with an electromagnetic field is

$$V_a(p) = q\gamma_a + \tfrac{1}{2}\mu_a(\not{p}\gamma_a - \gamma_a \not{p}) \tag{28}$$

where the 4-momentum, p, is that of the photon. The sign of the momentum is positive if the photon is leaving the vertex.

This vertex derived here is outwardly similar to that used by Rosenbluth (1950) for the vertex of the proton interacting with the electromagnetic field of the electron in his scattering cross-section calculation. However Rosenbluth has the photon momentum in the opposite sense to that of figure 1.

Rosenbluth's vertex is

$$\begin{aligned} V_a(p)_{\mathrm{R}} &= V_a(-p) \\ &= q\gamma_a - \tfrac{1}{2}\mu_a(\not{p}\gamma_a - \gamma_a \not{p}) \end{aligned} \tag{29}$$

and corresponds to a Pauli–Dirac Hamiltonian which has the Pauli modification with the opposite sign:

$$H_{\mathrm{PD,R}} = \not{p} - q\not{A} - m + \tfrac{1}{2}\mu_a \not{F}. \tag{30}$$

As we have shown in §2 this requires an incorrect sign for the anomalous magnetic moments.

Note that the usual Dirac vertex

$$v_a = q\gamma_a \tag{31}$$

is the special case of both equations (28) and (29) with $\mu_a = 0$.

4. Scattering cross section

We calculate the first-order scattering cross section for two non-identical fermions interacting via the Pauli–Dirac Hamiltonian. This is described diagramatically by figure 2.

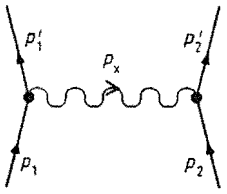

Figure 2. Interaction of two fermions (Pauli–Dirac vertices).

The Feynman amplitude of the interaction is

$$A = \bar{u}_1(p_1')V_{1\alpha}(p_x)u_1(p_1)\bar{u}_2(p_2')V_2^{\alpha}(-p_x)u_2(p_2)/p_x^2. \tag{32}$$

where the subscripts 1 and 2 refer to legs 1 and 2, respectively, p_x is the exchange momentum and we have suppressed the spin dependence of the spinors $u(p, s)$.

The intensity of the interaction is

$$\begin{aligned} M_{PD} = A^{\dagger}A = &[\bar{u}_1(p_1')V_{1\alpha}(p_x)u_1(p_1)]^{\dagger}\bar{u}_1(p_1')V_{1\beta}(p_x)u_1(p_1) \\ &\times [\bar{u}_2(p_2')V_2^{\alpha}(-p_x)u_2(p_2)]^{\dagger}\bar{u}_2(p_2')V_2^{\beta}(-p_x)u_2(p_2)/p_x^4. \end{aligned} \tag{33}$$

In general

$$[\bar{u}(p')V_{\alpha}(p)u(p'')]^{\dagger} = \bar{u}(p'')V_{\alpha}(-p)u(p') \tag{34}$$

so the intensity simplifies to

$$\begin{aligned} M_{PD} = &\bar{u}_1(p_1)V_{1\alpha}(-p_x)u_1(p_1')\bar{u}_1(p_1')V_{1\beta}(p_x)u_1(p_1) \\ &\times \bar{u}_2(p_2)V_2^{\alpha}(p_x)u_2(p_2')\bar{u}_2(p_2')V_2^{\beta}(-p_x)u_2(p_2)/p_x^4. \end{aligned} \tag{35}$$

Assuming that we do not know the initial polarisations of the particles and that we will not measure their final polarisations, the cross section measured will be a sum over the final polarisation states and an average over the $(2s_1+1)(2s_2+1)=4$ initial polarisation states. Thus any products $\bar{u}(p)u(p)$ may be replaced by their projection operators:

$$\bar{u}(p)u(p) \rightarrow \rho(p) = \tfrac{1}{2}(\not{p} + m). \tag{36}$$

We also use the identity (Berestetskii *et al* 1971, §29), for any F,

$$\sum^{\text{pol}} \bar{u}(p)Fu(p) = \text{tr}((\not{p} + m)F). \tag{37}$$

The intensity can now be expressed as a product of traces:

$$\begin{aligned} M_{PD} = &\text{tr}[(\not{p}_1 + m_1)V_{1\alpha}(-p_x)(\not{p}_1' + m_1)V_{1\beta}(p_x)] \\ &\times \text{tr}[(\not{p}_2 + m_2)V_2^{\alpha}(p_x)(\not{p}_2' + m_2)V_2^{\beta}(-p_x)]/(4p_x^4). \end{aligned} \tag{38}$$

The Dirac interaction intensity, M_D is simply the case where all the Pauli–Dirac vertices in the above equation are replaced by the Dirac vertices, v_a, of equation (31). Alternatively, we can calculate M_D by first calculating M_{PD} then setting $\mu_1 = \mu_2 = 0$.

Using the algebraic manipulation program REDUCE III, we find the complete intensity from equation (38) to be

$$\begin{aligned}16t^2M_{PD} = {} & 2q_1^2q_2^2[t(2s+t)+2(m_1^2+m_2^2-s)^2] \\ & + 4(q_1^2\mu_2^2+\mu_1^2q_2^2)t[s^2+(2s+t)(m_1^2+m_2^2-s)-(m_1^2-m_2^2)^2] \\ & + 4(q_1^2\mu_2^2m_2^2+\mu_1^2q_2^2m_1^2)t^2 \\ & + \mu_1^2\mu_2^2t^2[(2s+t)^2+8(m_1^2+m_2^2)(m_1^2+m_2^2-s)-4(m_1^2-m_2^2)^2] \\ & - 8q_1^2q_2\mu_2m_2t(t+2m_1^2)-8q_1\mu_1q_2^2m_1t(t+2m_2^2) \\ & - 4q_1\mu_1\mu_2^2m_1t^2(t+8m_2^2)-4\mu_1^2q_2\mu_2m_2t^2(t+8m_1^2) \\ & + 48q_1\mu_1q_2\mu_2m_1m_2t^2. \end{aligned} \tag{39}$$

The particles are always considered to be on mass-shell, i.e.

$$\begin{aligned} p_1^2 &= p_1'^2 = m_1^2 \\ p_2^2 &= p_2'^2 = m_2^2 \end{aligned} \tag{40}$$

and use is made of the Mandelstam invariants for elastic scattering:

$$\begin{aligned} s &= P^2 \qquad P = p_1+p_2 = p_1'+p_2' \\ t &= p_x^2 \qquad p_x = p_1-p_1' = p_2'-p_2. \end{aligned} \tag{41}$$

The intensity is invariant in form, but the values of the variables $(p_1, \ldots)$ are frame dependent. If we consider the scattering of electrons off protons in the laboratory frame, we have a stationary proton target (particle 2) being struck by a beam of electrons (particle 1). In the laboratory frame

$$\boldsymbol{p}_2 = 0 \tag{42}$$

and hence

$$\begin{aligned} E_2 &= m_2 \\ p_1'^2 &= m_1^2 = E_1'^2 - \boldsymbol{p}_1'^2 = E_1^2 - \boldsymbol{p}_1^2 = p_1^2 \\ p_1p_1' &= E_1E_2. \end{aligned} \tag{43}$$

The scattering cross section is (Berestetskii *et al* 1971, equation (65.19))

$$\left.\frac{d\sigma}{d\omega}\right|_{Lab} = \frac{E_1'^2}{E_1^2m_2^2}M_{PD}. \tag{44}$$

Landau and Lifshitz (1977, § 13) show that in general

$$E_1' = \frac{(E_1+m_2)(E_1m_2+m_1^2)+m_2(E_1^2-m_1^2)[1-(m_1/m_2)\sin^2\theta_1]^{1/2}m_2\cos\theta_1}{(E_1+m_2)^2-(E_1^2-m_1^2)\cos^2\theta_1} \tag{45}$$

where particle 1 is turned through an angle θ_1 from its original direction and E, E' are the initial and final energies respectively.

Rosenbluth calculated his cross section treating only the proton as interacting via the Pauli–Dirac term and used the incorrect sign for the proton's anomalous magnetic

moment. If we take the above intensity and follow Rosenbluth's approach it is possible, although somewhat of a struggle, to convert equation (39) to Rosenbluth's format:

$$M_R = \frac{q_e^2 q_p^2 E_e' \cos^2(\theta_e/2)}{4E_e^3 \sin^4(\theta_e/2)}\{1 + \tau[2(1+\kappa_p)^2 \tan^2(\theta_e/2) + \kappa_p^2]\} \tag{46}$$

where the subscript p refers to proton values, subscript e to electron values, $m_e = 0$, $\tau = -t/4m_p^2$ and $\kappa_p = (2m_p/q_p)\mu_{ap}$.

The next section compares these cross sections graphically and discusses some implications of the results.

5. Comparison with experiment

On the following graphs we have plotted the predicted and experimental curves for the scattering of electrons off protons in the laboratory frame, that is with a stationary proton target, for a range of energies from 188 MeV to 550 MeV. We have chosen to plot the following quantities.

(i) The experimental results, uncertainties shown (+). This data is from Hofstadter and McAllister (1956) and Hofstadter and Chambers (1956).

(ii) Rosenbluth's original expression (□). This result is that used by those modelling the internal distribution of the electric charge and magnetic dipole moment of the proton.

(iii) The full expression, both vertices Pauli–Dirac (▷).

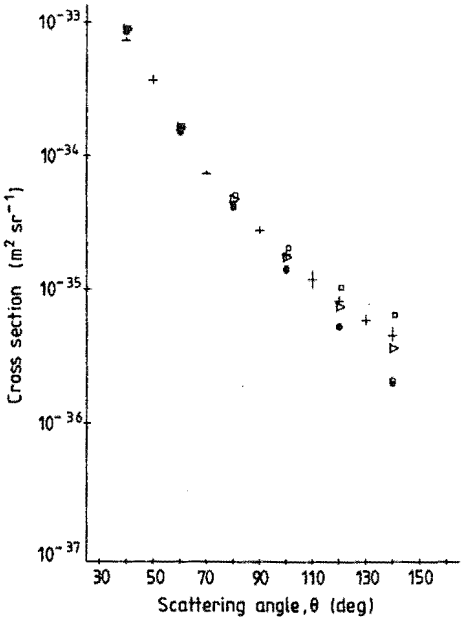

Figure 3. Scattering of electrons off protons; laboratory frame, 188 MeV. For explanation of symbols, see main text (§5).

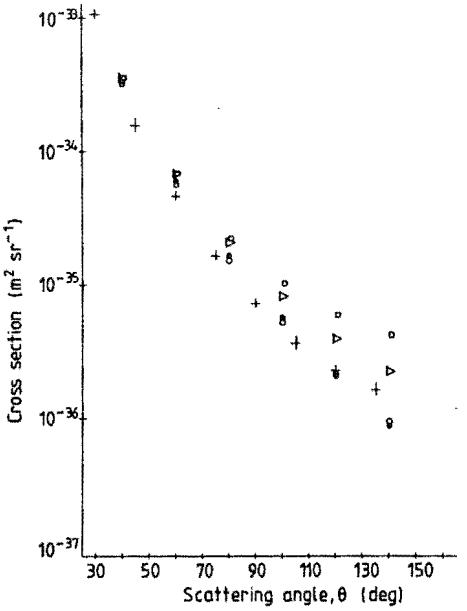

Figure 4. Scattering of electrons off protons; laboratory frame, 300 MeV. For explanation of symbols, see main text (§5).

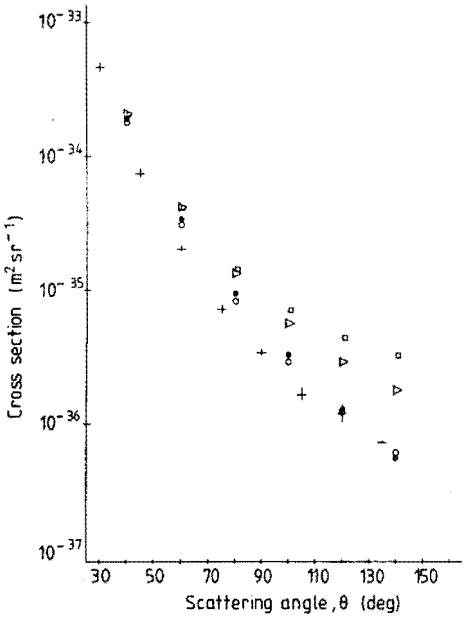

Figure 5. Scattering of electrons off protons; laboratory frame, 400 MeV. For explanation of symbols, see main text (§5).

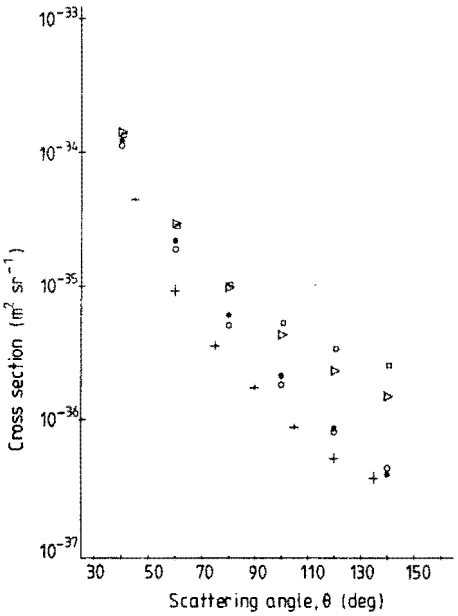

Figure 6. Scattering of electrons off protons; laboratory frame, 500 MeV. For explanation of symbols, see main text (§5).

(iv) The corrected form of Rosenbluth's results, namely with the proton vertex Pauli–Dirac and the electron vertex Dirac (●).

(v) The simple minimally coupled result for two spin-$\frac{1}{2}$ point particles, both vertices Dirac (○).

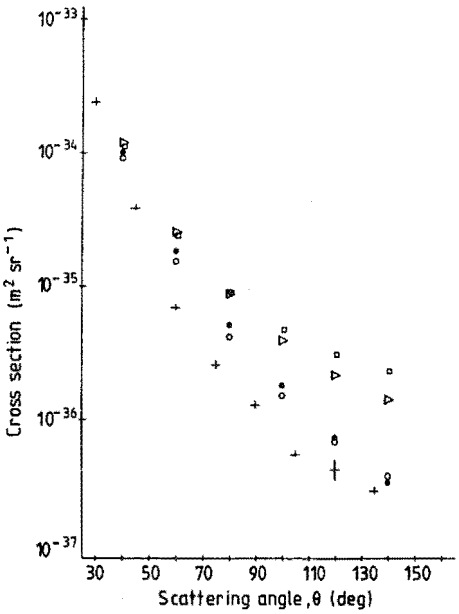

Figure 7. Scattering of electrons off protons; laboratory frame, 550 MeV. For explanation of symbols, see main text (§5).

In all of the plots, the original Rosenbluth cross section is larger than the experimental results. The full Pauli–Dirac cross section has much the same property but is always in better agreement than the Rosenbluth cross section. Note that at 188 MeV the Pauli–Dirac cross section is within two standard deviations of the experimental results.

The original Rosenbluth cross section, but with form factors to fit this curve to experimental results, is still in use (see for example Donnelly and Raskin (1986)). Yennie *et al* (1957), Hofstadter and Chambers (1956) and Kirk *et al* (1973), among others, compared the accuracy of several common form factors and attempted to fit physical charge distributions to these proton form factors with little success.

Recall that the Rosenbluth model treats only the proton as having an anomalous magnetic moment. However, we can see immediately from the graphs that with the correct vertex (●) this model deviates only slightly from the Dirac result (○). That is, the interaction between the anomalous magnetic dipole moment of the proton and the electric monopole charge of the electron is of little importance in this energy range.

This is quite contrary to the result obtained by using Rosenbluth's vertex. The only difference between Rosenbluth's original result and the corrected curve is a sign change on the anomalous magnetic moment of the proton. If $\mu_1 = 0$ in equation (39) we see that μ_2 occurs in various powers and combinations with q_1, q_2. Thus the correction of the sign causes a rather surprising cancellation of the effect of the proton's anomalous magnetic moment.

6. Conclusion

We have derived the Pauli–Dirac vertex for the anomalous magnetic moment from the gauge-invariant term that Pauli suggested adding to the Dirac Hamiltonian. The correct sign associated with the anomalous magnetic moment of the Pauli–Dirac vertex is the opposite of that used by Rosenbluth (1950).

The correct vertex has been used to derive a corrected version of Rosenbluth scattering and to derive the full expression for the Pauli–Dirac scattering of any two non-identical fermions. The resulting cross sections have been compared with experimental electron–proton scattering data for a range of energies from 188 MeV to 550 MeV.

There is substantial difference between Rosenbluth's cross section and the corrected cross section for his model. Those fitting Rosenbluth's result to experiment will have obtained quite misleading results for the form factors of the proton and no reliance can be placed on the charge distributions derived from these form factors (see Yennie *et al* 1957, Hofstadter *et al* 1958, Kirk *et al* 1973).

The corrected Rosenbluth cross section is close to the simple Dirac cross section, and cannot be fitted to the experimental results using Rosenbluth's original prescription for calculating the form factors. On the other hand, the Pauli–Dirac cross-section curves have a similar shape to the original Rosenbluth curves. While it may be possible to fit the full Pauli–Dirac curves to the experimental data using a method of finding form factors similar to that used for Rosenbluth's results, we see little worth in such an approach. Since the anomalous magnetic moment of the electron is about 10% larger than that of the proton, our suggestion is that one should consider the anomalous magnetic moments of both proton and electron to be of equal importance.

The anomalous magnetic moment of an electron is normally regarded in the standard model as being fixed by second- and higher-order QED effects. The scattering cross section analysis of this paper is a first-order calculation. The values of the anomalous magnetic moments that we quote are those derived from experiment, and there is no second-order effect brought into our calculation by our use of them. We introduce the Pauli modification with no appeal to higher-order terms in a perturbative expansion.

Our results show that the first-order Pauli–Dirac analysis has at least as good agreement with experiment as previous analyses based on either the Dirac Hamiltonian or on the corrected Rosenbluth vertex. We consider that if any form factors and charge distributions are to be derived using Rosenbluth's prescription, then it is necessary to use the full Pauli–Dirac cross section.

References

Aitchison I J R and Hey A J G 1982 *Gauge Theories in Particle Physics* (Bristol: Adam Hilger)

Barut A O 1981 *Group Theory and its Applications in Physics–1980* ed T H Selegman (AIP Conference Series 71) pp 73–108

Berestetskii V B, Lifshitz E M and Pitaevskii L P 1971 *Relativistic Quantum Theory* part 1 (Oxford: Pergamon)

Donnelly T W and Raskin A S 1986 *Ann. Phys., NY* **169** 247

Hofstadter R and Chambers E E 1956 *Phys. Rev.* **103** 1454

Hofstadter R and McAllister R W 1956 *Phys. Rev.* **102** 851

Hofstadter R, Bumiller F and Yearian M R 1958 *Rev. Mod. Phys.* **30** 482

Itzykson C and Zuber J-B 1980 *Quantum Field Theory* (New York: McGraw-Hill)

Jackson J D 1975 *Classical Electrodynamics* (New York: Wiley) 2nd edn

Kirk P N *et al* 1973 *Phys. Rev.* D **8** 63

Landau L D and Lifshitz E M 1977 *Quantum Mechanics* (Oxford: Pergamon)

Messiah A 1965 *Quantum Mechanics* vol II (Amsterdam: North-Holland)

Pauli W and Weisskopf V 1934 *Helv. Phys. Acta* **7** 709

Rosenbluth M N 1950 *Phys. Rev.* **79** 615

Yennie D R, Levy M M and Ravenhall D G 1957 *Rev. Mod. Phys.* **29** 144

Appendix B

Neutron β Decay from Maximally Coupled Quantum Electrodynamics

The following pages are a photocopy of the article *Neutron β Decay from Maximally Coupled Quantum Electrodynamics* (Burling-Claridge and Butler 1989).

J. Phys. G: Nucl. Part. Phys 15 (1989) L201–L207. Printed in the UK

LETTER TO THE EDITOR

Neutron β decay from maximally coupled quantum electrodynamics

Philip H Butler and G Robert Burling-Claridge
Physics Department, University of Canterbury, Christchurch 1, New Zealand

Received 27 April 1989, in final form 26 June 1989

Abstract. Maximally coupled quantum electrodynamics is shown to give a closed first-order expression for the β decay spectrum for a neutron, and a realistic value for the lifetime.

1. Introduction

Soon after Dirac introduced his relativistic quantum mechanics for spin-$\frac{1}{2}$ particles, Pauli pointed out that an additional electromagnetic term could be included in the Dirac Hamiltonian (Pauli 1933). It is well known that the Dirac Hamiltonian describes the minimal coupling of a spin-$\frac{1}{2}$ particle to the electromagnetic field, the particle's interaction being characterised by two scalar quantities (mass, m, and electric charge, q) and one spin quantity (s). The inclusion of Pauli's term describes the maximal coupling (Barut and McEwan 1984) of a spin-$\frac{1}{2}$ particle to the electromagnetic field, the particle's interaction now being characterised by the two scalar quantities (m, q) and two spin quantities (s and μ_a). The fourth quantity is known as the anomalous magnetic moment. However, only one extra parameter, μ_a, is introduced since μ_a is parallel to the spin vector s:

$$\mu_a = 2\mu_a s = \mu_a \sigma. \tag{1}$$

(We choose units so that $\hbar = c = 1$.)

With these parameters the Pauli–Dirac Hamiltonian is

$$H_{PD} = p - q\not{A} - m - \tfrac{1}{2}\mu_a \not{F}. \tag{2}$$

Pauli's term has not found favour with developments in the formulation of quantum electromagnetism for a number of reasons. One of the most important may have been an emphasis placed on a minimally coupled theory. The major use for the Pauli term has been in analysing the elastic scattering of electrons off protons and neutrons. In the usual model (Rosenbluth 1950) of electron–nucleon scattering, the electron is treated as a Dirac particle while the nucleon is modelled as having the electric monopole charge q (zero for the neutron), and a magnetic dipole charge μ_a, so that the laboratory-frame magnetic moment is a combination of the Dirac moment $2\mu_D s$ ($\mu_D = q/2m$) and the anomalous moment $2\mu_a s$. This model shows that above transfer momenta of 100 MeV c^{-1}, the predominant interaction is between the electron's electric monopole charge and the nucleon's anomalous magnetic

0954-3899/89/100201 + 07 $02.50

dipole charge. The Dirac moment, although behaving as a magnetic dipole in a uniform magnetic field, scales with distance (and transfer momentum) like the electric monopole charge.

It is usual to adjust the fit between experiment and the Rosenbluth point-particle scattering formula by means of adjustable form factors. These form factors are justified in terms of a model of a point electron and a distributed nucleon:

> 'The development of our present theory of strong interactions has been much influenced by measurement of form factors and by their theoretical interpretation'.
>
> Omnès (1971)

The widespread use of the form factors has led to a view that anomalous moments can only be the result of real electric charge (and electric current) distributions. This view conflicts with the treatment of the intrinsic angular momentum of point particles. Particles usually regarded as structureless (e.g. the electron) or both structureless and massless (e.g. the neutrino) nevertheless have a non-zero moment of their momentum about their centre, their intrinsic spin. Some of the conceptual and philosophical issues raised by this are discussed for example by Biedenharn and Louck (1981).

In a previous paper (Burling-Claridge and Butler 1989) we re-analysed electron proton scattering by treating both as Pauli–Dirac particles with ignorable internal structure. Our initial motivation was partly the above reasoning and partly that the anomalous magnetic moment for the electron is some 15% larger than for the proton. This latter fact is not widely appreciated because of the nearly universal use of g-factors. (It was pointed out to us by Barut in his lectures in Mexico, but not recorded in his notes, Barut 1981.) We were unable to find any analysis of the scattering of two maximally coupled spin-$\frac{1}{2}$ particles, nor were we able to find any published second-order corrections to the Rosenbluth result. (See, however, Hubert 1985.) Further, we were unable to find a derivation of the vertex operator as used by Rosenbluth and corresponding to the Pauli–Dirac Hamiltonian.

To our surprise, our derivation of the vertex operator gave the opposite sign of the magnetic dipole term. The use of this corrected sign for the anomalous moment, and the inclusion of it for the electron, produces a better fit to the scattering data. We therefore raised the issue of the validity of the proton form factors.

In this letter we offer a further calculation using anomalous magnetic moments. The neutron lifetime calculated here is in line with experimental results. We find this even more intriguing than the nucleon form factor re-analysis discussed above.

2. Assumptions

Our principal hypothesis is based upon the near equality of the magnitude of the electron, proton and neutron anomalous moments. We assume that these three particles, and also the (electron) neutrino, carry a quantised magnetic dipole charge

$$\mu_a = \frac{\alpha}{2\pi}\mu_B = \frac{\alpha}{2\pi}\frac{e}{2m_e} \tag{3}$$

and that the experimental (or laboratory frame, or weak field) moments arise as some (only approximately linear) combination of $\mu_a = (\alpha/2\pi)(e/2m_e)2s$ and $\mu_D =$

$(q/2m)2s$. We have

$$\begin{aligned} &\mu_a^{\text{quant}}(e^-) = -\mu_a \qquad && \mu_a^{\text{lab}}(e^-) \simeq -0.998\mu_a \\ &\mu_a^{\text{quant}}(p^+) = +\mu_a && \mu_a^{\text{lab}}(p^+) \simeq 0.841\mu_a \\ &\mu_a^{\text{quant}}(n) = -\mu_a && \mu_a^{\text{lab}}(n) \simeq -0.898\mu_a \\ &\mu_a^{\text{quant}}(\bar{\nu}_e) = -\mu_a. \end{aligned} \tag{4}$$

Since the neutrino's mass is known to be less than 30 eV, we are proposing a neutrino g-factor of less than 6×10^{-8}.

Our second assumption is based upon the observation that there is no requirement to assume equality of the masses associated with the parts of a fermion line. The form of the Pauli–Dirac vertex operator associated with the diagram in figure 1 is

$$V_\alpha(p_x) = q\gamma_\alpha + \tfrac{1}{2}\mu(\not{p}_x\gamma_\alpha - \gamma_\alpha\not{p}_x) \tag{5}$$

where q and μ are the electric monopole and magnetic dipole charges associated with the fermion line.

These assumptions allow us to draw the generalised Feynman diagram shown in figure 2, which we may interpret using the usual Feynman rules. The diagram of figure 2 models a neutron as decaying initially to a neutrino and a virtual photon, which later decays to an electron–proton pair. The diagram gives a closed expression for the β^- particle's energy spectrum and for the lifetime of the neutron. The maximally coupled vertex leads to a spin dependence in β-decay. We postpone for future work analysis of this spin dependence (and thus the possible parity violation (see appendix 3 of Wilkinson 1982)) of the first-order diagram (figure 2).

The diagram of figure 2 appears to be able to describe the decays of various particles. The non-baryon-conserving decay $p^+ \rightarrow e^+e^-e^+$ would need to be analysed in terms of three identical fermions. The muon decay $\mu^+ \rightarrow e^+\nu_\mu\nu_e$ is not related to this diagram because the laboratory frame anomalous moment of the muon is less than $0.01\mu_a$, quite different from (4) and thus a vertex $\mu^+ \rightarrow e^+\gamma$ is not allowed.

The decay channel $n \rightarrow \bar{\nu}_e e^+ p^-$ for the neutron gives, in this first-order analysis, the same result as in figure 2. It is, however, well known that first-order scattering theory does not distinguish between attractive and repulsive potentials. We expect the second-order diagrams to be important in resolving between particle and antiparticle channels.

3. Evaluation of the decay spectrum

Pilkuhn (1979) gives detailed examples of how to calculate a decay rate, Γ, for the decay of a single particle into three particles. We have

$$\Gamma = \frac{1}{2m_1}\int M \, \mathrm{d}\,\mathrm{Lips}(s : p_2, p_3, p_4) \tag{6}$$

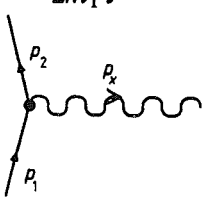

Figure 1. The Pauli–Dirac vertex operator.

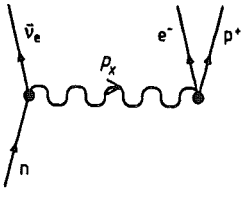

Figure 2. Neutron decaying to a neutrino and virtual photon.

where m_1 is the mass of the initial particle, $M = A\dagger A$ is the matrix element calculated from the amplitude A of the interaction and d Lips$(s : p_2, p_3, p_4)$ is the Lorentz-invariant element of phase space.

Pilkuhn (1979, § 4.6) evaluates d Lips in the rest frame of the initial particle (where $s = m_1^2$) as

$$\text{d Lips}(s : p_2, p_3, p_4) = (4\pi)^{-4}\pi^{-1}\,\mathrm{d}E_2\,\mathrm{d}E_3\,\mathrm{d}E_4\delta(m_1 - E_2 - E_3 - E_4)\,\mathrm{d}\Omega_4\,\mathrm{d}\phi \tag{7}$$

where Ω_4, ϕ define the orientation of the 3-momentum plane formed by $\boldsymbol{p}_2, \boldsymbol{p}_3, \boldsymbol{p}_4$. The spin-averaged matrix element is independent of Ω_4, ϕ and the δ function may be used to remove any one of three energy integrals, giving

$$\text{d Lips}(s : p_2, p_3, p_4) = (4\pi)^{-3}\,\mathrm{d}E_2\,\mathrm{d}E_3 \qquad \text{with } E_4 = m_1 - E_2 - E_3. \tag{8}$$

The limits of the E_2, E_3 integrals occur when $\boldsymbol{p}_2$, $\boldsymbol{p}_3$ and $\boldsymbol{p}_4$ are colinear, i.e. when

$$|\boldsymbol{p}_2| \pm |\boldsymbol{p}_3| \pm |\boldsymbol{p}_4| = 0. \tag{9}$$

Since

$$|\boldsymbol{p}_2|^2 = E_2^2 - m_2^2 \qquad \text{etc} \tag{10}$$

it is merely a matter of some algebra to find lower and upper limits on E_2, E_3 or equivalently on the kinetic energies, $K_i = E_i - m_i$.

The tracing and simplifications required to obtain the matrix element M_{PD} for the diagram of figure 2 was performed using REDUCE 3.3, running on a SUN workstation. (The program listing is given in figure 3.)

This part of the program is essentially that used to evaluate the Pauli–Dirac scattering cross section (Burling-Claridge and Butler 1989). The REDUCE output may be factorised to show that

$$\begin{aligned}
&16(m_{\mathrm{n}}^2 - 2m_{\mathrm{n}}E_\nu)^2 M_{\mathrm{PD}} \\
&\quad = \mu_1^2 q_2^2\{m_{\mathrm{n}}^2 X^2 + \tfrac{1}{2}m_{\mathrm{n}}E_\nu[4m_{\mathrm{n}}^2 m_{\mathrm{p}}^2 + 4m_{\mathrm{n}}^2 E_{\mathrm{e}}(m_{\mathrm{n}} - 2E_\nu) \\
&\qquad - 2m_{\mathrm{n}}(3m_{\mathrm{n}} - 4E_{\mathrm{e}} - 2E_\nu)X - m_{\mathrm{n}}(3m_{\mathrm{e}} - 2E_\nu)(m_{\mathrm{p}} + m_{\mathrm{e}})^2 - (m_{\mathrm{p}}^2 - m_{\mathrm{e}}^2)^2]\} \\
&\qquad - \mu_1^2 q_2 \mu_2 m_{\mathrm{n}}^2 E_\nu (m_{\mathrm{p}} - m_{\mathrm{e}})(3m_{\mathrm{n}} - 2E_\nu) \\
&\qquad \times [m_{\mathrm{n}}^2 - 2m_{\mathrm{n}}E_\nu - (m_{\mathrm{p}} + m_{\mathrm{e}})^2] \\
&\qquad + \mu_1^2 \mu_2^2 m_{\mathrm{n}}^2 [\![-m_{\mathrm{n}}^2 X^2 + \tfrac{1}{2}m_{\mathrm{n}}E_\nu(m_{\mathrm{n}}^4 - 2(m_{\mathrm{p}}^2 - m_{\mathrm{e}}^2)^2 \\
&\qquad + (m_{\mathrm{n}} - 2E_\nu)\{(3m_{\mathrm{n}} - 2E_\nu)[4X - (m_{\mathrm{p}} + m_{\mathrm{e}})^2 - 2m_{\mathrm{n}}E_\nu] \\
&\qquad + 4m_{\mathrm{n}}(m_{\mathrm{n}}^2 + m_{\mathrm{p}}^2 + m_{\mathrm{e}}^2) - 8m_{\mathrm{p}}^2 E_\nu\} - 4m_{\mathrm{n}}^2(m_{\mathrm{n}} - E_\nu)^2 \\
&\qquad - 4X(4m_{\mathrm{n}}E_{\mathrm{e}} - 4E_{\mathrm{e}}E_\nu - 2m_{\mathrm{n}}E_\nu + m_{\mathrm{p}}^2 - m_{\mathrm{e}}^2)]\!]
\end{aligned} \tag{11}$$

where

$$X = m_{\mathrm{n}}^2 - m_{\mathrm{p}}^2 + m_{\mathrm{e}}^2 - 2m_{\mathrm{e}}E_{\mathrm{e}}.$$

Either of the two integrations may be performed analytically by REDUCE; however, the substitution of the analytic limits causes problems, so we have evaluated both integrals numerically. The REDUCE procedure is included in the program listing (figure 3) as are the physical constants used (Cohen and Taylor 1986).

The decay probability $\Gamma(E_{\mathrm{e}}, E_\nu)$ varies less than 1% over each range of E_ν allowed by a fixed E_{e}. The size of this range is drawn in figure 4 together with the

```
%  REDUCE progam for maximally-coupled QED neutron lifetime
OFF RAISE;
     % pn to pnu + photon
     % photon to pe+pp

MASS     pn=mn, pe=me, pnu=mnu, pp=mp;
MSHELL   pn,pe,pnu,pp;
VECTOR   px;
INDEX    al,bt;
OPERATOR vertex,q,mu;
NONCOM   G,vertex;

FOR ALL  line,al,p LET
  vertex(line,al,p)=q(line)*G(line,al)
    + mu(line)*( G(line,p)*G(line,al)-G(line,al)*G(line,p) )/2;

trace := (G(1,pn )+mn ) * vertex(1,al,-px)
       * (G(1,pnu)+mnu) * vertex(1,bt, px)
       * (G(2,pe )+me ) * vertex(2,al, px)
       * (G(2,pp )+mp ) * vertex(2,bt,-px);

LET   px  = pn-pnu,    % momentum conservation at vertex
      pp  = pn-pe-pnu, % momentum conservation overall
   pn.pe  = mn*Ee,     % pn=(mn,0,0,0) in lab frame
   pn.pnu = mn*Enu,    %  ditto
                % because pn=pe+pnu+pp => (pe+pnu)^2 = (pn-pp)^2
   pe.pnu = (mn^2 - me^2 - mnu^2 + mp^2)/2 - pn.pp;

q(1) := 0 ;       mu(1) := mua;
q(2) := e ;       mu(2) := mua;

matrixelem:= trace/16/(px.px)^2;
% integral:=INT(INT(matrixelem,Knu),Ke) with the limits below;
life       := 2*mn*(4*PI)^3/integral;

%   Evaluate the boundaries of the Dalitz plot.
pe2  :=Ee^2-me^2;
pnu2 :=Enu^2-mnu^2;
pp2  :=Ep^2-mp^2;
Ep   :=mn-Ee-Enu;
z    :=pe2^2+pnu2^2+pp2^2-2*pe2*pnu2-2*pnu2*pp2-2*pp2*pe2;
%  checks sqrt(pe2) +- sqrt(pnu2) +- sqrt(pp2) => z=0
upKnu:= (-b+SQRT(discr))/(2*a) - mnu;
loKnu:= (-b-SQRT(discr))/(2*a) - mnu;
upKe :=(mn^2+me^2-(mnu+mp)^2)/(2*mn) - me;
loKe := me - me;
list :=COEFF(z,Enu);
c    :=FIRST(list);
b    :=SECOND(list);
a    :=THIRD(list);
discr:=16*(Ee^2-me^2)*(mn^2+me^2-2*mn*Ee- (mnu-mp)^2)
                    *(mn^2+me^2-2*mn*Ee- (mnu+mp)^2);
check:= b^2 - 4*a*c -discr;
Ee   := Ke+me;
Enu  := Knu+mnu;
```

(a)

Figure 3. The REDUCE program used for the calculations in this letter.

```
PROCEDURE numint(numKestep,numKnustep);
%      evaluate both the integrals numerically.
BEGIN
   MeV     := 1;
   numel   := matrixelem;
   numloKnu:= loKnu;
   numupKnu:= upKnu;
   Ke      := loKe;
   dKe     := (upKe-Ke)/numKestep;
   gamma   := 0;
   FOR i:=0:numKestep DO BEGIN
      Knu :=numloKnu; delKnu:=numupKnu-Knu;
      dKnu:=delKnu/numKnustep;
      WRITE "Ke=",Ke,"  delKnu=",delKnu;
      FOR j:=0:numKnustep DO BEGIN
         d2gam:=numel;
         WRITE "Knu=",Knu,"  d2gam=",d2gam;
         IF j=0 THEN dgam:=0 ELSE dgam:=dgam+d2gam*dKnu;
         Knu:=Knu+dKnu; END;
      WRITE "dne=",dgam/dKe;
      gamma:=gamma+dgam*dKe;
      Ke:=Ke+dKe; END;
   MeV:=MeVsec;
   integral:= gamma*MeV^2;
   WRITE Life:=life;
   CLEAR MeV,Ke,Knu;
END;

ON NUMVAL, BIGFLOAT; PRECISION 30;
   % h-cross = c = 1
alpha := 1/137.0359895   ;  % +/- 61
e     := SQRT(alpha);
mua   := alpha * e /4/PI/me;
metre := second/ 2.99792458E+8;
MeVsec:= 1/6.5821220E-22/second ;  % +/- 20
mn    := 939.56563    *MeV;  % +/- 28
me    :=   0.51099906*MeV;  % +/- 15
mnu   :=   0.000000   *MeV;  % +/- 30
mp    := 938.27231    *MeV;  % +/- 28

numint(30,3);
```

(b)

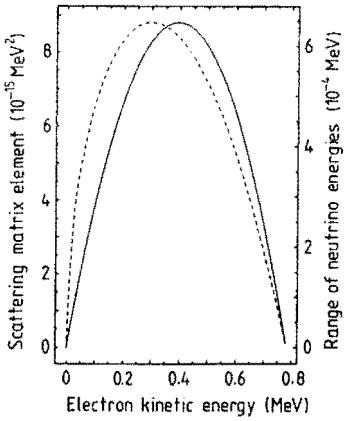

Figure 4. The two factors contributing to the β spectrum. The scattering matrix element $\Gamma(E_e, E_\nu)$ averaged over allowed E_ν (full curve), and the neutrino energy range, $E_\nu(\max) - E_\nu(\min)$ (broken curve).

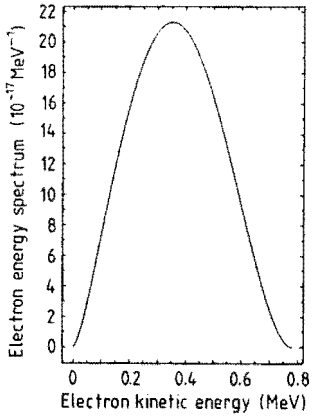

Figure 5. The β^- energy spectrum for neutron decay, as given by first-order maximally-coupled QED.

average value of $\Gamma(E_e, E_\nu)$. These two factors are combined in figure 5 to give the spectrum of electron energies.

4. The neutron lifetime

The calculation of the previous section gives a neutron lifetime, $\tau_n = 1015$ s. This value is startlingly close to the experimental values. The most recent experiment (Last *et al* 1988) gives $\tau_n = 876 \pm 21$ s; however, other experiments claiming similar accuracy (see Bryne (1988) for a brief review) give a range of values, one as high as 1013 ± 26 s. Last *et al* use the decay spectrum as determined from the standard model of weak interactions (the Glashow–Salam–Weinberg model) to extrapolate to the entire spectrum from a count of decays with $K_e \geq 363.7$ keV. Does the use of the β^- spectrum calculated from maximal electromagnetic coupling (figure 5) bring the value determined by Last *et al* into line with the lifetime measured by other techniques?

The value for τ_n computed here is very sensitive to the value of μ_a chosen for the e^-p^+ fermion line. Its large value depends on the near cancellation of the $q_2\mu_2$ term with the sum of the q_2^2 and μ_2^2 terms in the matrix element. A 0.1% change in μ_2 away from our assumed value of $\mu_a = (\alpha/2\pi)\mu_B$ gives a 4% change in τ_n. Using the Rosenbluth sign for the anomalous magnetic moment gives a calculated neutron lifetime of 1.1 s.

As we see it, the situation is as follows. Spin-$\frac{1}{2}$ fermions may be coupled to the electromagnetic field through two terms; the monopole electric charge, q, which is quantised in units of e, and the anomalous magnetic dipole moment, μ_a, which may be quantised in units of $(\alpha/2\pi)(e/2m_e)$. Pauli and others have been aware since 1933 that these two terms constituted maximal coupling. However, there has been an emphasis in the literature on minimal coupling. Rosenbluth, in following a suggestion by Feynman, chose an incorrect sign when studying the scattering of minimally coupled electrons off maximally coupled protons. This led to the

introduction and use of adjustable form factors. A maximally coupled theory of electrons and protons gives a better (first-order) fit to the scattering experiments (Burling-Claridge and Butler 1989). The calculation of the present letter shows that a maximally coupled, purely electromagnetic theory gives a realistic value of the neutron lifetime.

References

Barut A O 1981 *Group Theory and its Applications in Physics, 1980 (AIP Conf. Series* **71**) ed. T H Seligman (New York: AIP) pp 73–108

Barut A O and McEwan J 1984 *Phys. Lett.* **135** 172

Biedenharn L C and Louck J D 1981 *Encyclopedia of Mathematics and its Applications* vol 8 (Reading, MA: Addison-Wesley) pp 1–26

Burling-Claridge G R and Butler P H 1989 *J. Phys. G: Nucl. Part. Phys.* **15** 571

Byrne J 1988 *Nature* **333** 398

Cohen E R and Taylor B N 1986 *The 1986 adjustment of the fundamental physical constants, CODATA Bulletin No 63* (Oxford: Pergamon) (reprinted 1987 *Rev. Mod. Phys.* **59** 1121)

Hubert A 1985 *MSc thesis* University of Canterbury

Last J, Arnold M, Döhner J, Dubbers D and Freedman S J 1988 *Phys. Rev. Lett.* **60** 995

Omnès 1971 *Introduction to Particle Physics* (New York: Wiley) p 380

Pauli W 1933 *Handbuch der Physik* Band 34/1 p 233

Pilkuhn 1979 *Relativistic Particle Physics* (Berlin: Springer)

Rosenbluth M N 1950 *Phys. Rev.* **79** 615

Wilkinson D H 1982 *Nucl. Phys.* A **377** 474